Figure 23

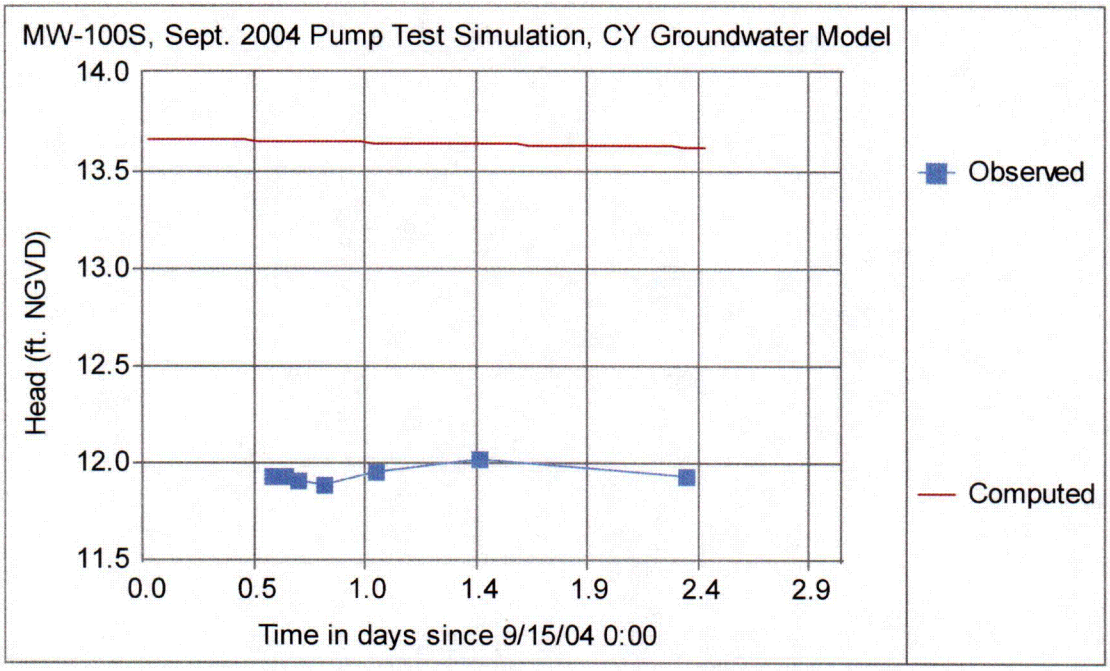
MW-100S, Sept. 2004 Pump Test Simulation, CY Groundwater Model
14.0
13.5
13.0
12.5
12.0
11.5
Head (ft. NGVD)
0.0
0.5
1.0
1.4
1.9
2.4
2.9
Time in days since 9/15/04 0:00
Observed
Computed

(a)

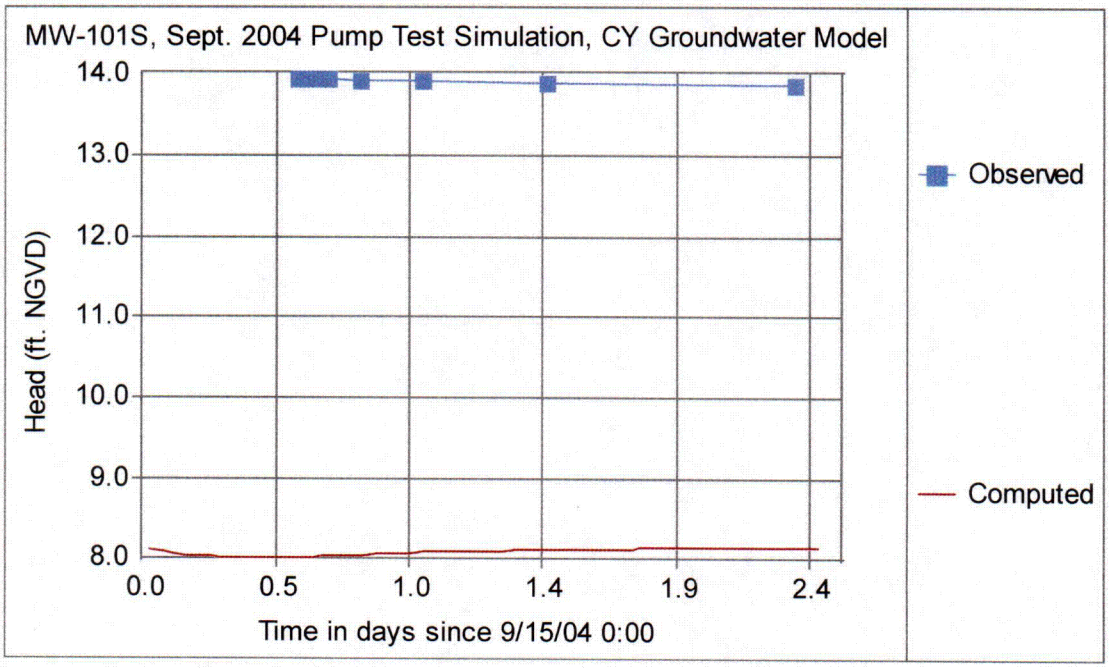
MW-101S, Sept. 2004 Pump Test Simulation, CY Groundwater Model
14.0
13.0
12.0
11.0
10.0
9.0
8.0
Head (ft. NGVD)
0.0
0.5
1.0
1.4
1.9
2.4
Time in days since 9/15/04 0:00
Observed
Computed

(b)

Figure 23

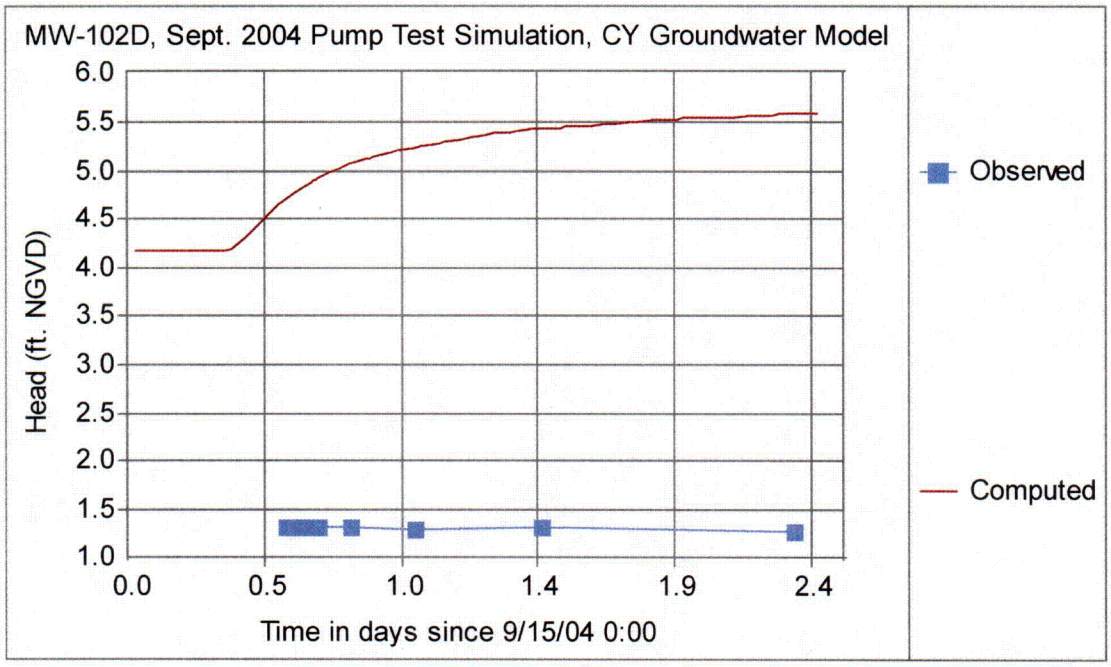
MW-102D, Sept. 2004 Pump Test Simulation, CY Groundwater Model
Head (ft. NGVD)
6.0
5.5
5.0
4.5
4.0
3.5
3.0
2.5
2.0
1.5
1.0
0.0
0.5
1.0
1.4
1.9
2.4
Time in days since 9/15/04 0:00
Observed
Computed

(c)

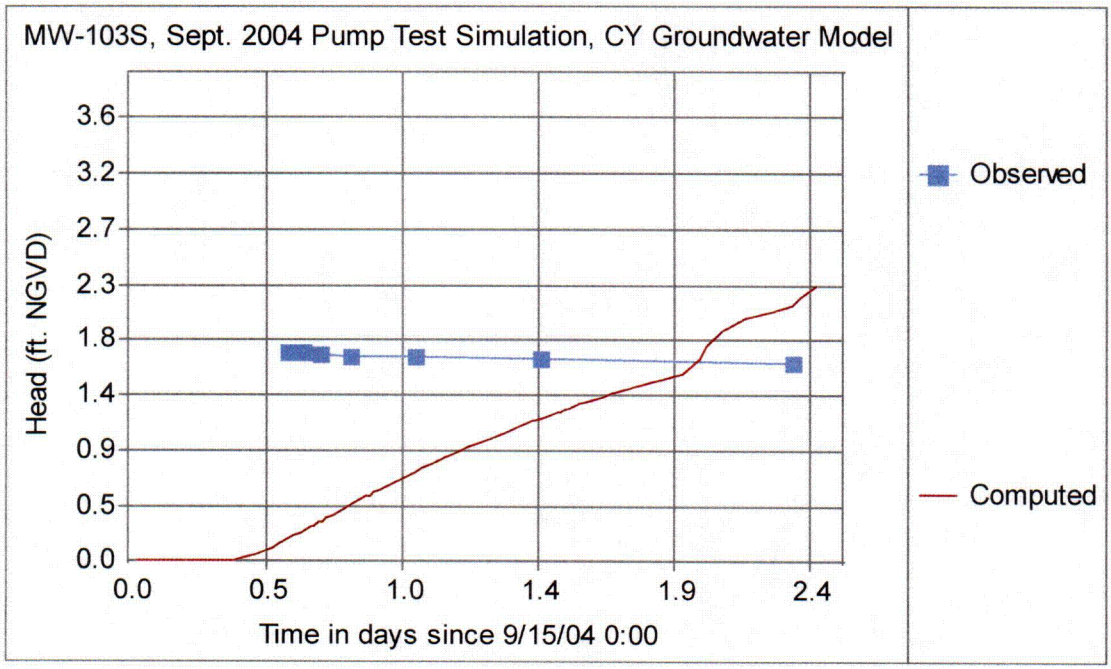
MW-103S, Sept. 2004 Pump Test Simulation, CY Groundwater Model
Head (ft. NGVD)
3.6
3.2
2.7
2.3
1.8
1.4
0.9
0.5
0.0
0.0
0.5
1.0
1.4
1.9
2.4
Time in days since 9/15/04 0:00
Observed
Computed

(d)

Figure 23

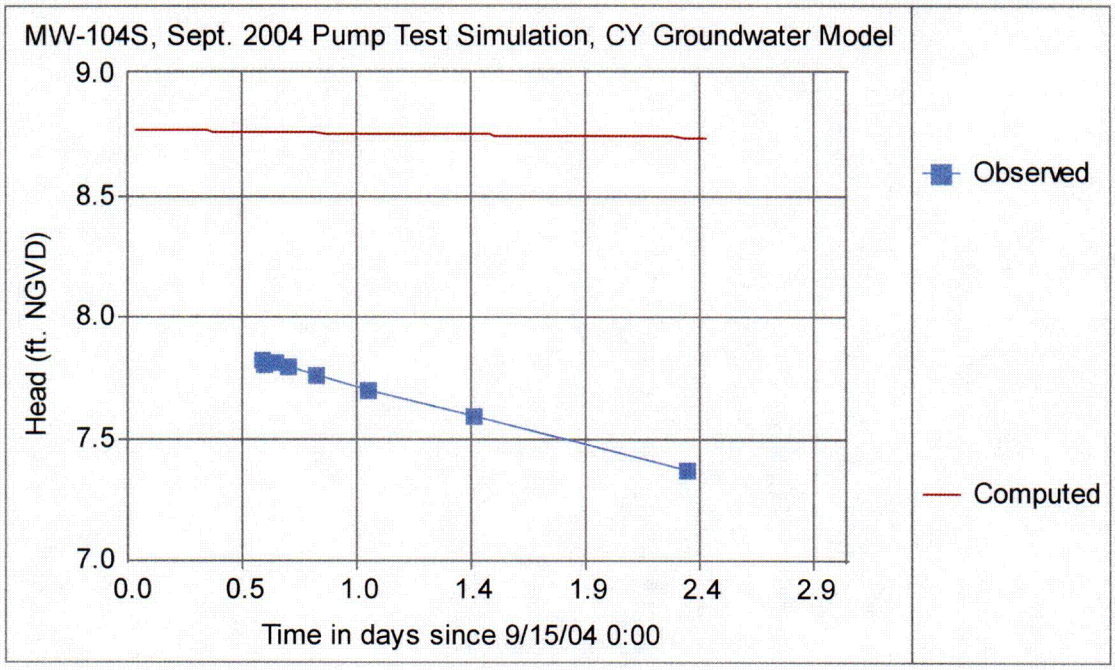

(e)

MW-107S Comparison of Predicted versus Measured Head, September 2004 pumping test at AT-1

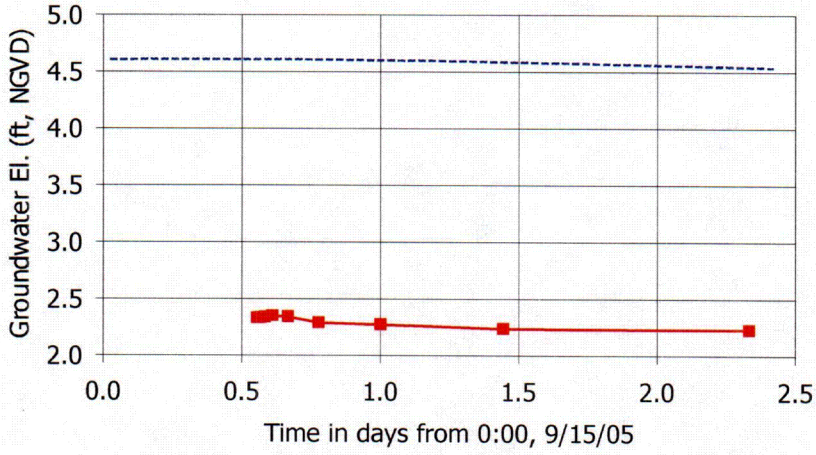

(f)

Figure 23

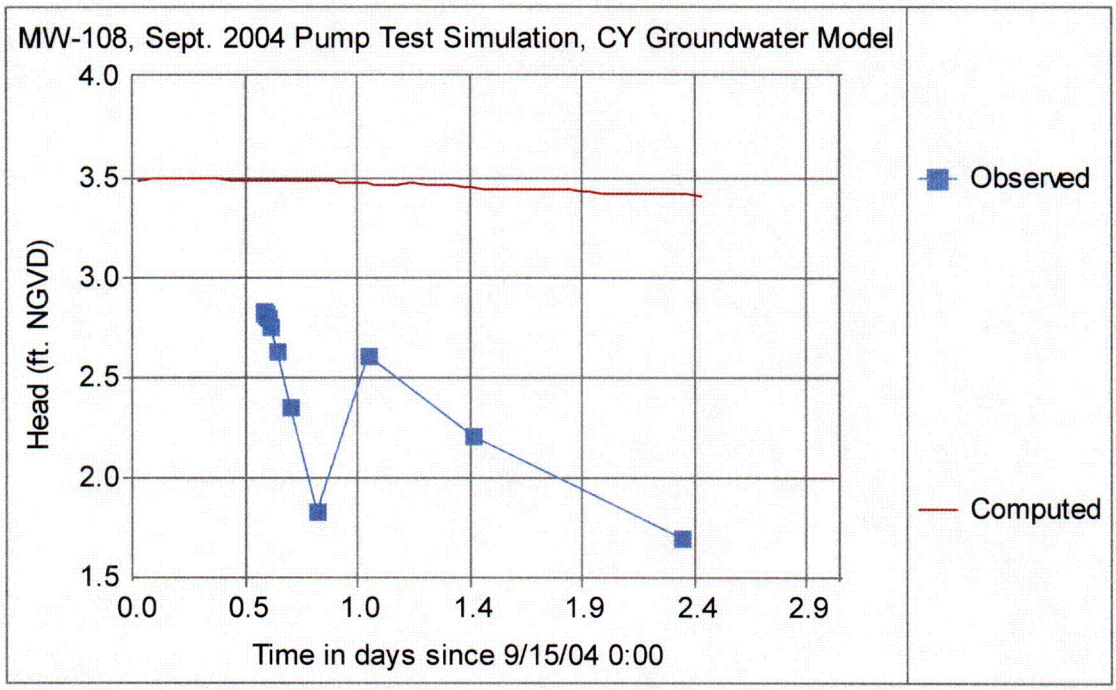
MW-108, Sept. 2004 Pump Test Simulation, CY Groundwater Model
4.0
3.5
3.0
2.5
2.0
1.5
Head (ft. NGVD)
0.0
0.5
1.0
1.4
1.9
2.4
2.9
Time in days since 9/15/04 0:00
Observed
Computed

(g)

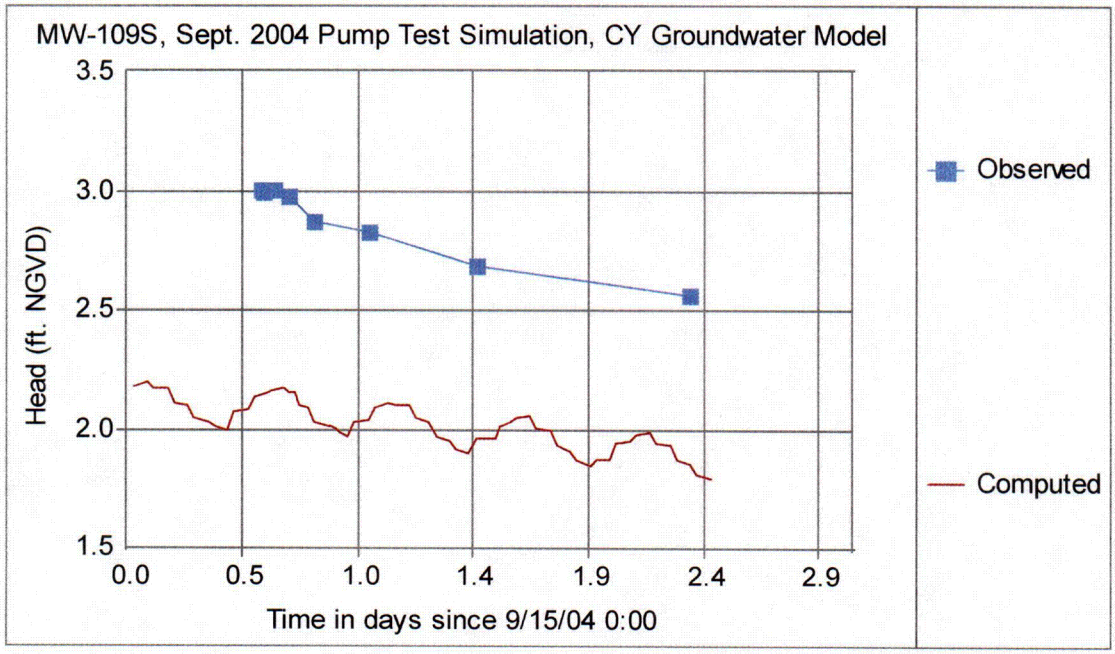
MW-109S, Sept. 2004 Pump Test Simulation, CY Groundwater Model
3.5
3.0
2.5
2.0
1.5
Head (ft. NGVD)
0.0
0.5
1.0
1.4
1.9
2.4
2.9
Time in days since 9/15/04 0:00
Observed
Computed

(h)

Figure 23

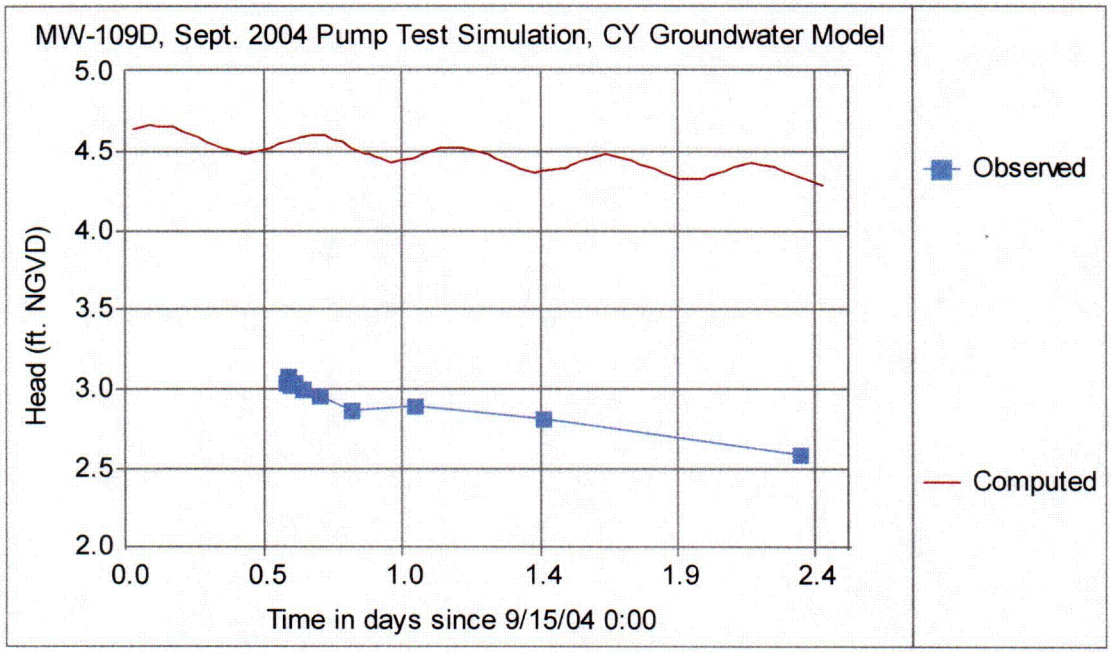
MW-109D, Sept. 2004 Pump Test Simulation, CY Groundwater Model
Head (ft. NGVD)
5.0
4.5
4.0
3.5
3.0
2.5
2.0
0.0
0.5
1.0
1.4
1.9
2.4
Time in days since 9/15/04 0:00
Observed
Computed

(i)

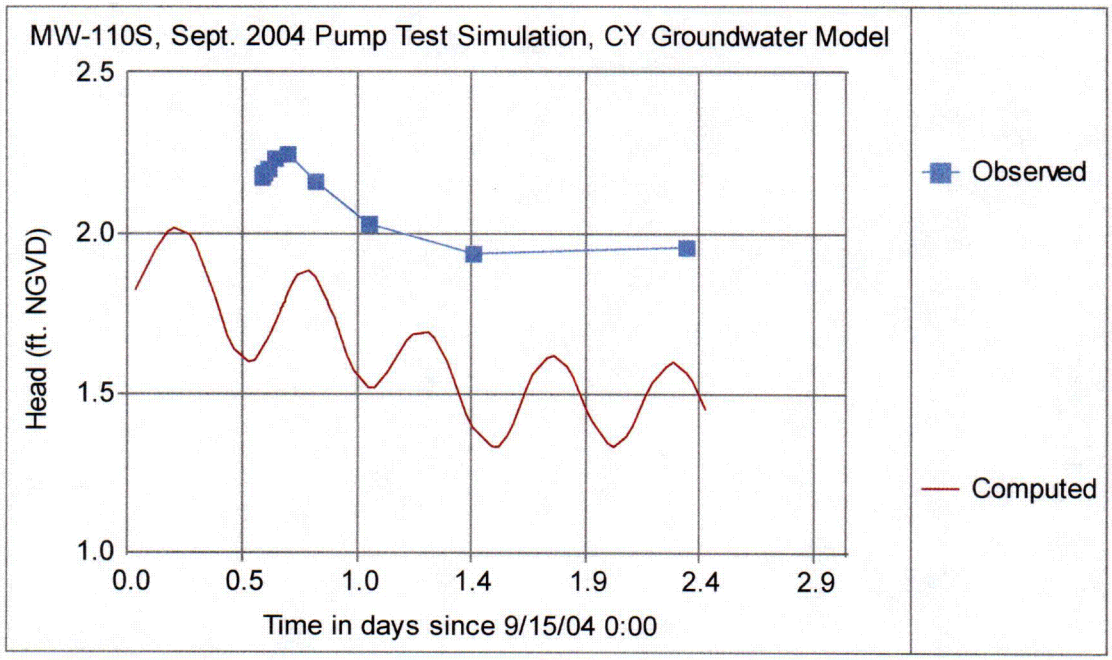
MW-110S, Sept. 2004 Pump Test Simulation, CY Groundwater Model
Head (ft. NGVD)
2.5
2.0
1.5
1.0
0.0
0.5
1.0
1.4
1.9
2.4
2.9
Time in days since 9/15/04 0:00
Observed
Computed

(j)

Figure 23

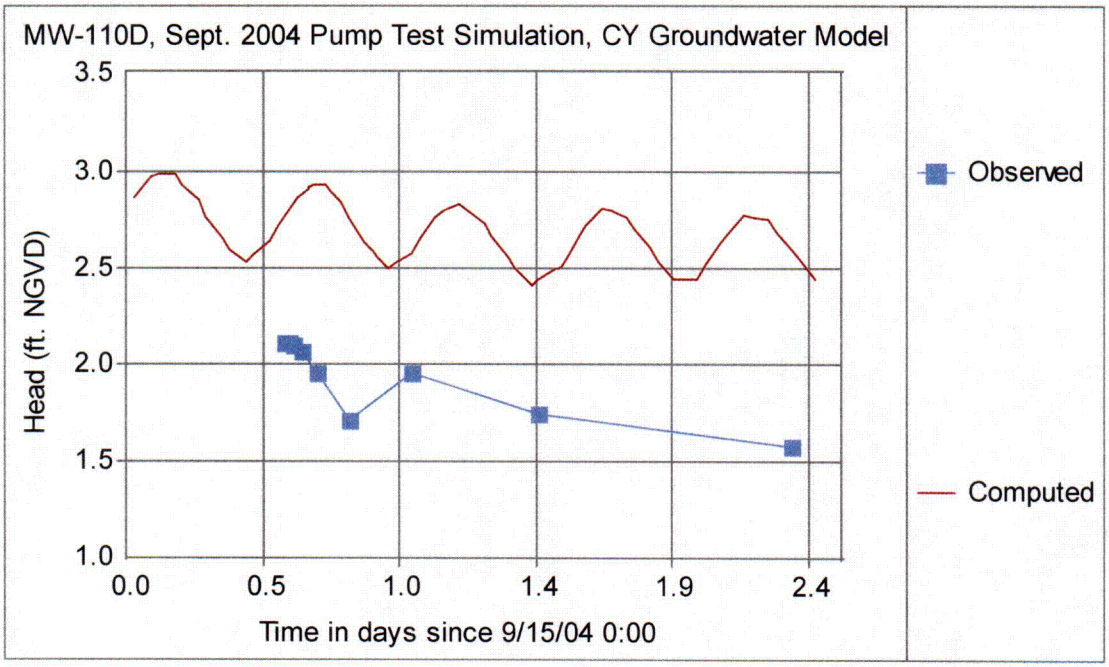
MW-110D, Sept. 2004 Pump Test Simulation, CY Groundwater Model
Head (ft. NGVD)
3.5
3.0
2.5
2.0
1.5
1.0
0.0
0.5
1.0
1.4
1.9
2.4
Time in days since 9/15/04 0:00
Observed
Computed

(k)

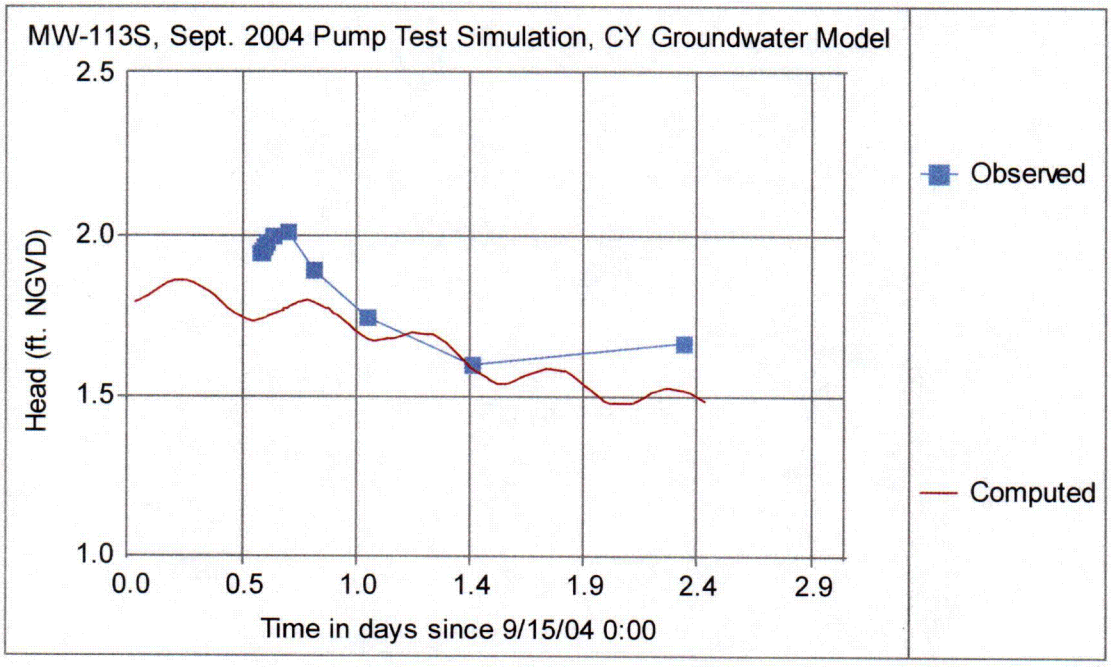
MW-113S, Sept. 2004 Pump Test Simulation, CY Groundwater Model
Head (ft. NGVD)
2.5
2.0
1.5
1.0
0.0
0.5
1.0
1.4
1.9
2.4
2.9
Time in days since 9/15/04 0:00
Observed
Computed

(l)

Figure 23

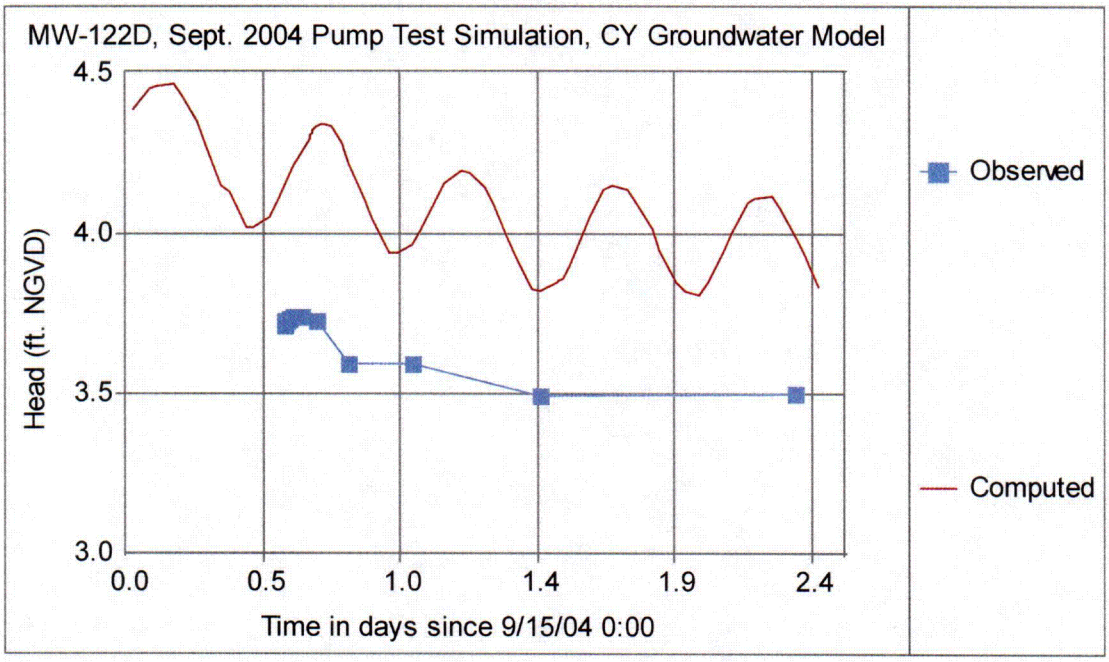
MW-122D, Sept. 2004 Pump Test Simulation, CY Groundwater Model
Head (ft. NGVD)
4.5
4.0
3.5
3.0
0.0
0.5
1.0
1.4
1.9
2.4
Time in days since 9/15/04 0:00
Observed
Computed

(m)

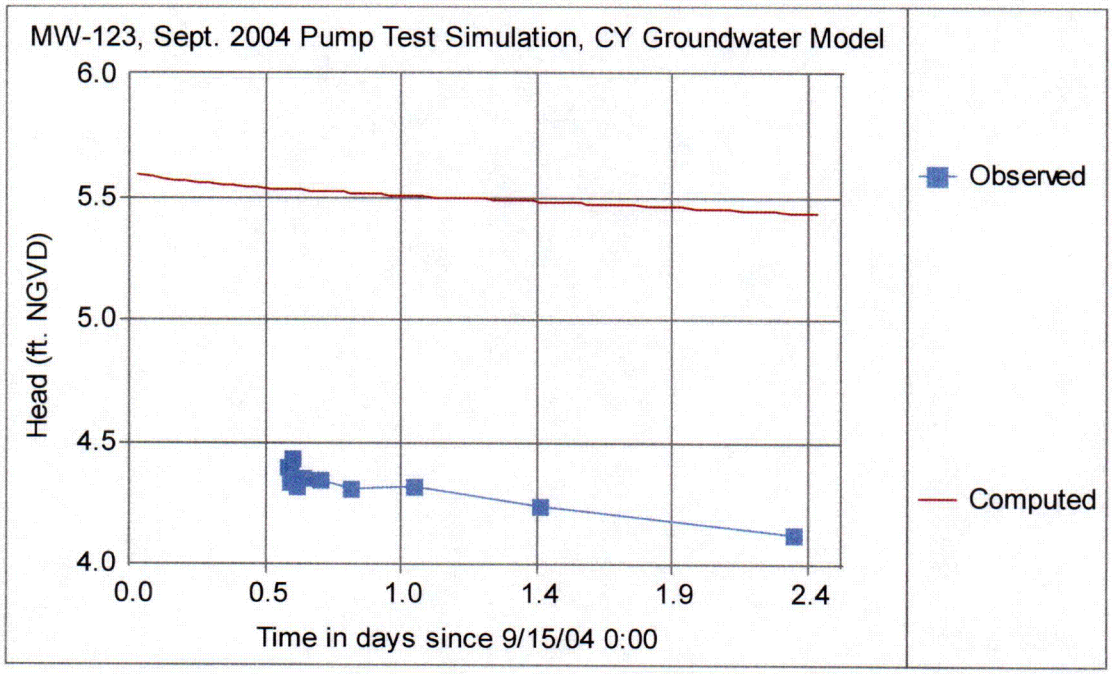
MW-123, Sept. 2004 Pump Test Simulation, CY Groundwater Model
Head (ft. NGVD)
6.0
5.5
5.0
4.5
4.0
0.0
0.5
1.0
1.4
1.9
2.4
Time in days since 9/15/04 0:00
Observed
Computed

(n)

Figure 23

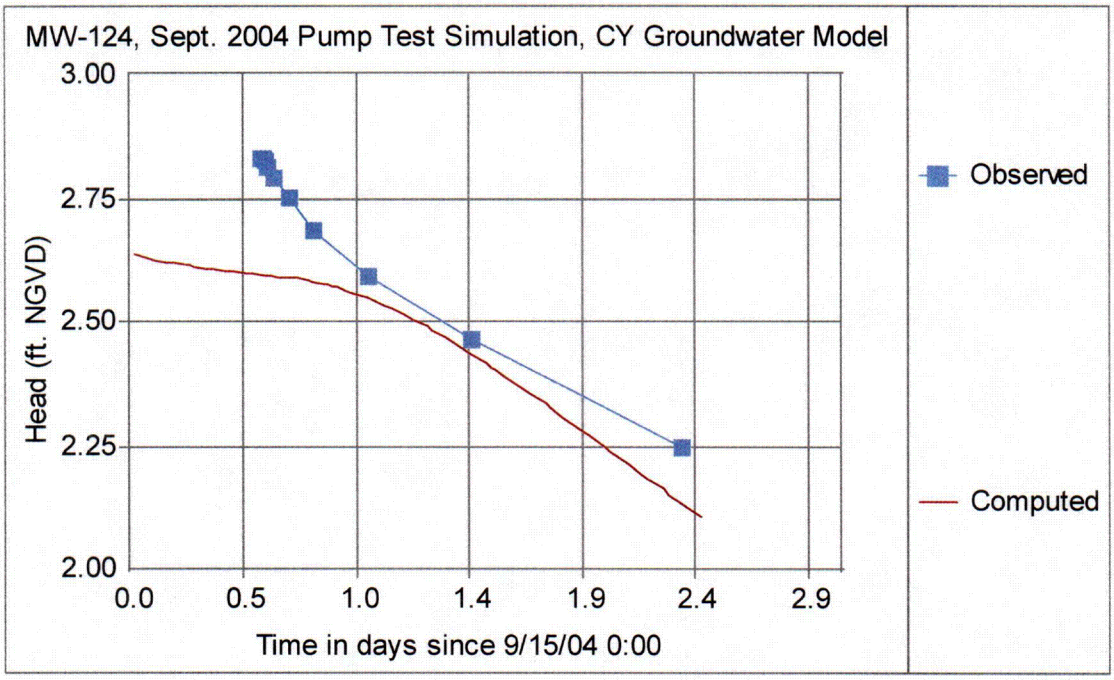
MW-124, Sept. 2004 Pump Test Simulation, CY Groundwater Model
3.00
2.75
2.50
2.25
2.00
Head (ft. NGVD)
0.0
0.5
1.0
1.4
1.9
2.4
2.9
Time in days since 9/15/04 0:00
Observed
Computed

(o)

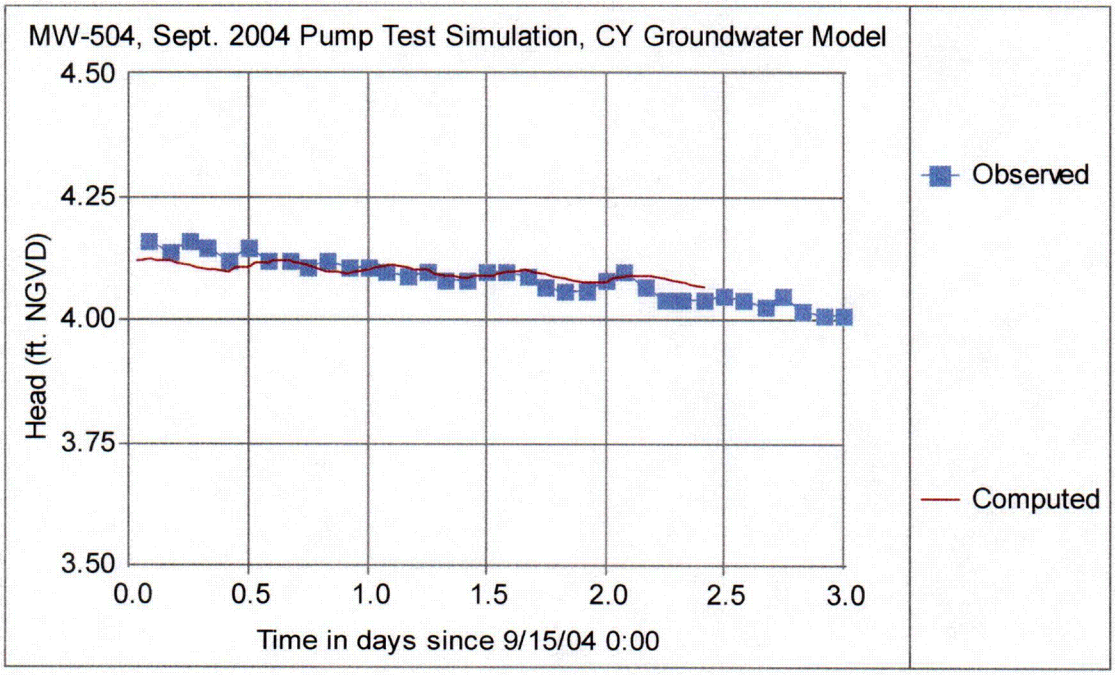
MW-504, Sept. 2004 Pump Test Simulation, CY Groundwater Model
4.50
4.25
4.00
3.75
3.50
Head (ft. NGVD)
0.0
0.5
1.0
1.5
2.0
2.5
3.0
Time in days since 9/15/04 0:00
Observed
Computed

(p)

Figure 23

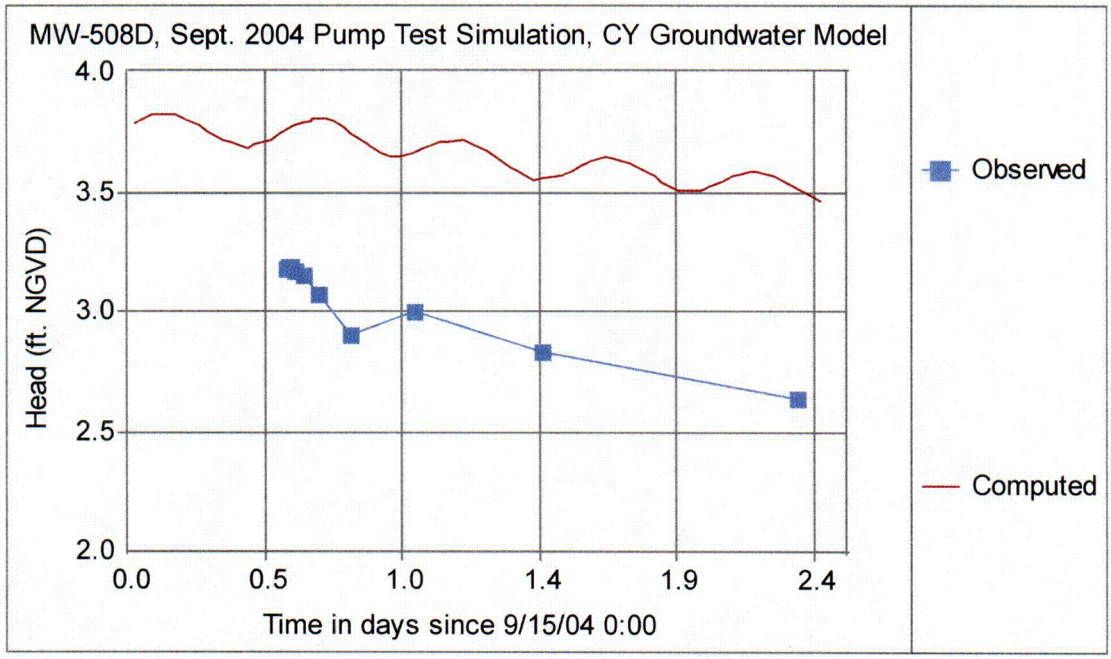
MW-508D, Sept. 2004 Pump Test Simulation, CY Groundwater Model
4.0
3.5
3.0
2.5
2.0
Head (ft. NGVD)
0.0
0.5
1.0
1.4
1.9
2.4
Time in days since 9/15/04 0:00
Observed
Computed

(q)

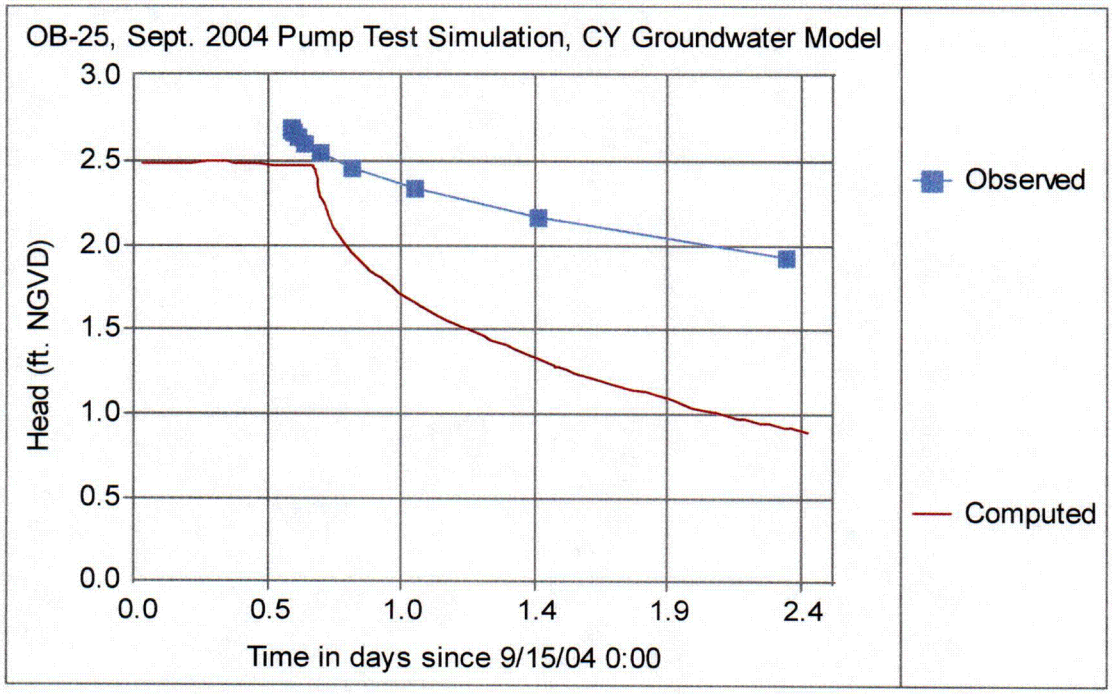
OB-25, Sept. 2004 Pump Test Simulation, CY Groundwater Model
3.0
2.5
2.0
1.5
1.0
0.5
0.0
Head (ft. NGVD)
0.0
0.5
1.0
1.4
1.9
2.4
Time in days since 9/15/04 0:00
Observed
Computed

(r)

Figure 23

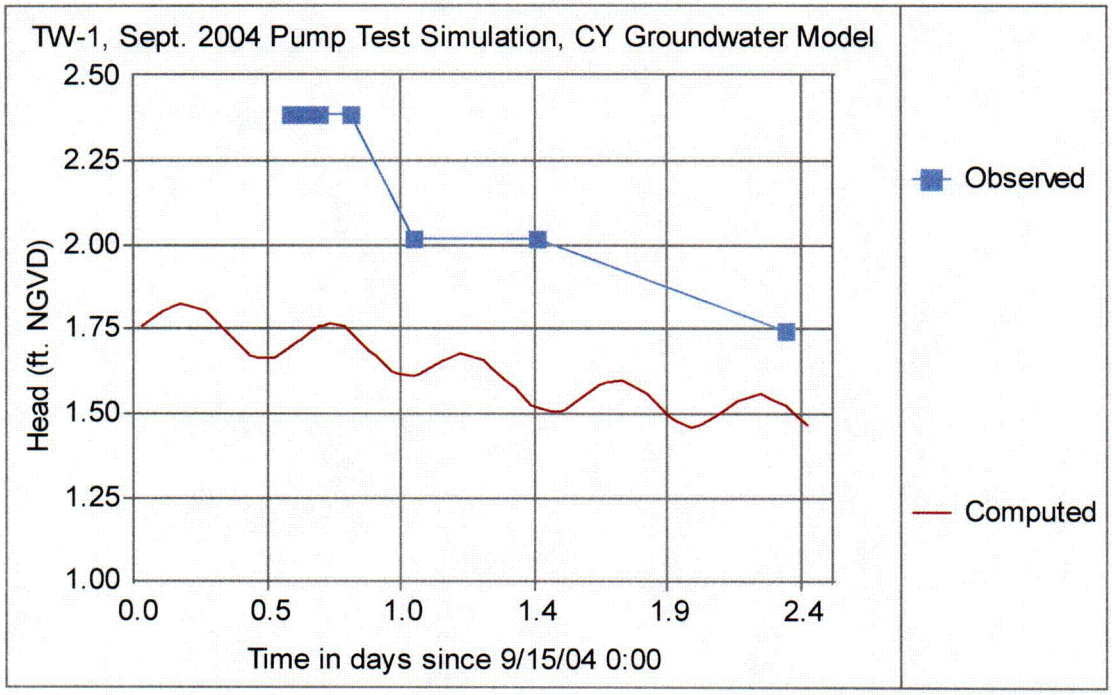
TW-1, Sept. 2004 Pump Test Simulation, CY Groundwater Model
2.50
2.25
2.00
1.75
1.50
1.25
1.00
Head (ft. NGVD)
0.0
0.5
1.0
1.4
1.9
2.4
Time in days since 9/15/04 0:00
Observed
Computed

(s)

Figure 24

Sensitivity Analysis, Recharge Zone 2
CY Groundwater Model

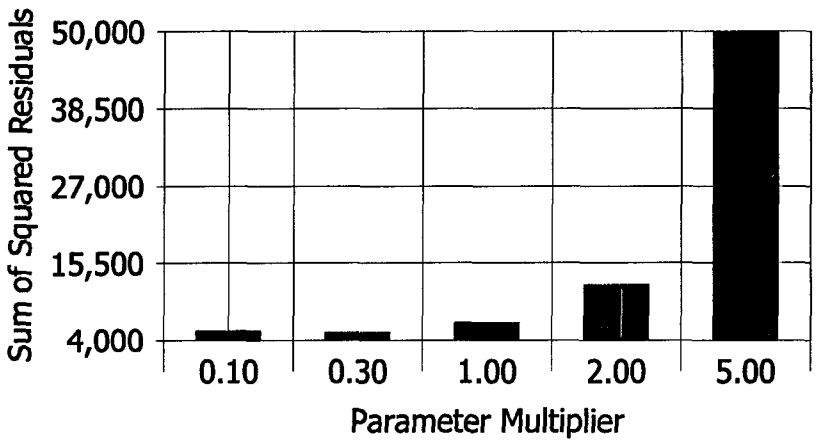

(a)

Sensitivity Analysis, Recharge Zone 3
CY Groundwater Model

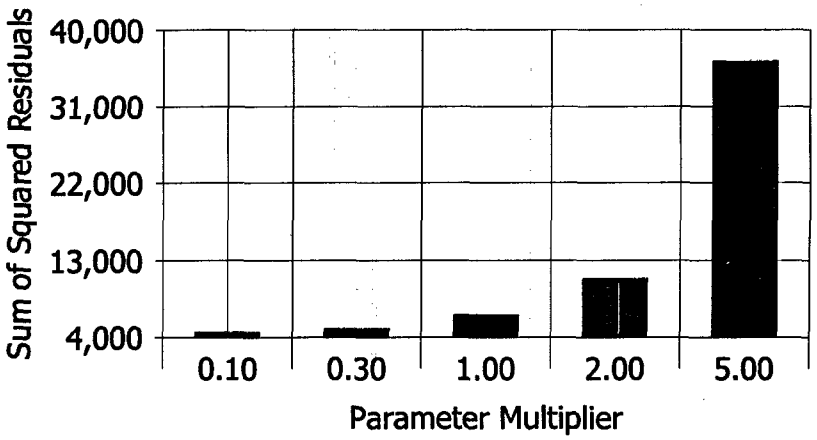

(b)

Figure 24

Sensitivity Analysis, Recharge Zone 4 CY Groundwater Model

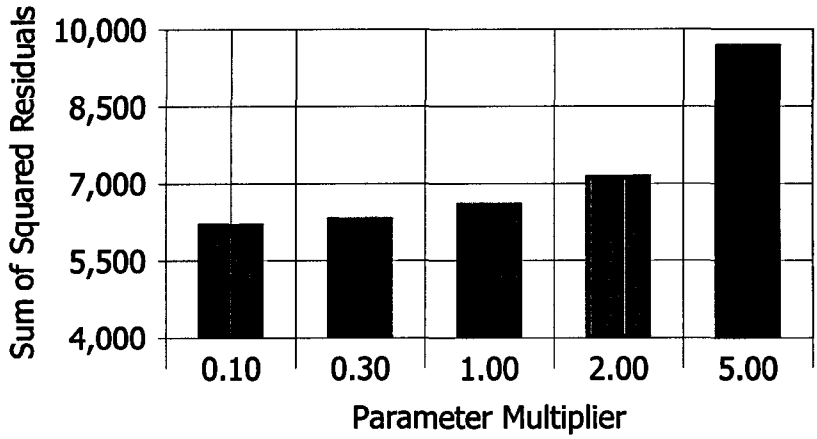

(c)

Sensitivity Analysis, Recharge Zone 7 CY Groundwater Model

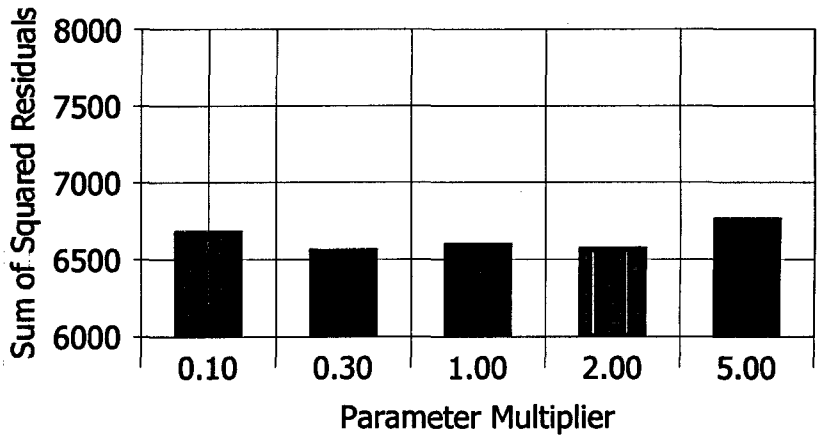

(d)

Figure 24

Sensitivity Analysis, Recharge Zone 11
CY Groundwater Model

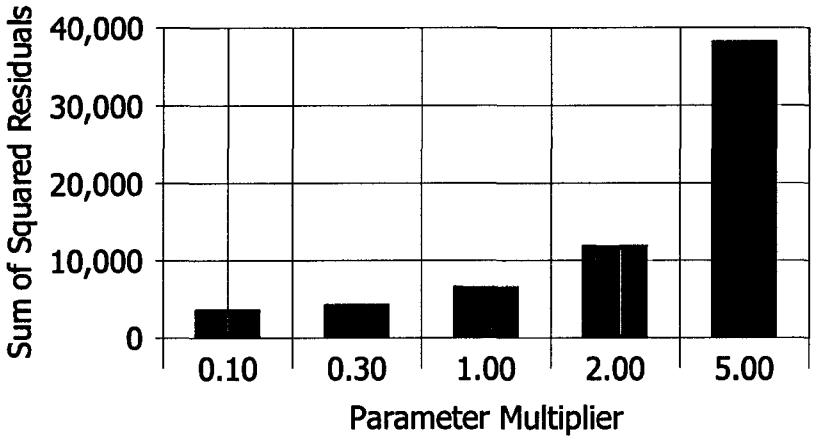

(e)

Figure 25

Sensitivity Analysis, Kxy Zone 1 CY Groundwater Model

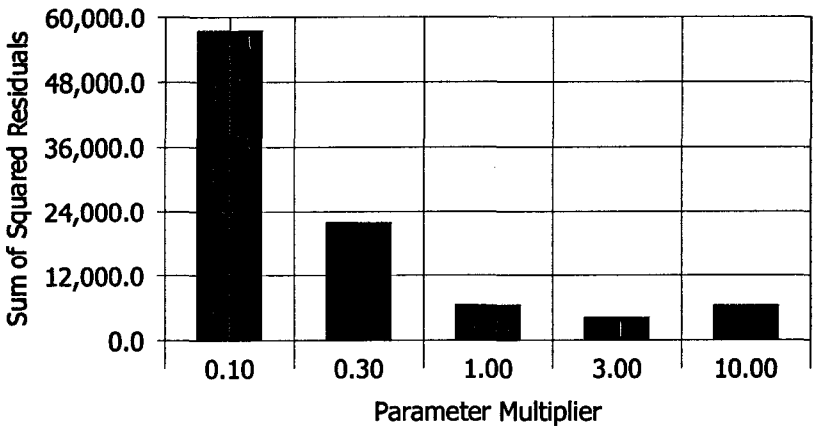

(a)

Sensitivity Analysis, Kxy Zone 3 CY Groundwater Model

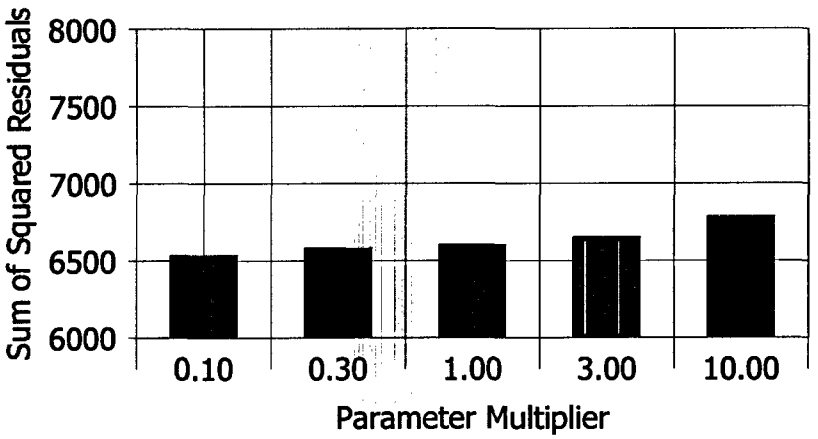

(b)

Figure 25

Sensitivity Analysis, Kxy Zone 14 CY Groundwater Model

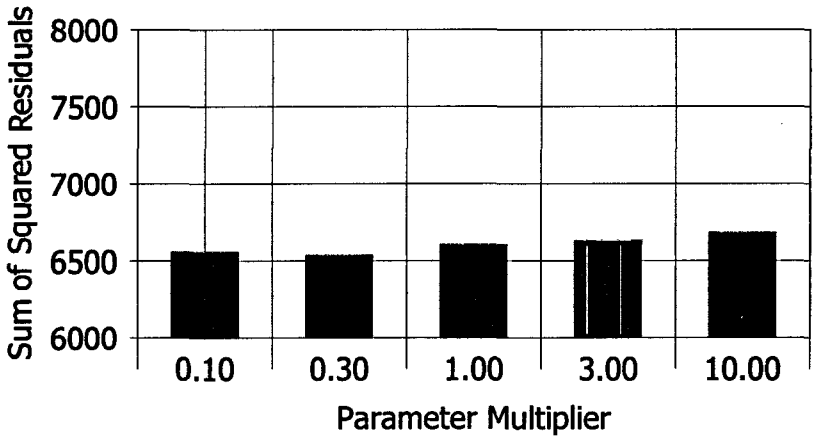

(c)

Sensitivity Analysis, Kxy Zone 17 CY Groundwater Model

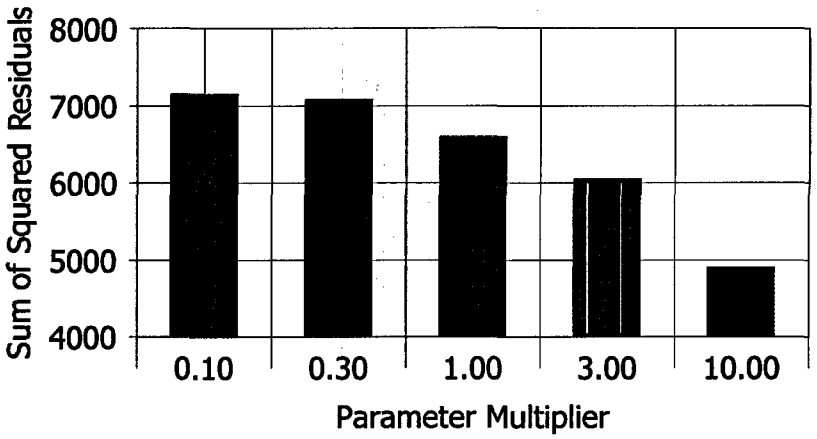

(d)

Figure 25

Sensitivity Analysis, Kxy Zone 18 CY Groundwater Model

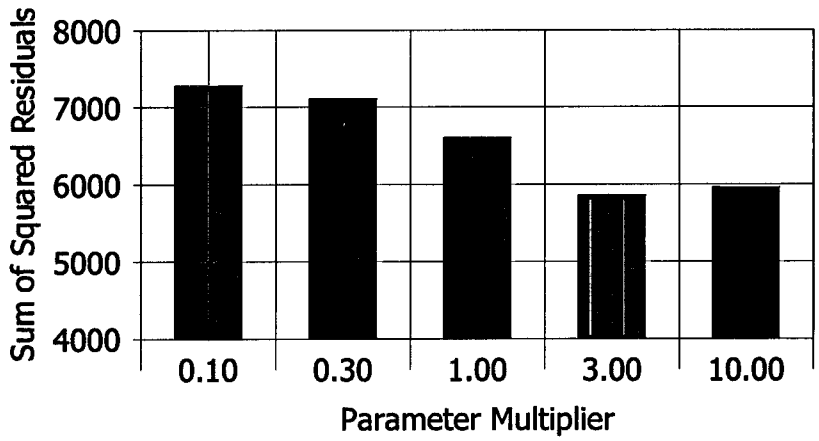

(e)

Sensitivity Analysis, Kxy Zone 20 CY Groundwater Model

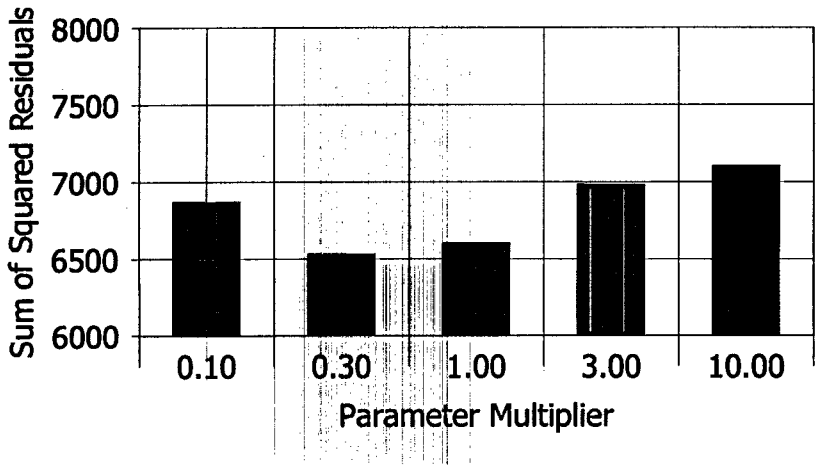

(f)

Figure 25

Sensitivity Analysis, Kxy Zone 21
CY Groundwater Model

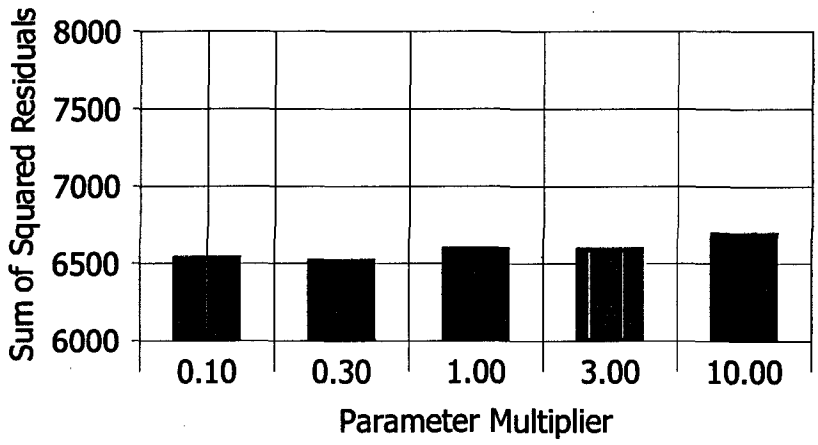

(g)

Sensitivity Analysis, Kxy Zone 24
CY Groundwater Model

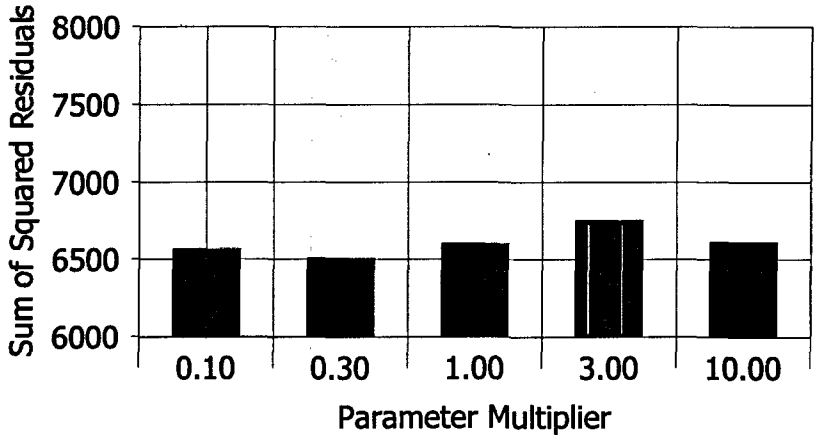

(h)

Figure 25

Sensitivity Analysis, Kxy Zone 27 CY Groundwater Model

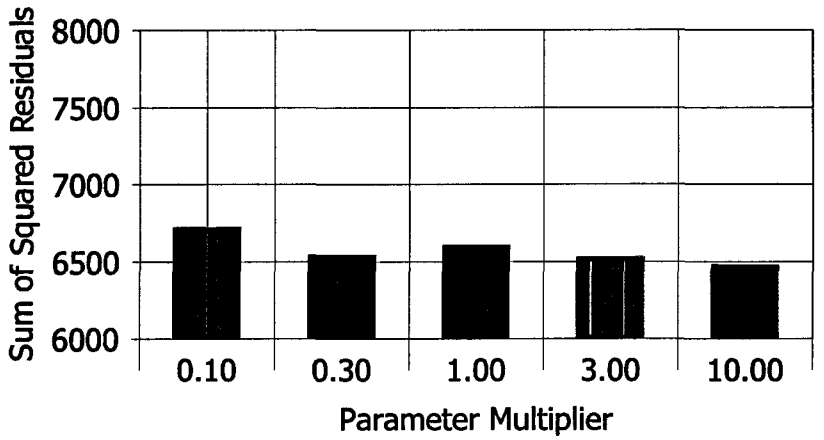

(i)

Sensitivity Analysis, Kxy Zone 29 CY Groundwater Model

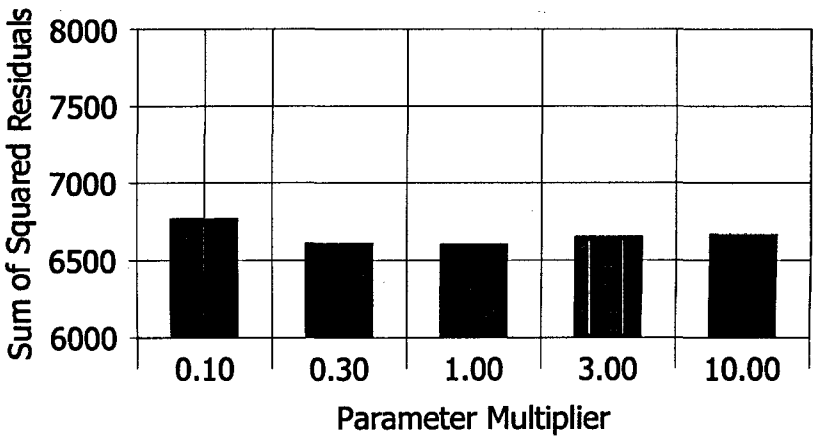

(j)

Figure 25

Sensitivity Analysis, Kxy Zone 33
CY Groundwater Model

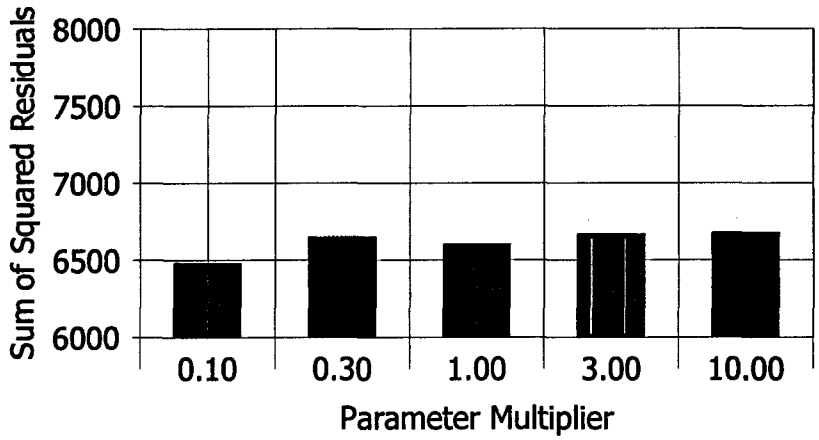

(k)

Sensitivity Analysis, Kxy Zone 40
CY Groundwater Model

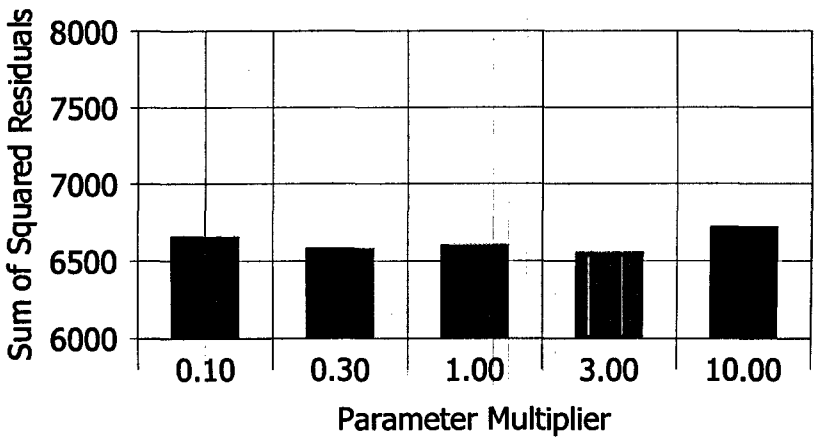

(l)

Figure 26

Sensitivity Analysis, Kz Zone 20
CY Groundwater Model

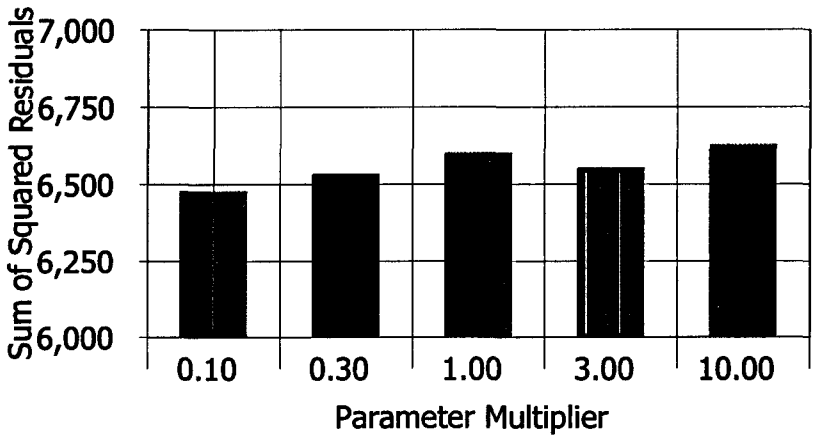

(a)

Sensitivity Analysis, Kz Zone 21
CY Groundwater Model

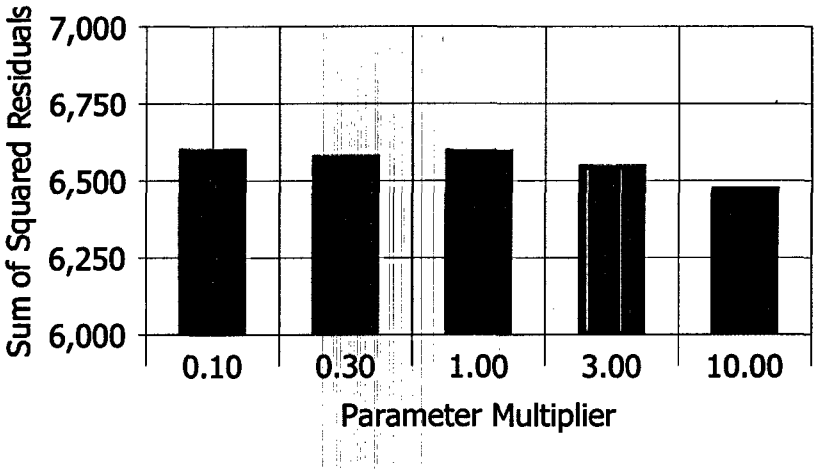

(b)

Figure 26

Sensitivity Analysis, Kz Zone 24
CY Groundwater Model

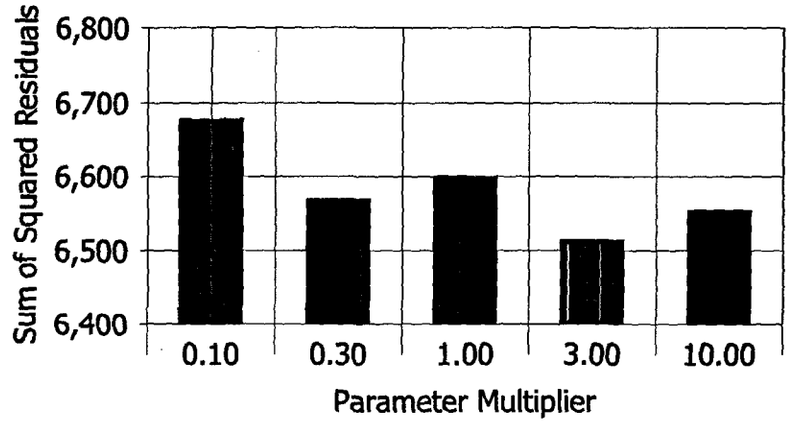

(c)

Sensitivity Analysis, Kz Zone 25
CY Groundwater Modeling

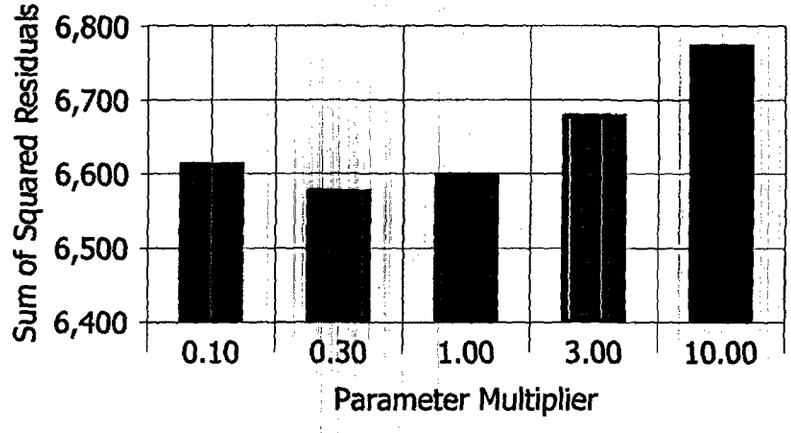

(d)

Figure 26

Sensitivity Analysis, Kz Zone 26
CY Groundwater Model

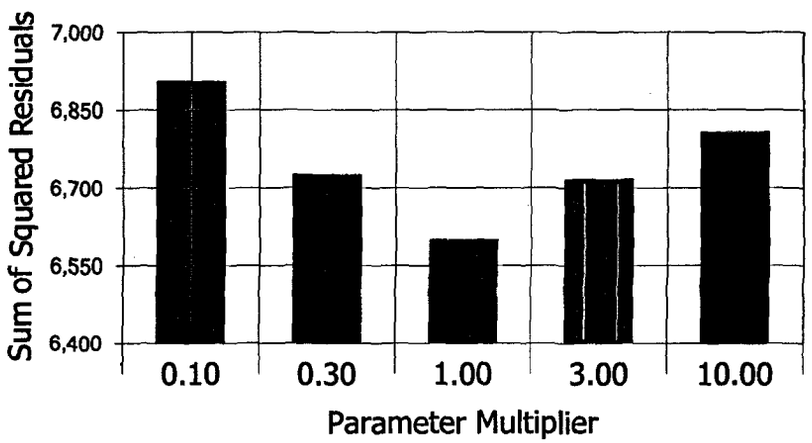

(e)

Sensitivity Analysis, Kz Zone 27
CY Groundwater Model

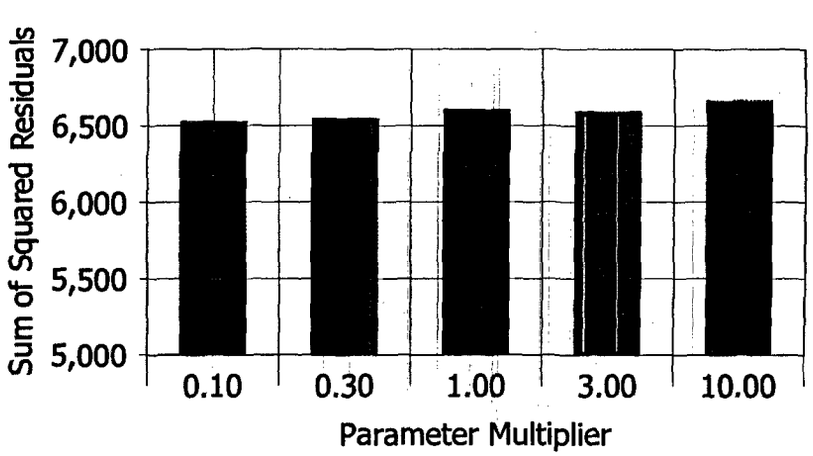

(f)

Figure 26

Sensitivity Analysis, Kz Zone 40
CY Groundwater Model

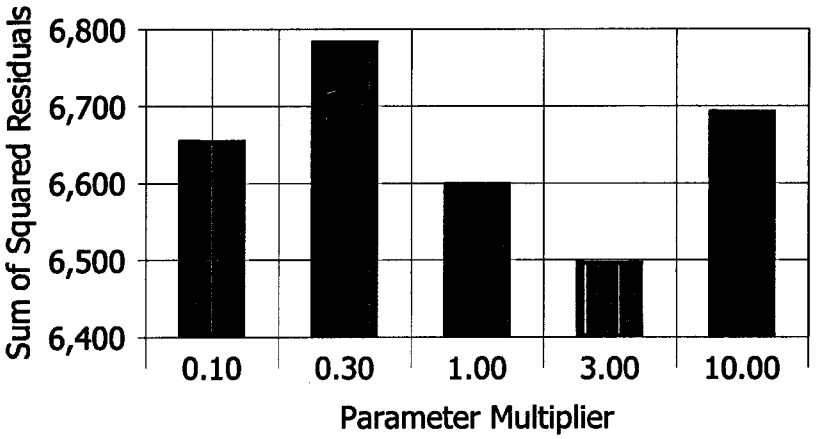

(g)

Figure 27
Sensitivity Analysis, Anisotropy Ratio, Ky/Kx
CY Groundwater Model

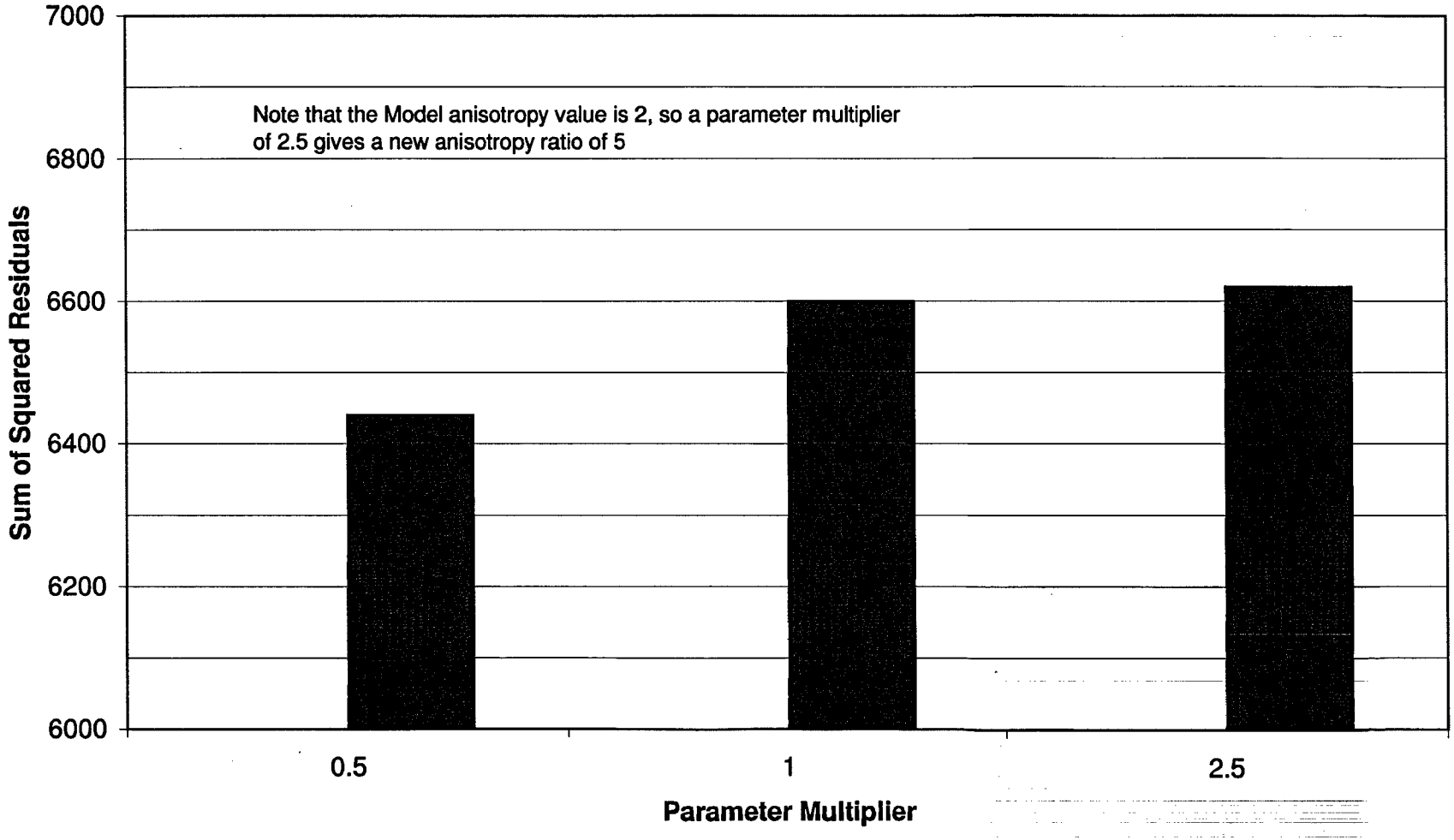

Figure 28
Sensitivity Analysis, Leakance
CY Groundwater Model

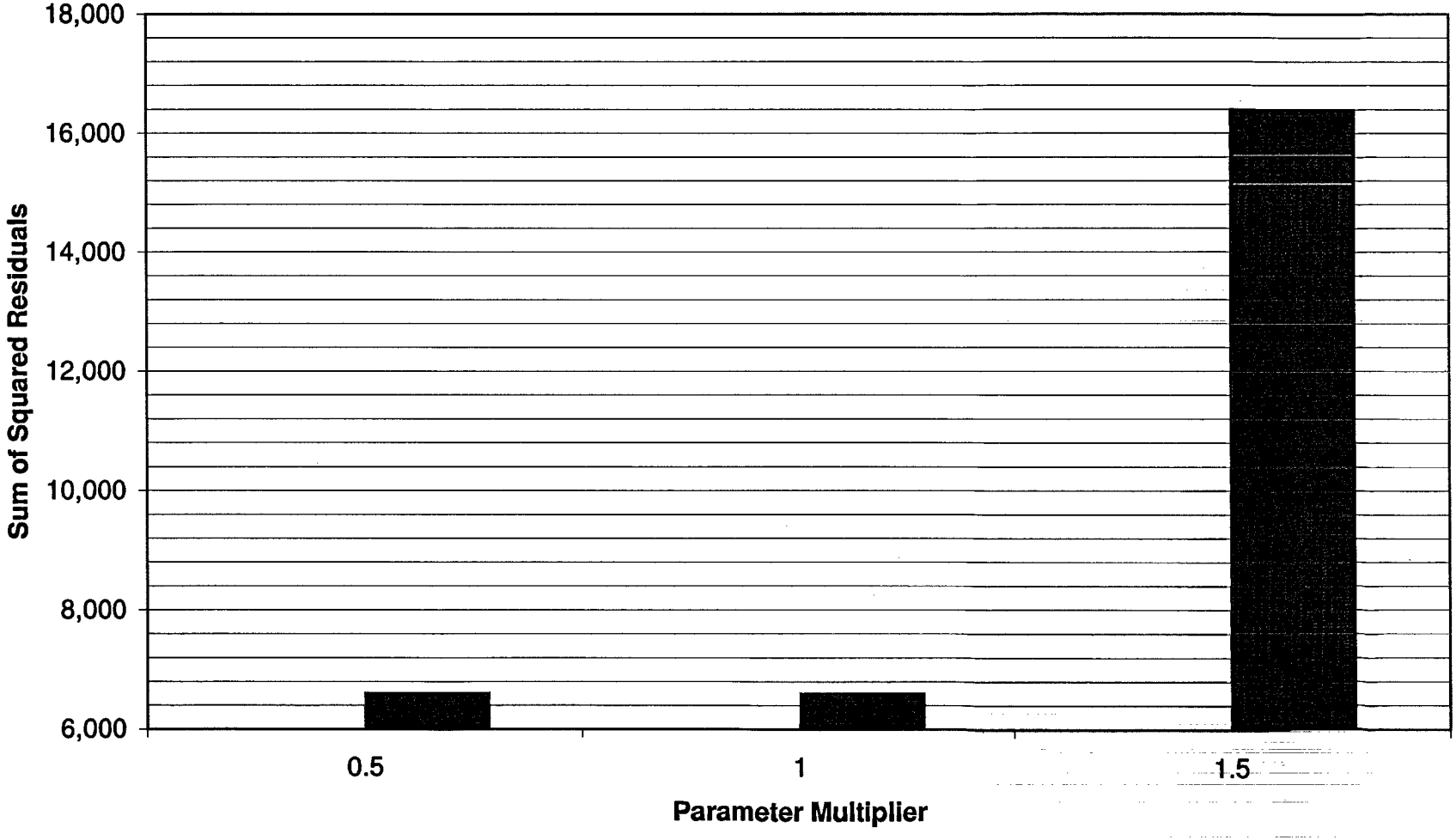

Figure 29
Sensitivity Analysis, Specific Yield Zone 1
CY Groundwater Model

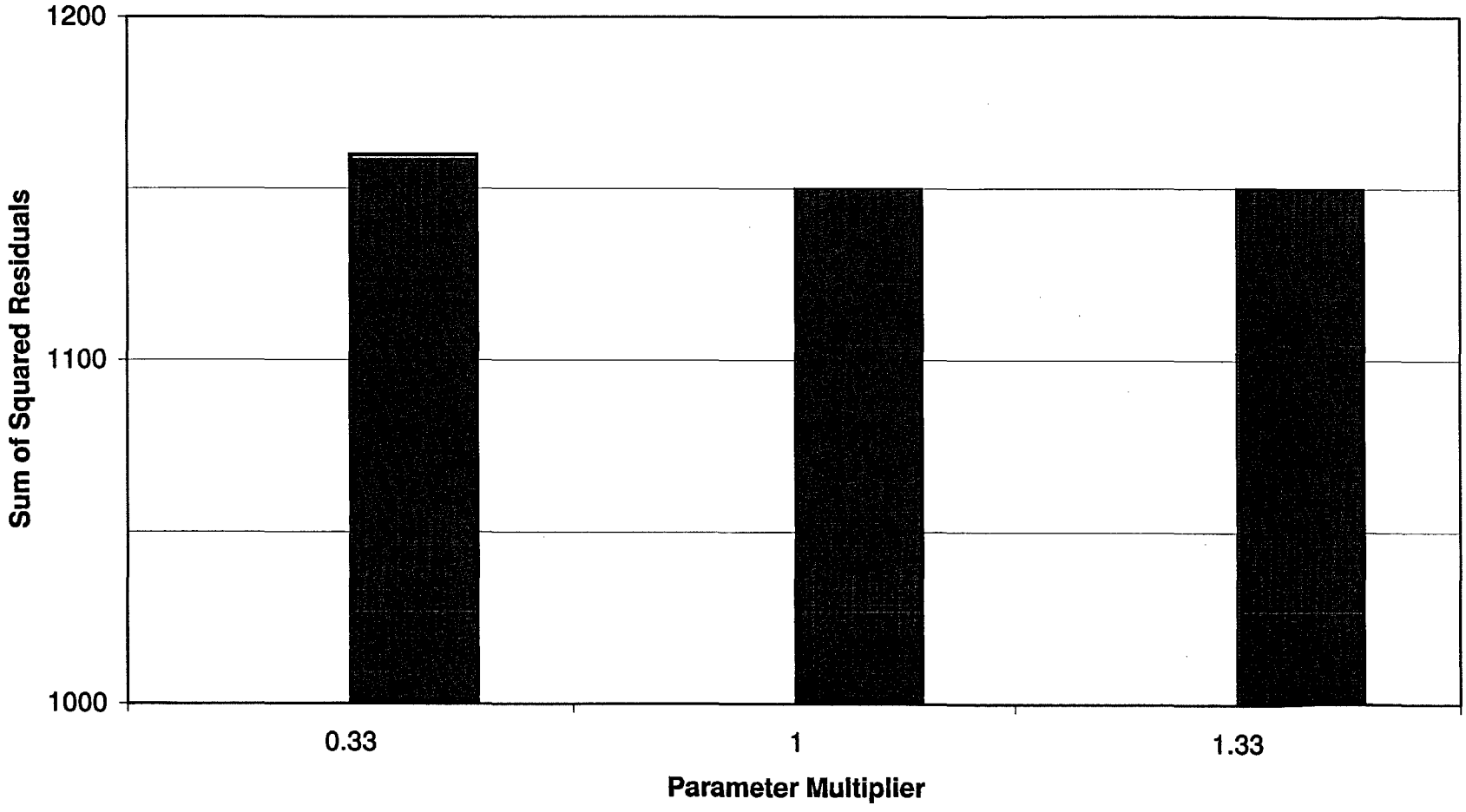

Figure 30
Sensitivity Analysis, Specific Storage Zone 2
CY Groundwater Model

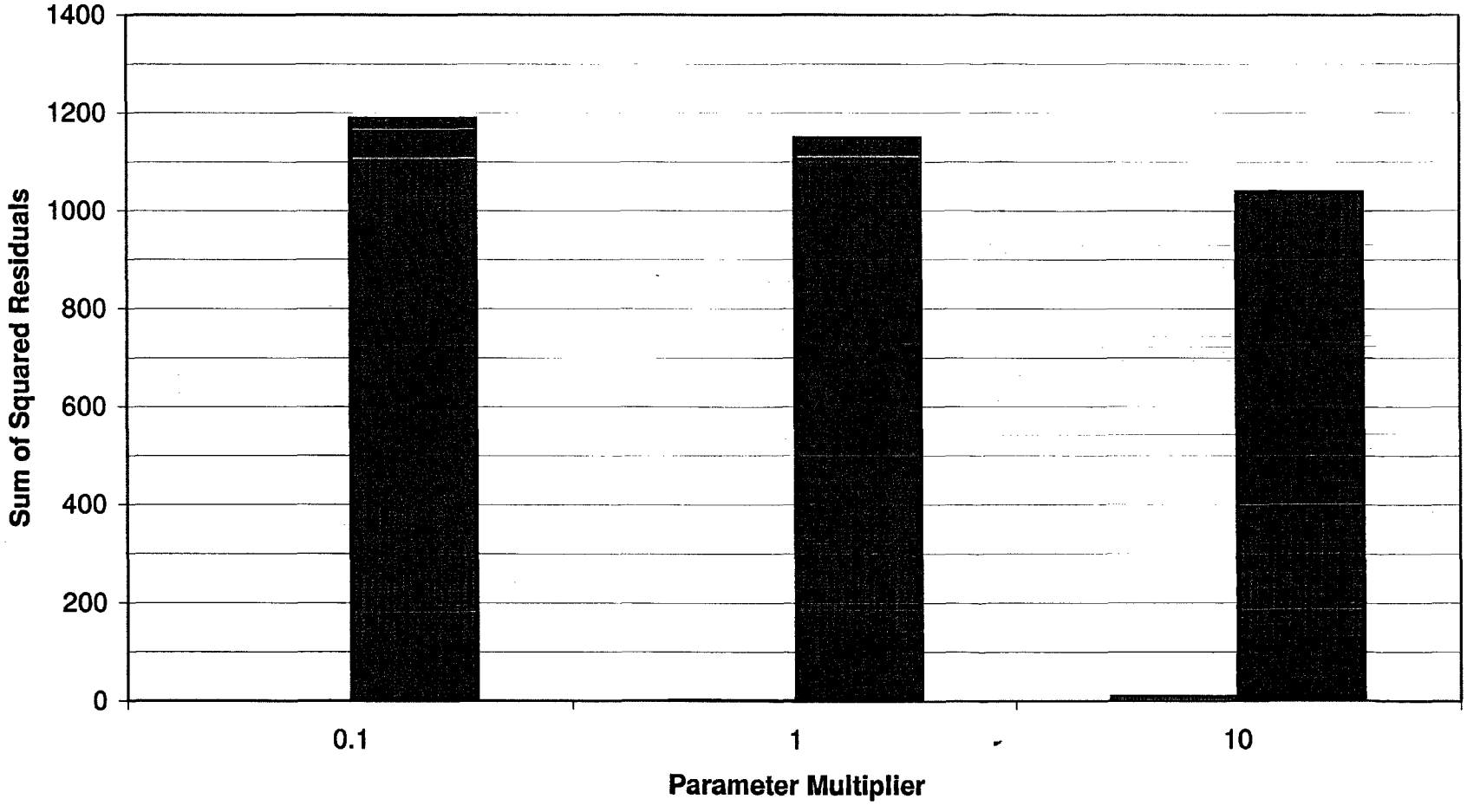

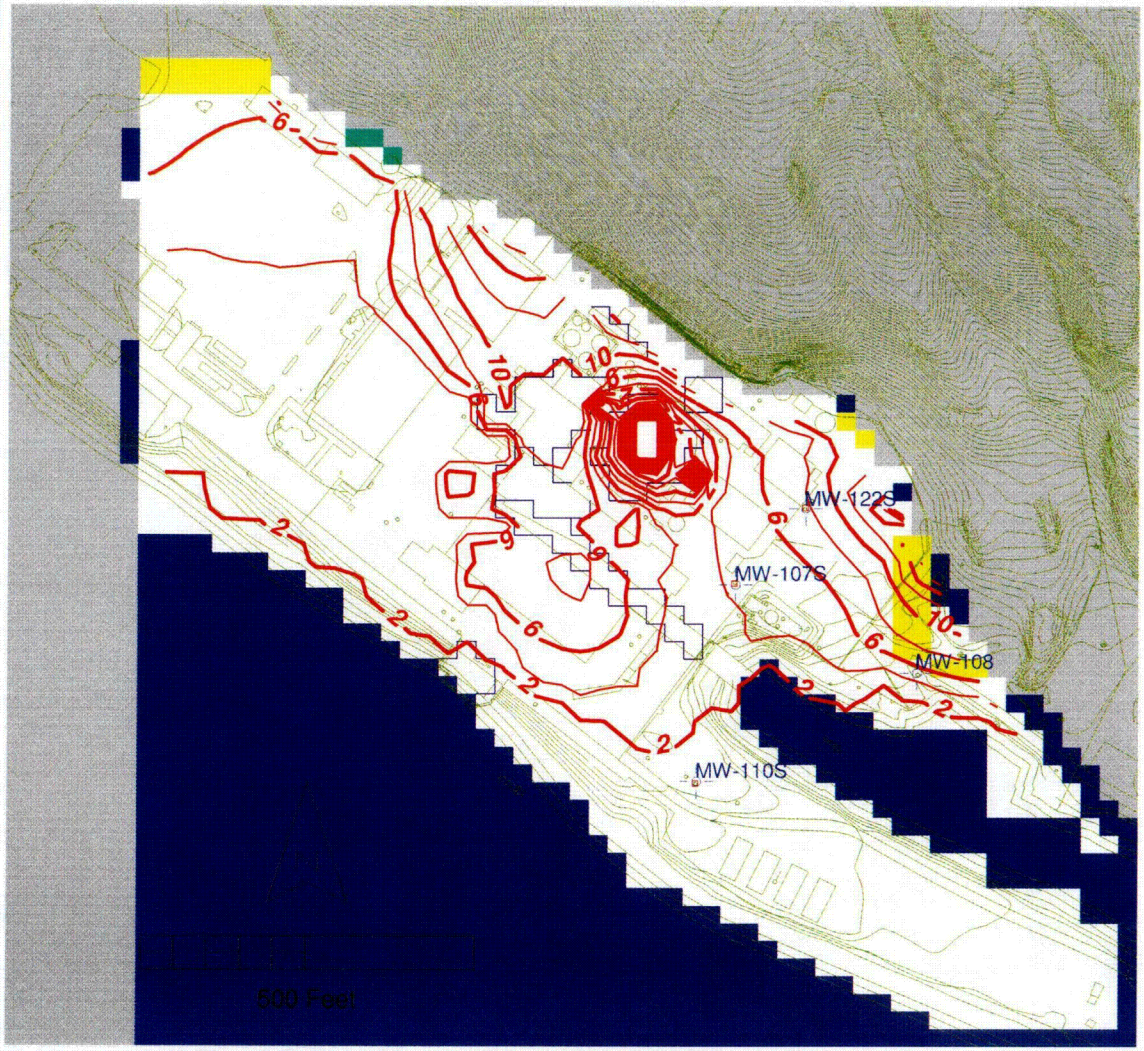

Figure 31---Steady-state operational phreatic surface heads

CY Groundwater Model

Heads are in feet above NGVD29

8/23/05

STRATEX strategic consulting

C43

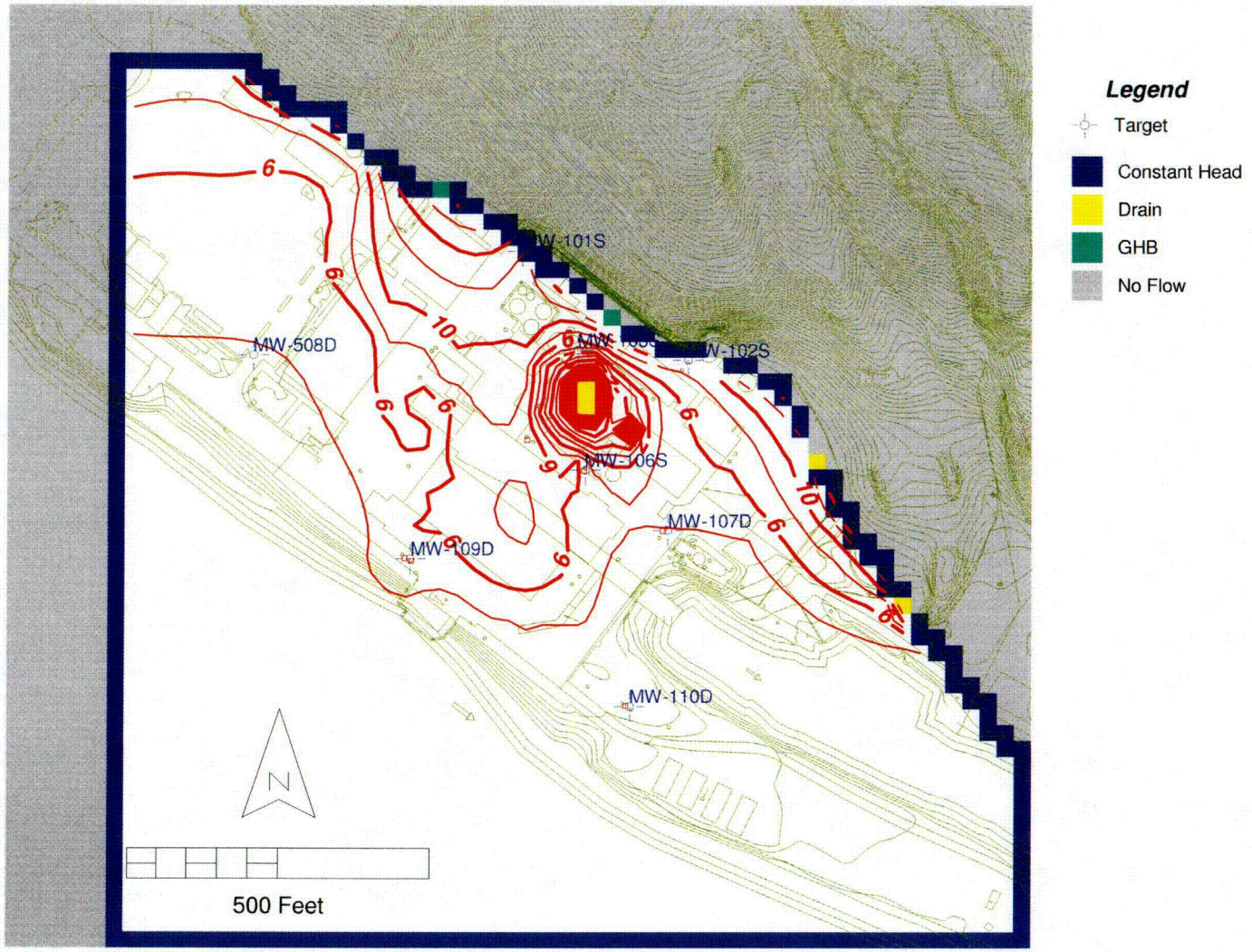

Figure 32--Steady-state operational heads in Model Layer 4--Top of Rock

CY Groundwater Model

Heads are in feet above NGVD29

8/23/05

STRATEX strategic consulting

C44

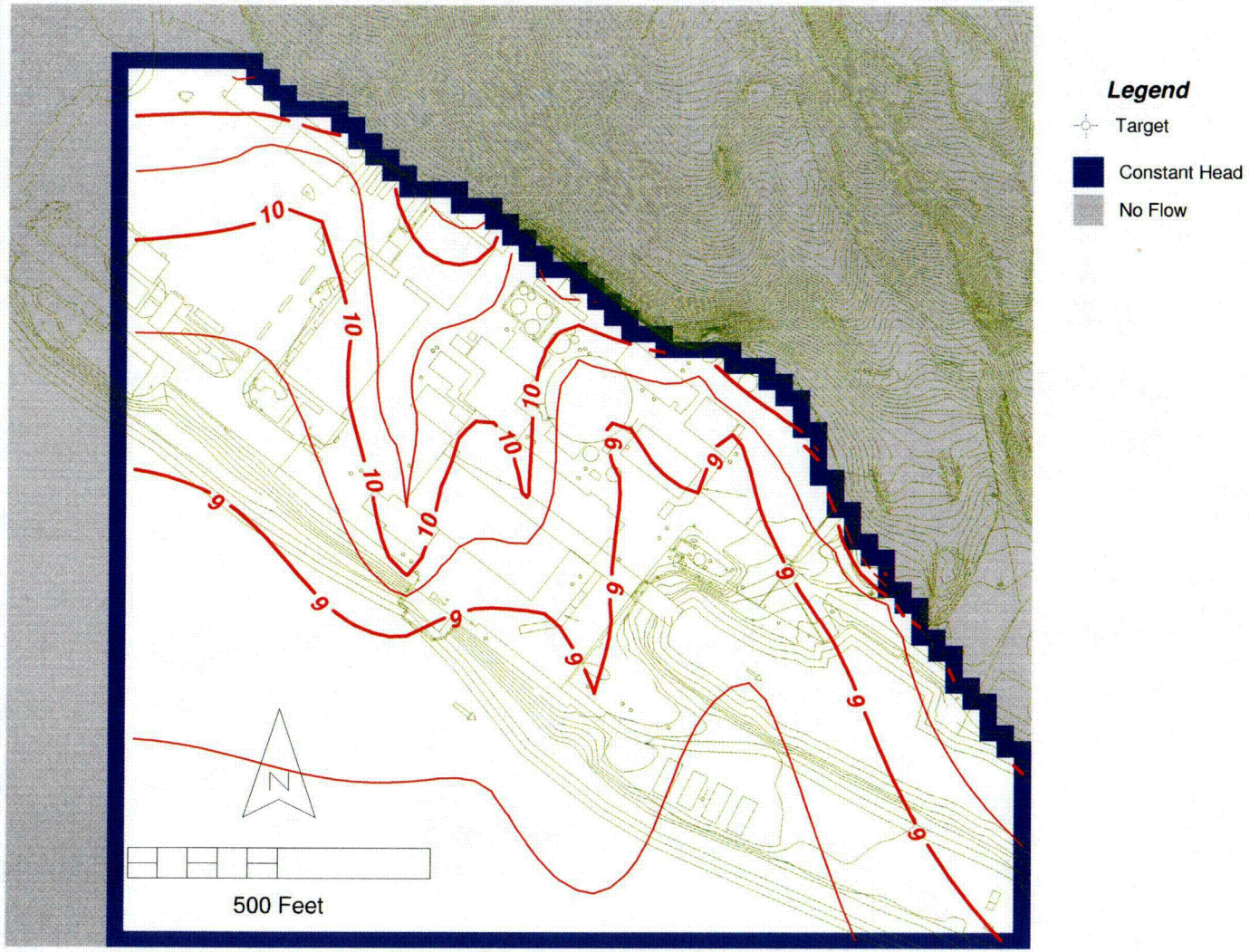

Legend

Target

Constant Head

No Flow

Figure 33--Steady-state operational heads in Model Layer 6--3rd Rock Layer

CY Groundwater Model

Heads are in feet above NGVD29

8/23/05

STRATEX strategic consulting

C45

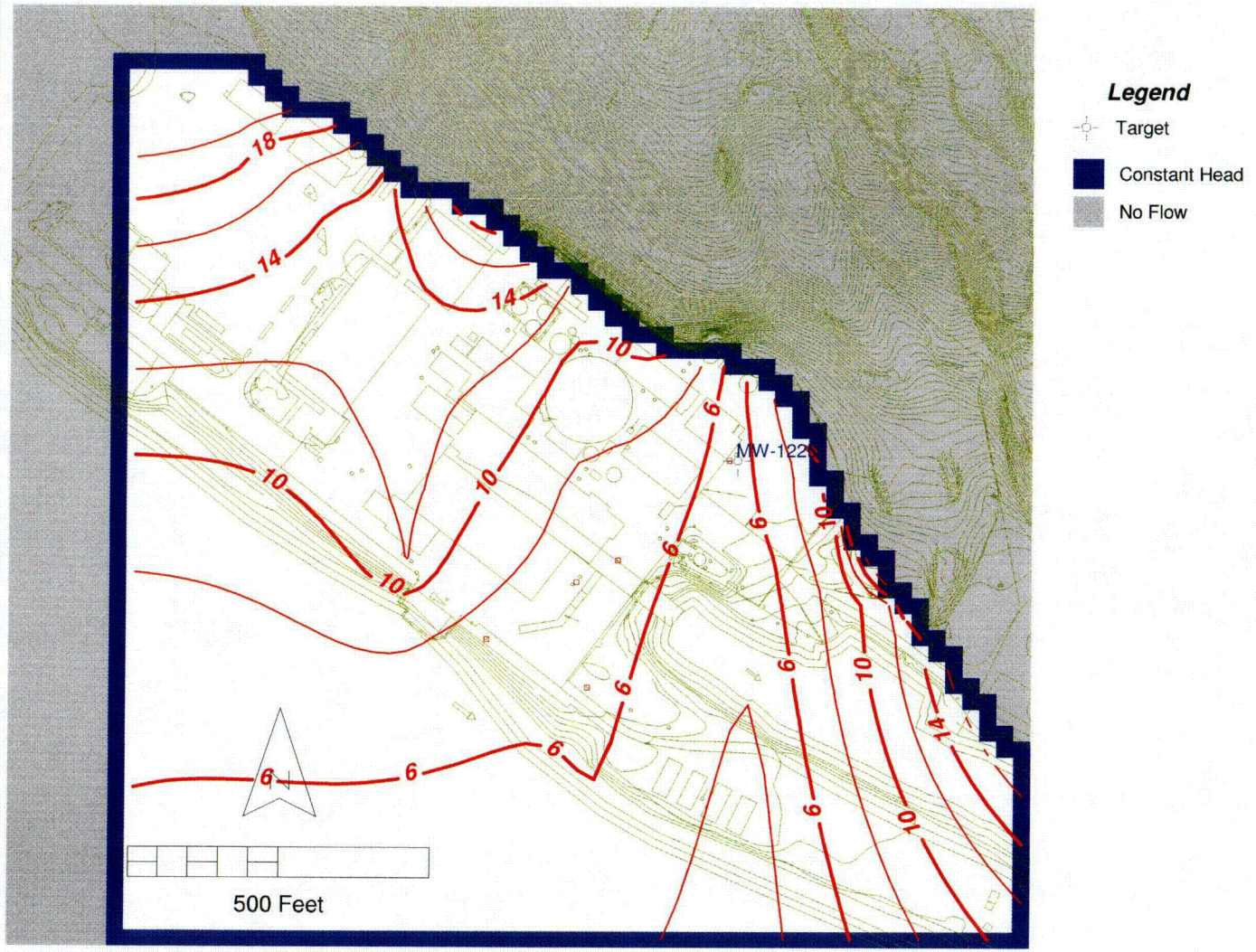

Figure 34--Steady-state operational heads in Model Layer 8--Next to Bottom Rock Layer

CY Groundwater Model

Heads are in feet above NGVD29

8/23/05

STRATEX strategic consulting

C46

CY Groundwater Model

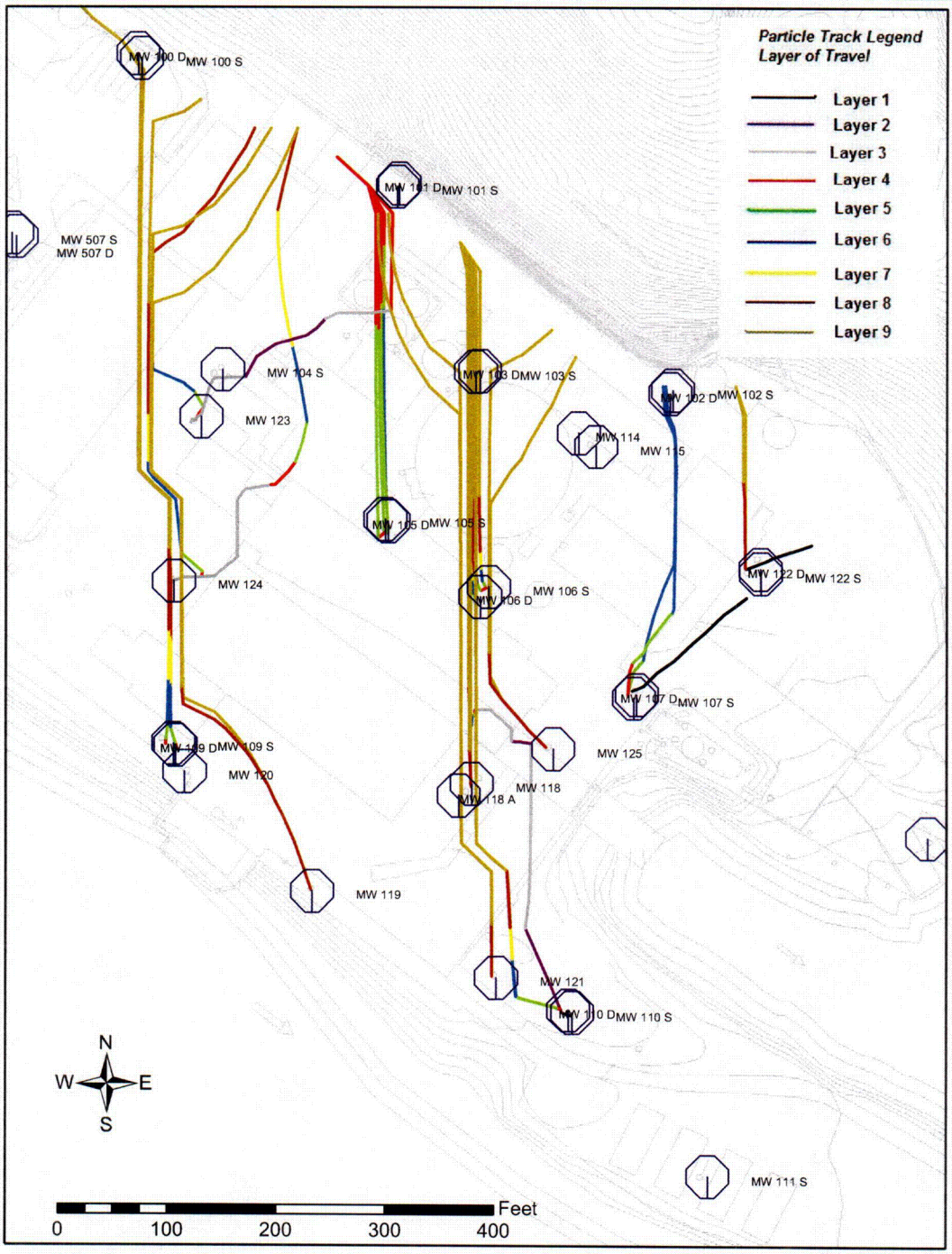

Legend

- Constant Head
- Drain
- General Head Boundary
- Barrier Wall

Reverse Particle Tracking from Major Monitoring Wells in Steady-state Operational Mode

Particles started at 0.1 and 0.9 times depth of layer in which each monitoring well is located

STRATEX
strategic consulting

8/24/05

Figure 35

C47

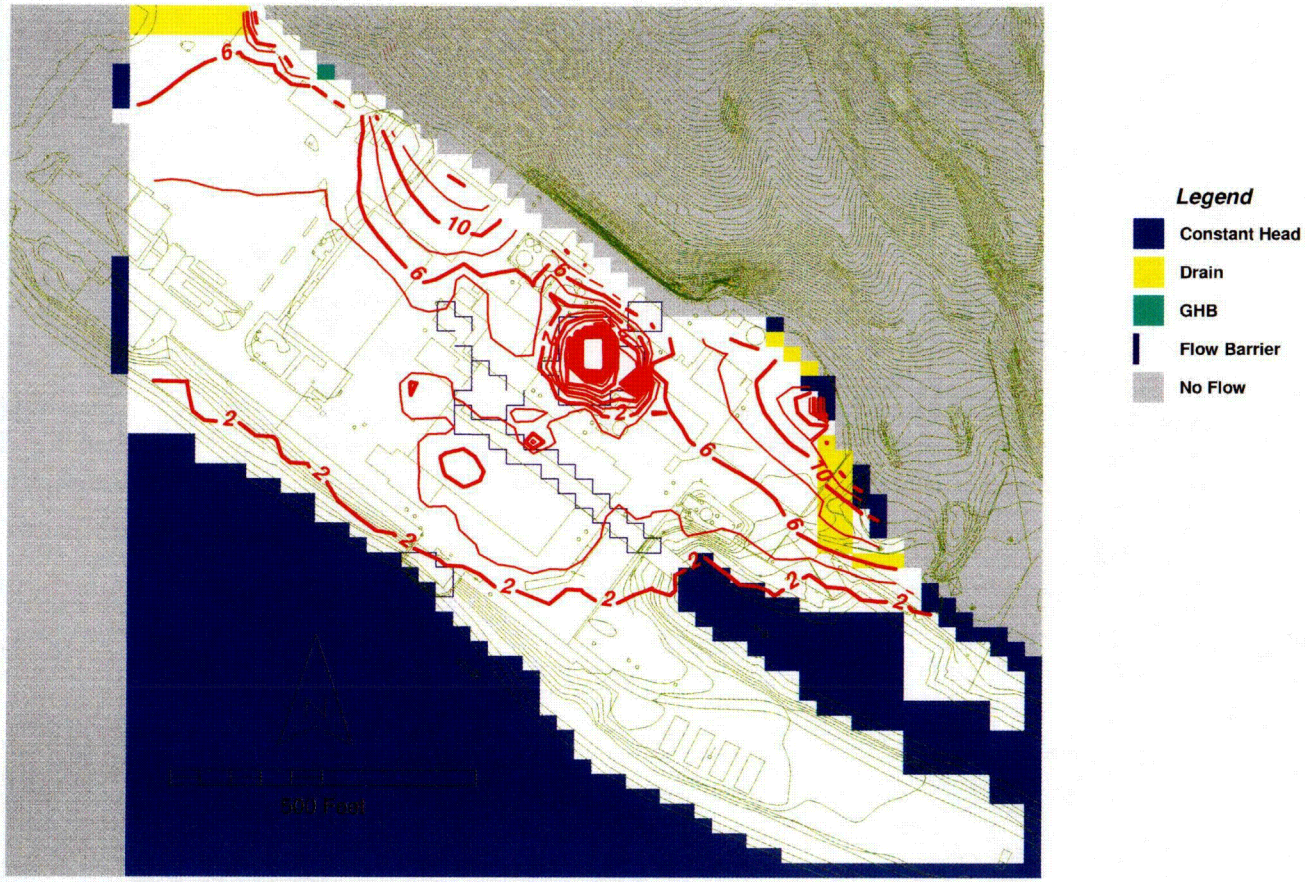

Figure 36--Phreatic contours during maximum dewatering

CY Groundwater Model

Heads are in feet above NGVD29 under average annual recharge conditions

8/24/05

STRATEX strategic consulting

C48

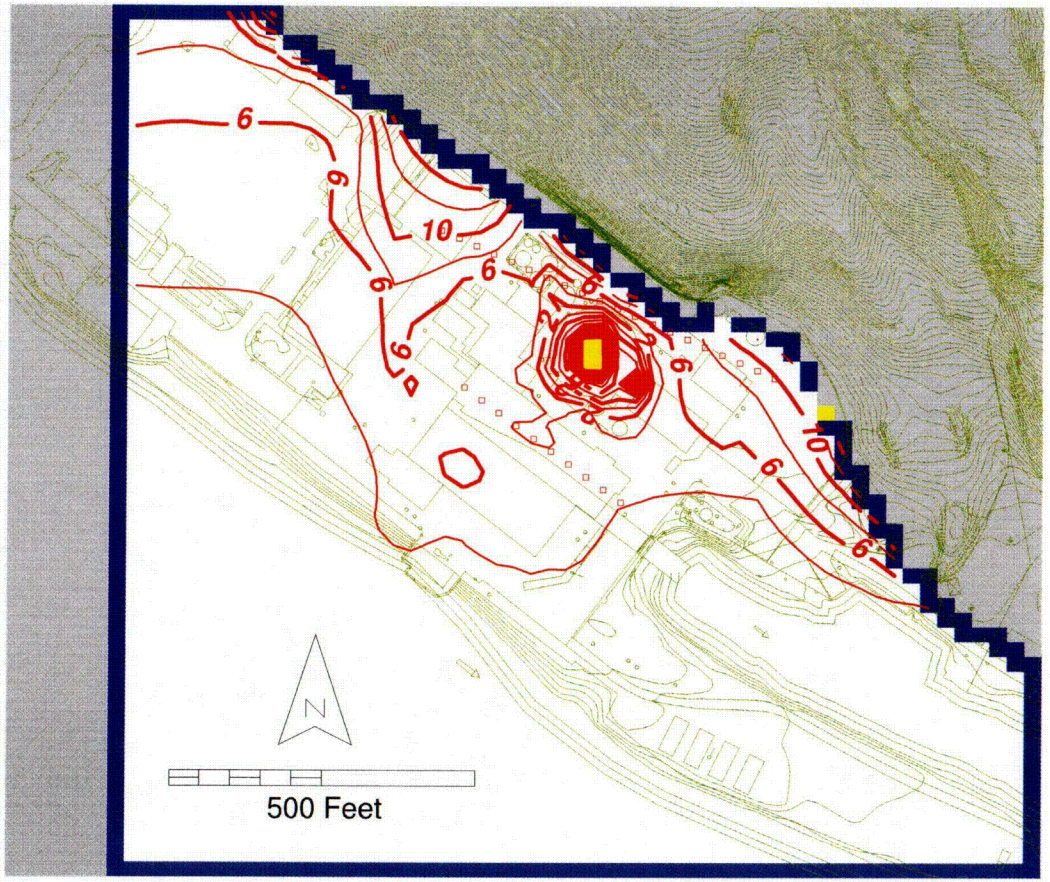

Legend

- Constant Head
- Drain
- No Flow

Figure 37--Head contours in Layer 4 during maximum dewatering

CY Groundwater Model

Heads are in feet above NGVD29 under average annual recharge conditions

8/24/05

STRATEX strategic consulting

C49

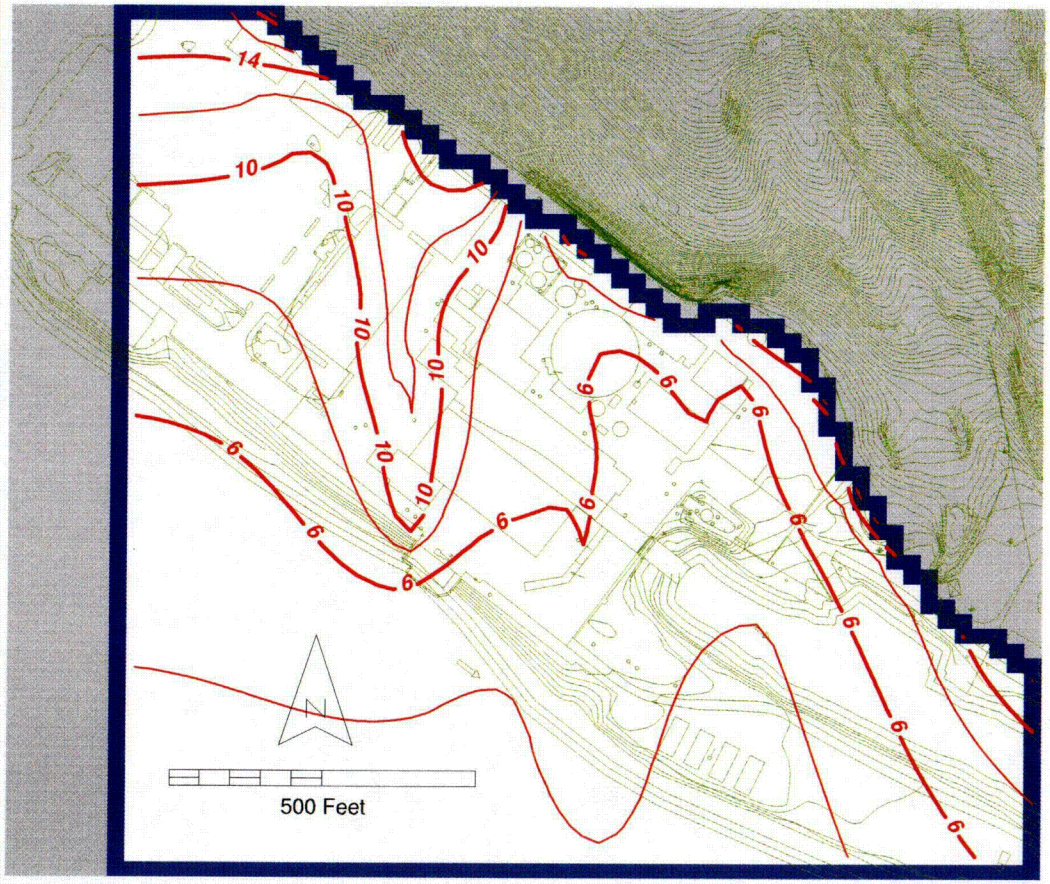

Legend

Constant Head

No Flow

Figure 38--Layer 6 head contours during maximum dewatering

CY Groundwater Model

Heads are in feet above NGVD29 under average annual recharge conditions

8/24/05

STRATEX strategic consulting

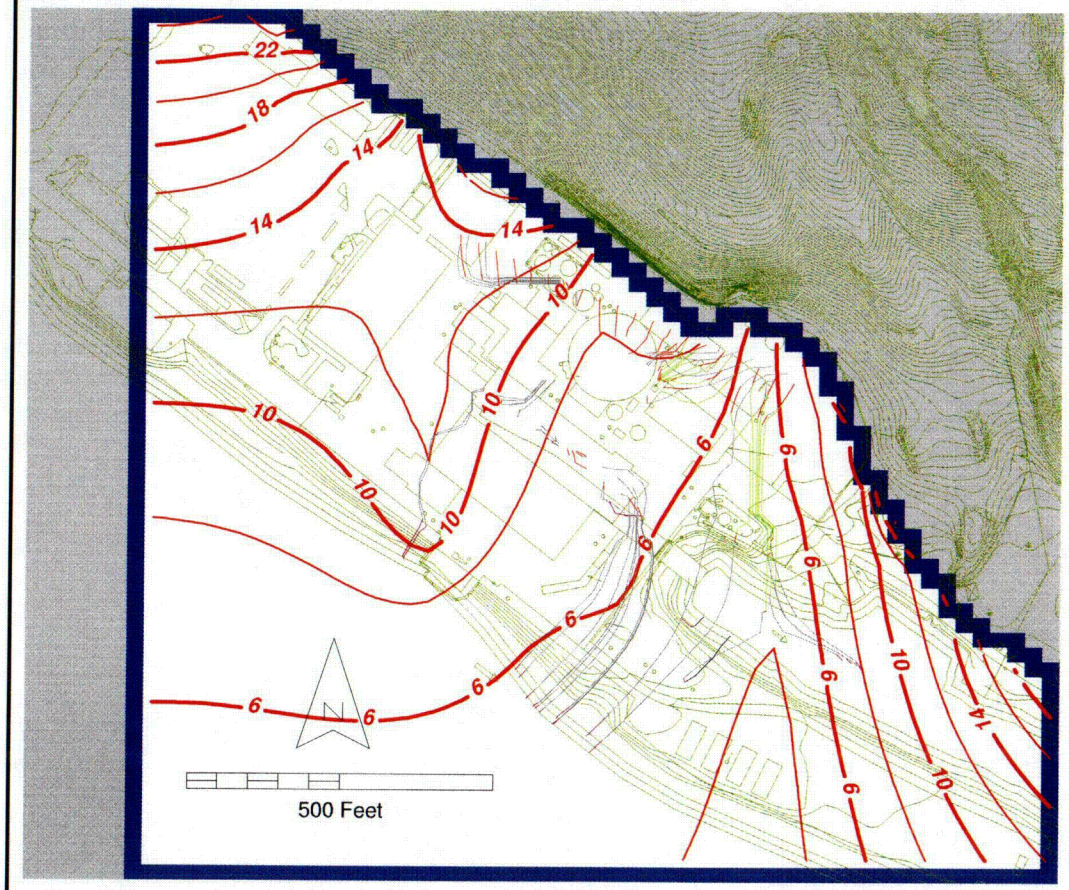

Legend

Constant Head

No Flow

Figure 39--Layer 8 head contours during maximum dewatering

CY Groundwater Model

Heads are in feet above NGVD29 under average annual recharge conditions

8/24/05

STRATEX strategic consulting

C51

CY Groundwater Model

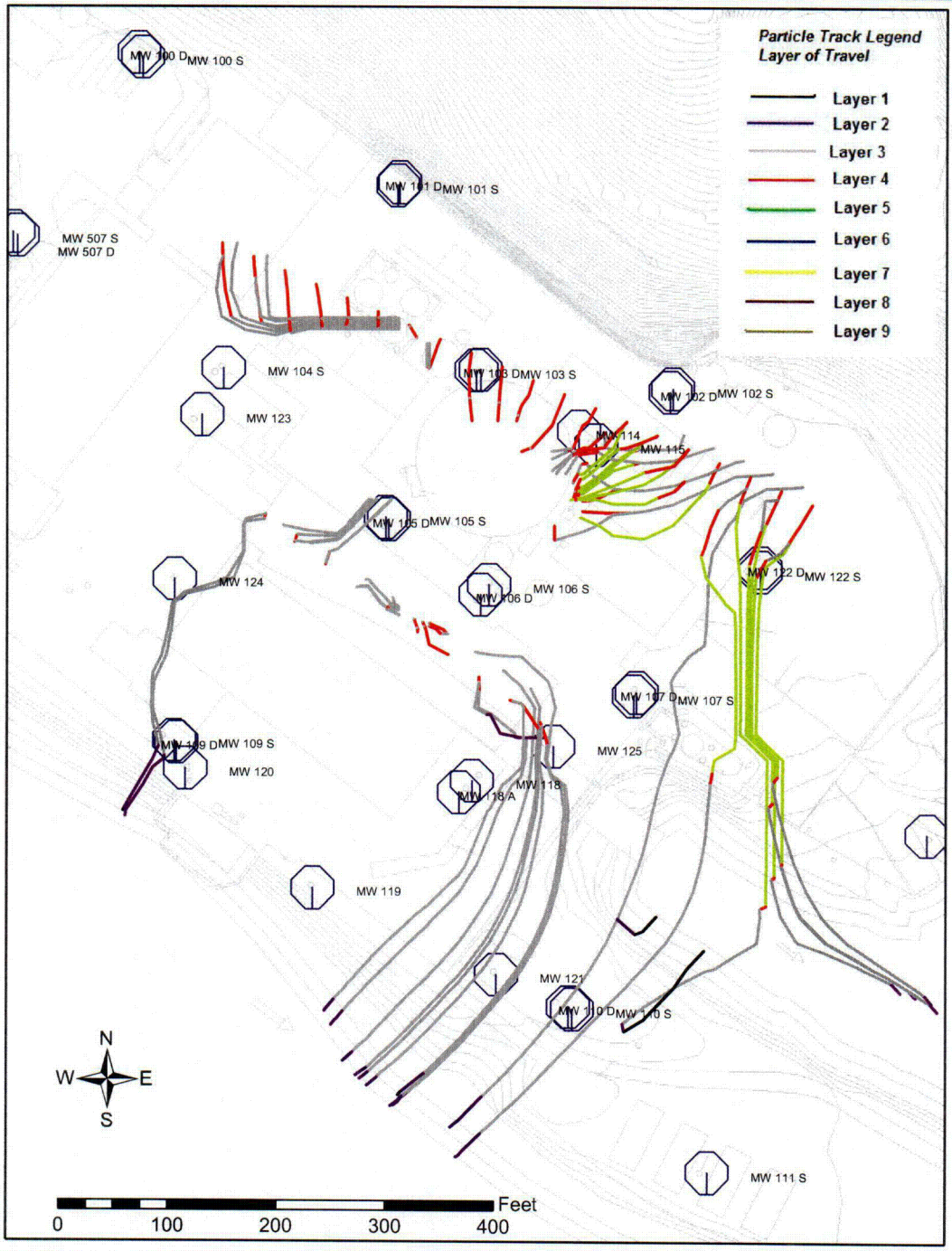

Legend

- Constant Head
- General Head Boundary
- Drain
- Barrier Wall

Forward Particle Tracking from two rows of arbitrary points during maximum dewatering under average annual recharge

Particles started at 0.1 and 0.9 times depth of layer. Particles were started in model layers 3 and 4

STRATEX
strategic consulting

8/24/05

Figure 40

C52

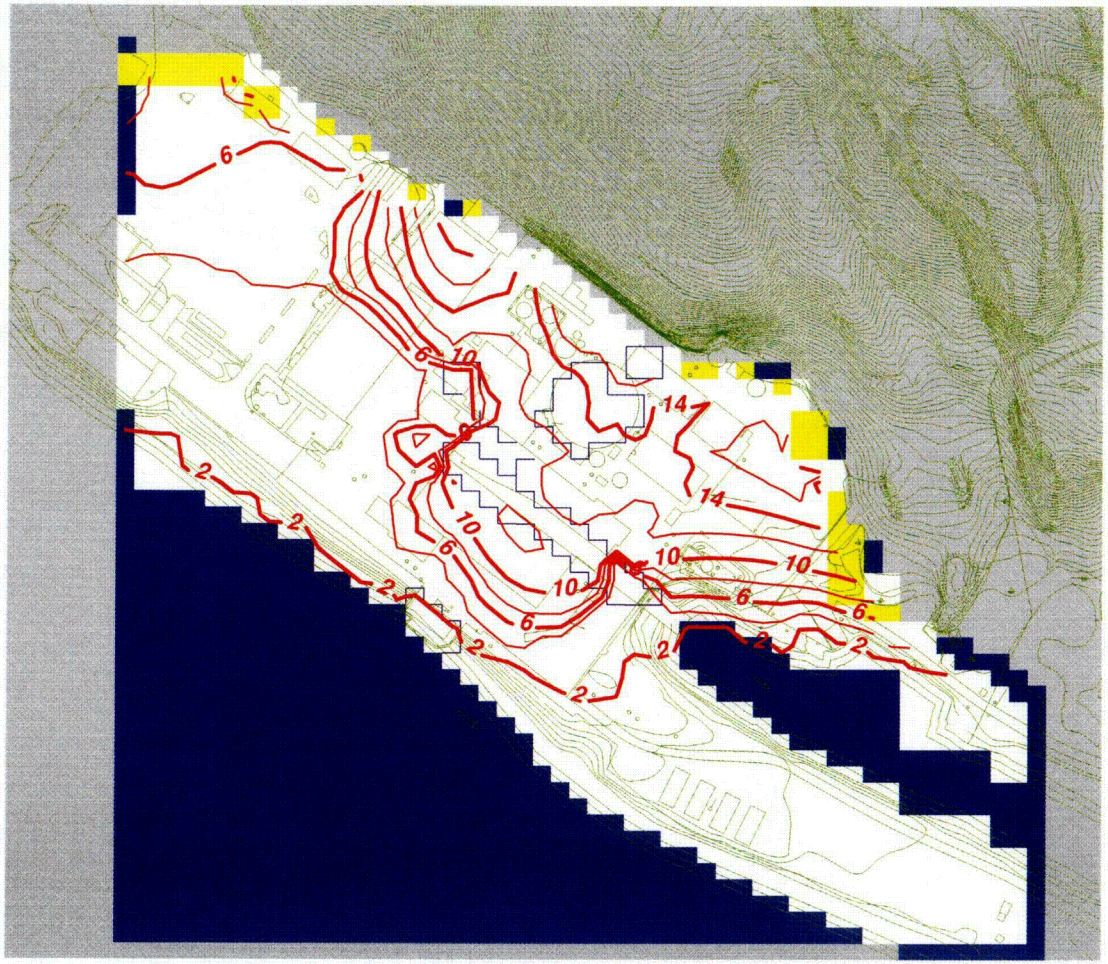

Figure 41--Phreatic contours post demolition

CY Groundwater Model

Heads are in feet above NGVD29 under average annual recharge conditions

8/24/05

STRATEX
strategic consulting

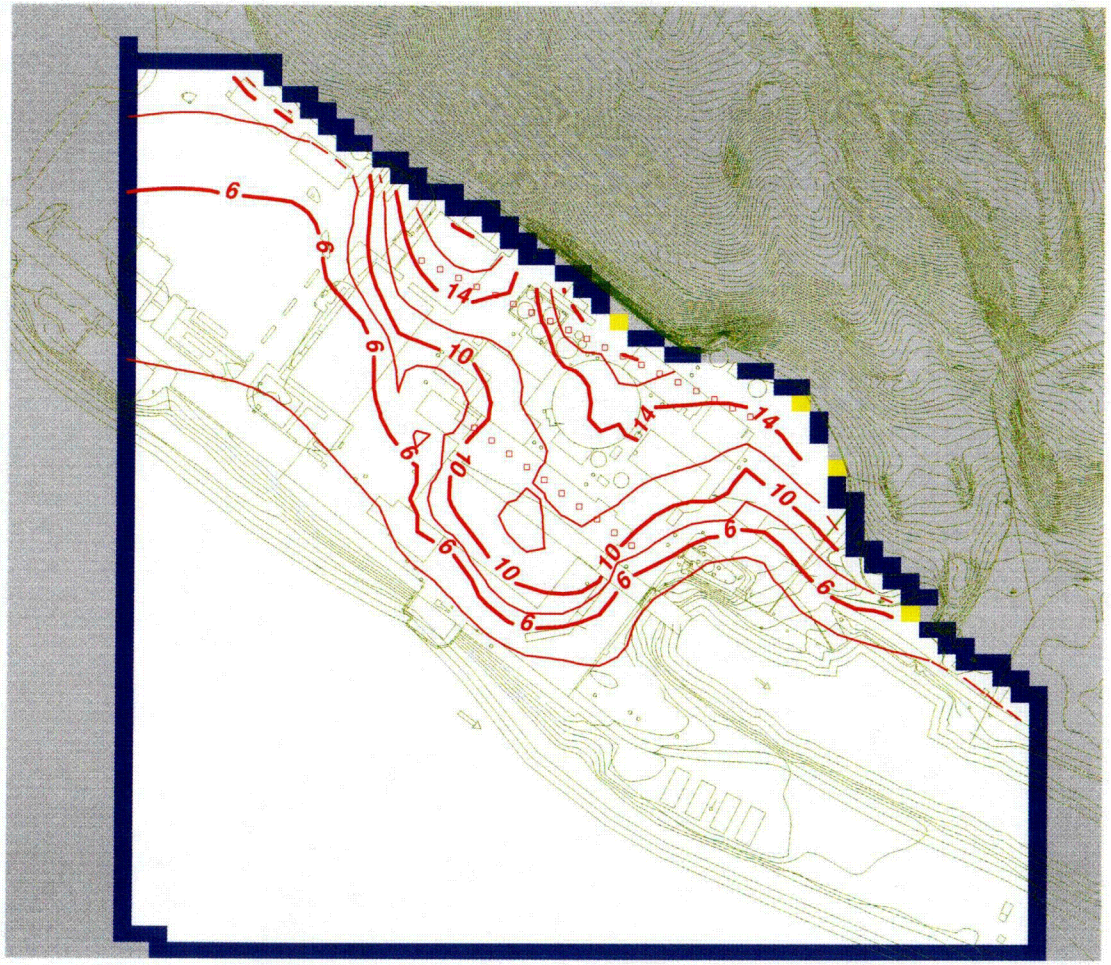

Legend

- Constant Head
- Drain
- GHB
- No Flow

Figure 42--Model Layer 4 groundwater head contours post demolition

CY Groundwater Model

Heads are in feet above NGVD29 under average annual recharge conditions

8/24/05

STRATEX strategic consulting

C54

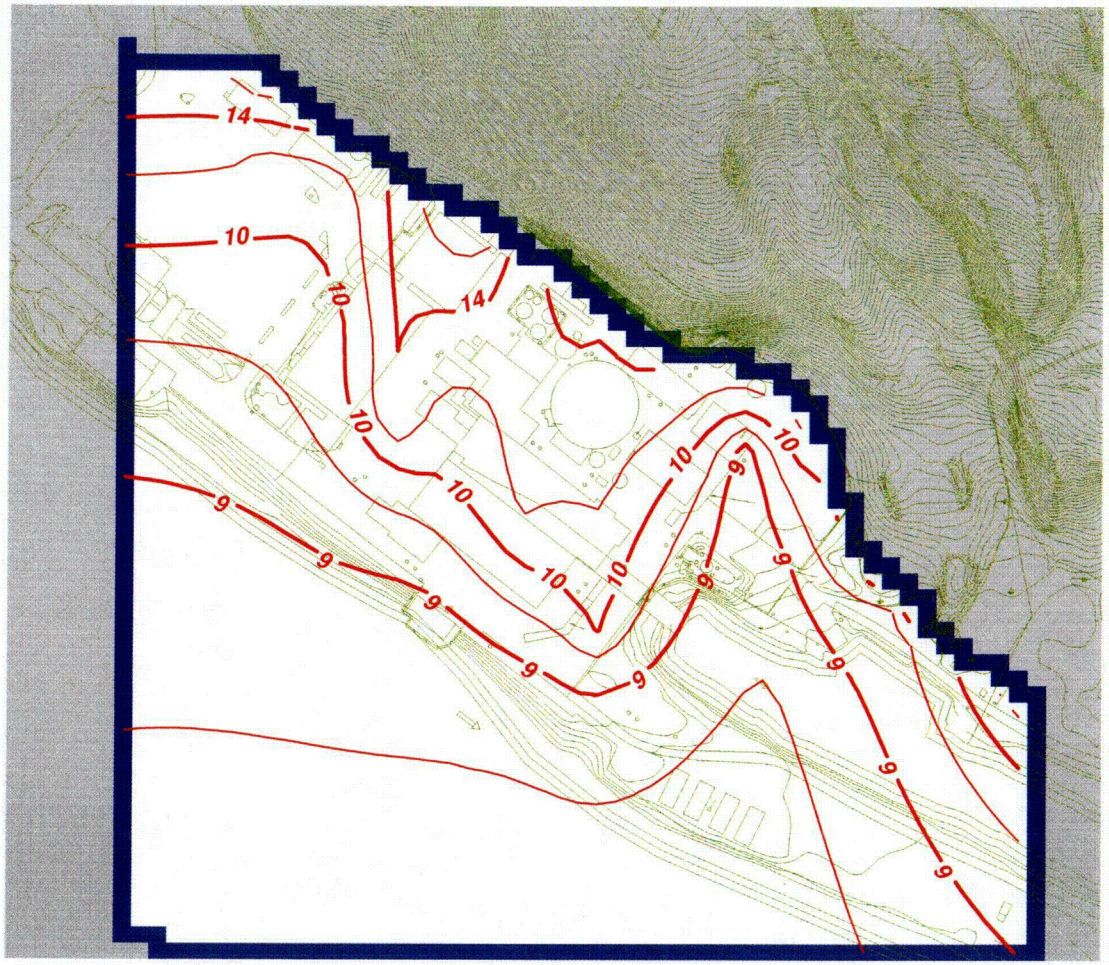

Legend

- Constant Head
- No Flow

Figure 43--Model Layer 6 groundwater head contours post demolition

CY Groundwater Model

Heads are in feet above NGVD29 under average annual recharge conditions

8/24/05

STRATEX strategic consulting

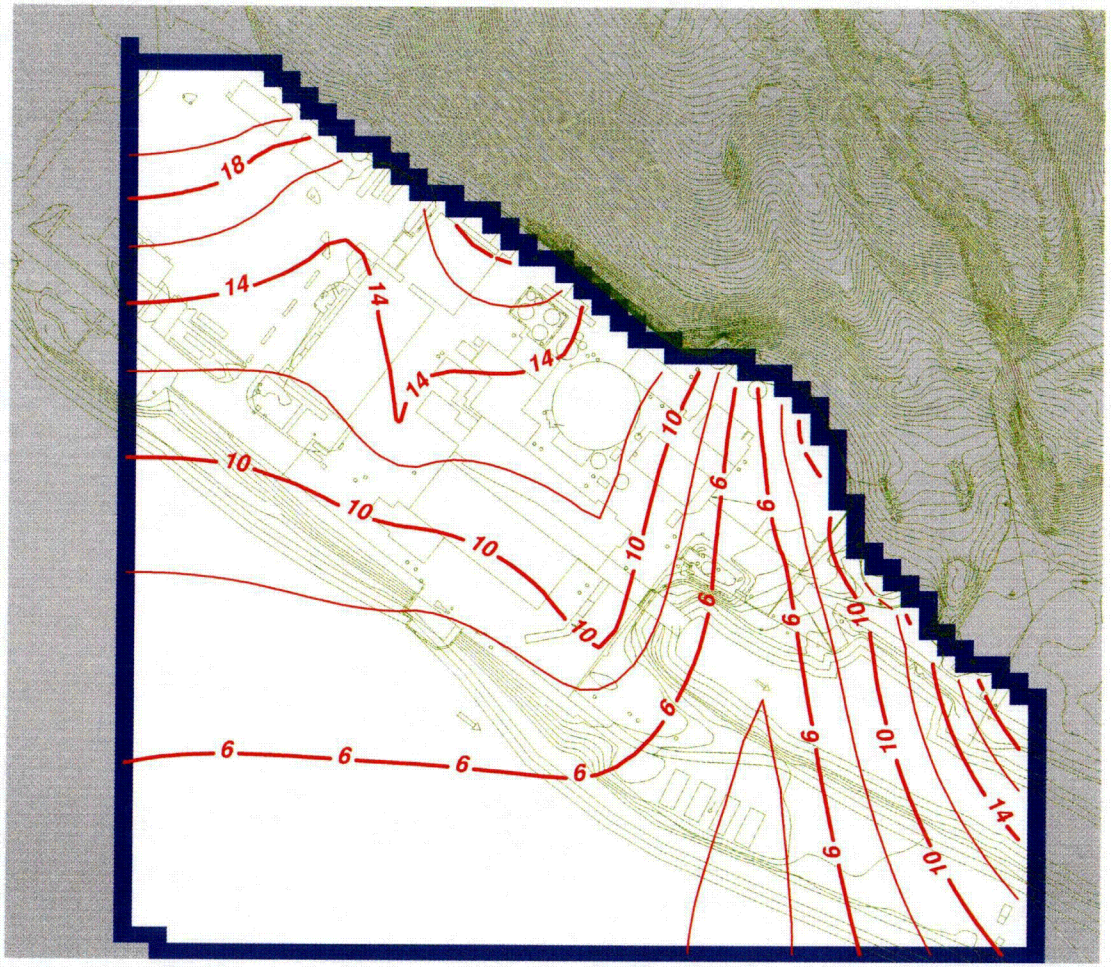

Legend

- Constant Head
- No Flow

Figure 44--Model Layer 8 groundwater head contours post demolition

CY Groundwater Model

Heads are in feet above NGVD29 under average annual recharge conditions

8/24/05

STRATEX strategic consulting

C56

CY Groundwater Model

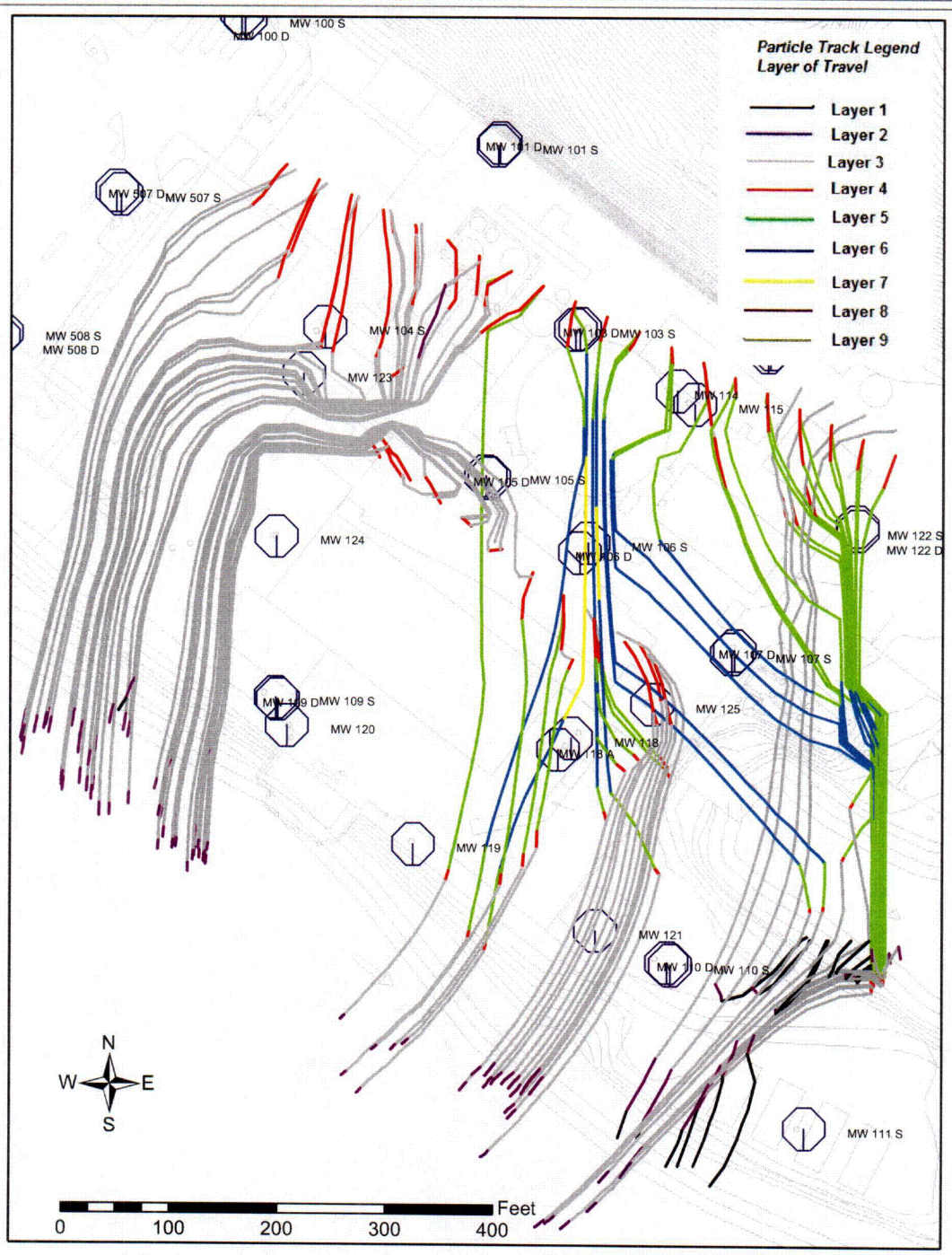

Legend

- Constant Head
- Drain
- General Head Boundary
- Barrier Wall

Forward Particle Tracking from two rows of arbitrary points during post demo conditions under average annual recharge

Particles started at 0.1 and 0.9 times depth of layer. Particles were started in model layers 3 and 4

STRATEX
strategic consulting

8/24/05

Figure 45

C57

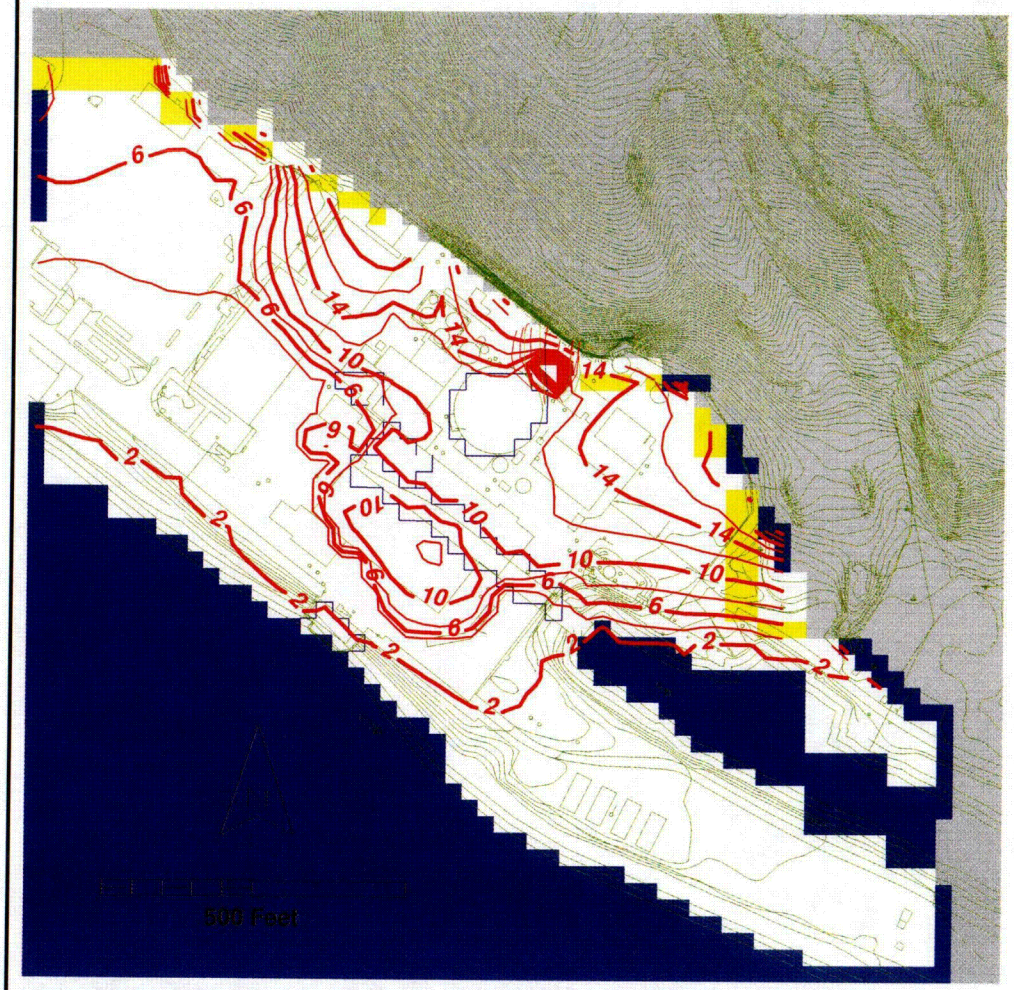

Legend

- Constant Head
- Drain
- Flow Barrier
- No Flow

Figure 46--Phreatic contours 60 days after start of dewatering spent fuel pool in post demo state

CY Groundwater Model

Heads are in feet above NGVD29 starting with average annual conditions

8/24/05

STRATEX strategic consulting

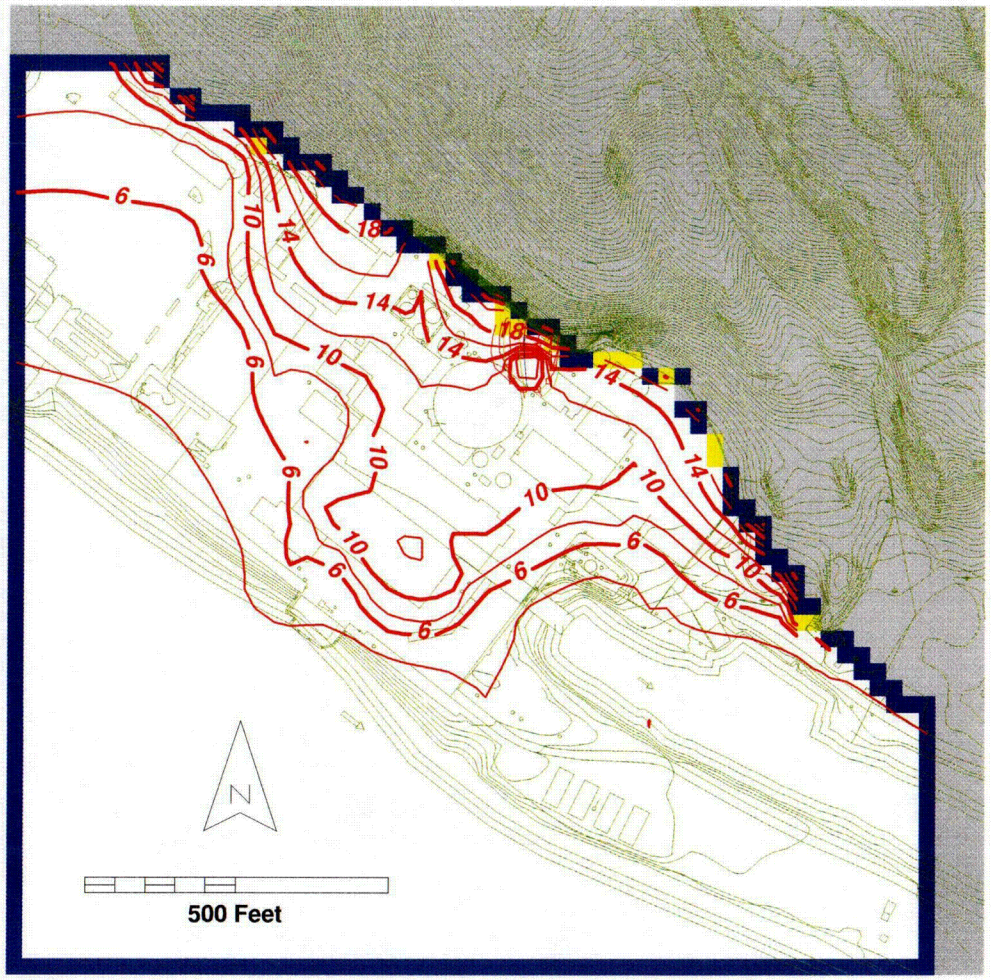

Legend

- Constant Head
- Drain
- GHB
- No Flow

Figure 47--Layer 4 heads 60 days after start of dewatering spent fuel pool in post demo state

CY Groundwater Model

Heads are in feet above NGVD29 starting with average annual conditions

8/24/05

STRATEX strategic consulting

C59

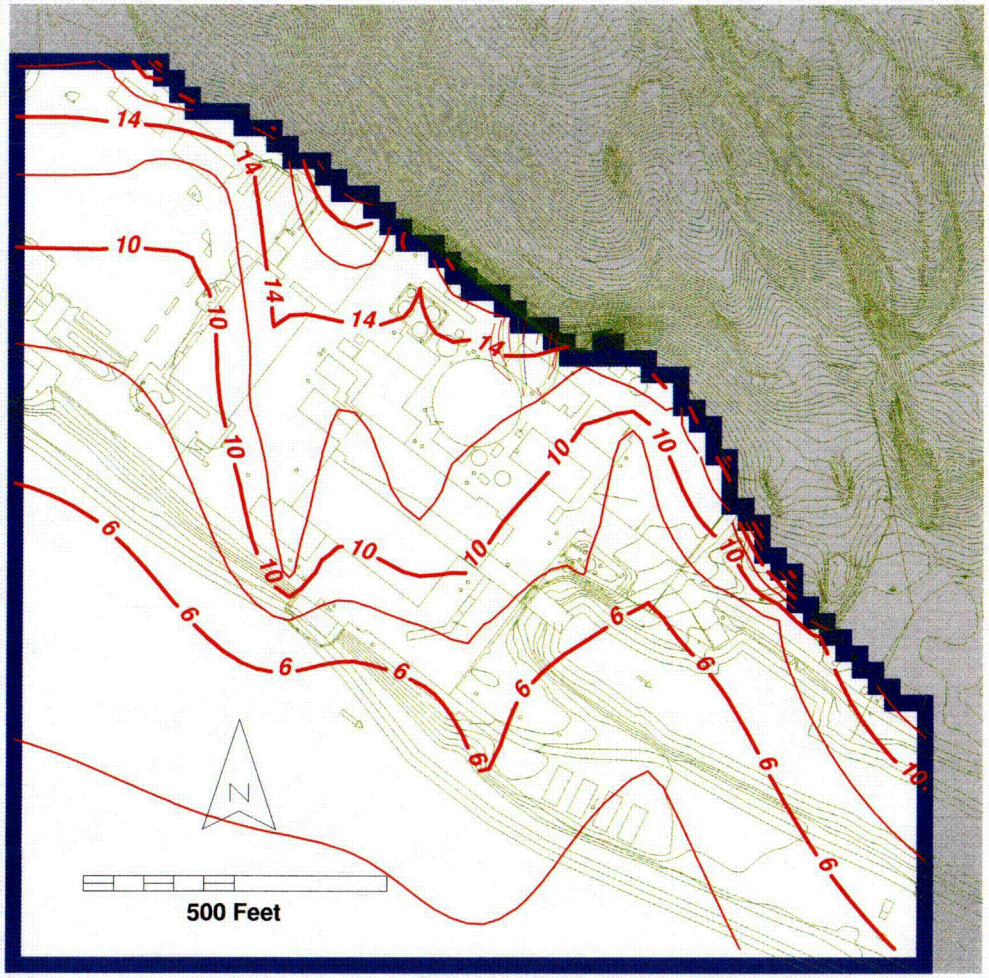

Legend

- Constant Head
- No Flow

Figure 48--Layer 6 heads 60 days after start of dewatering spent fuel pool in post demo state

CY Groundwater Model

Heads are in feet above NGVD29 starting with average annual conditions

8/24/05

STRATEX strategic consulting

C60

CY Groundwater Model

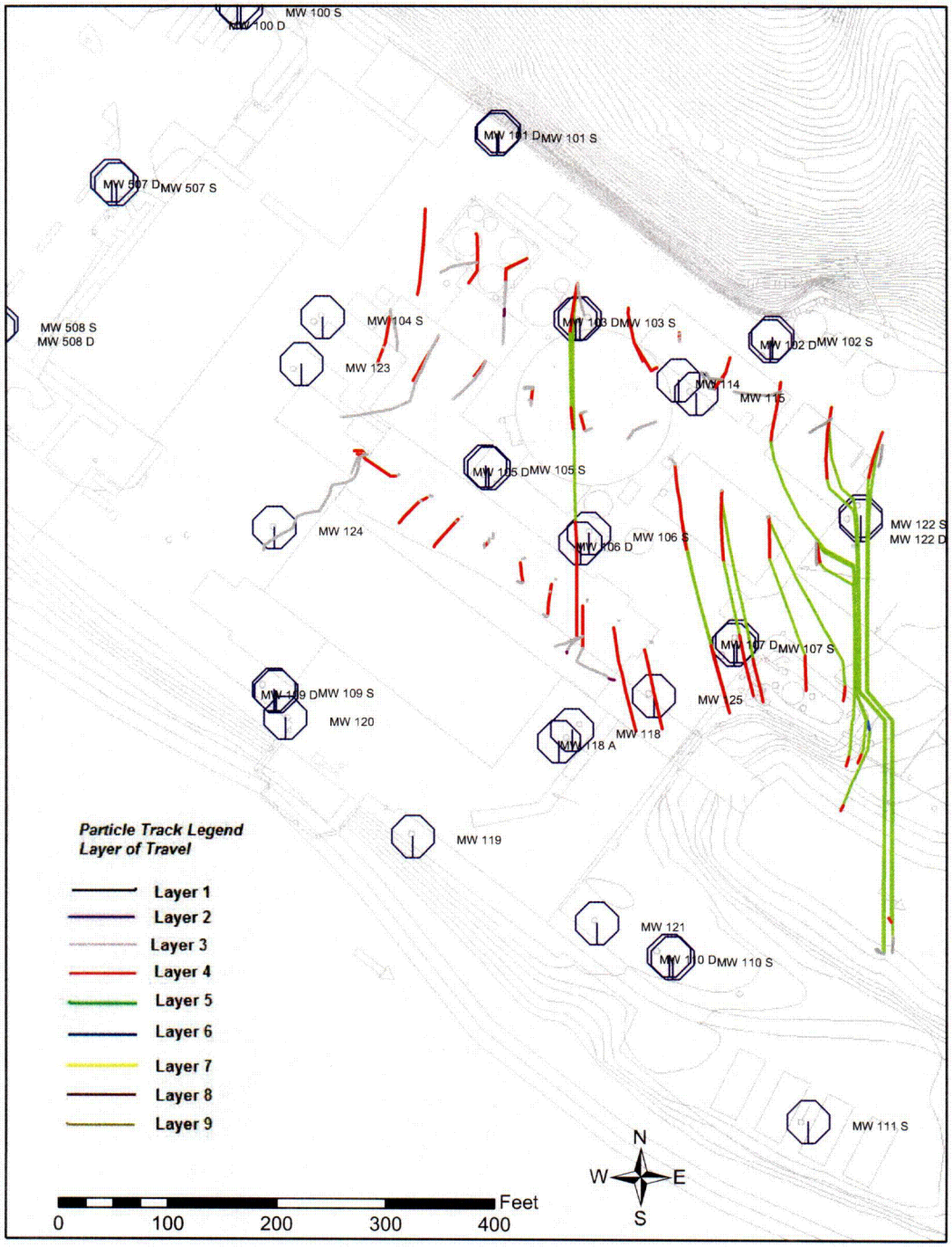

Forward Particle Tracking during simulation of 60 day post-demo dewatering of spent fuel pool to -2' NGVD during post demo conditions under average annual recharge

Particles started at 0.1 and 0.9 times depth of layer. Particles were started in model layers 3 and 4

STRATEX
strategic consulting

Figure 49

8/24/05

C61

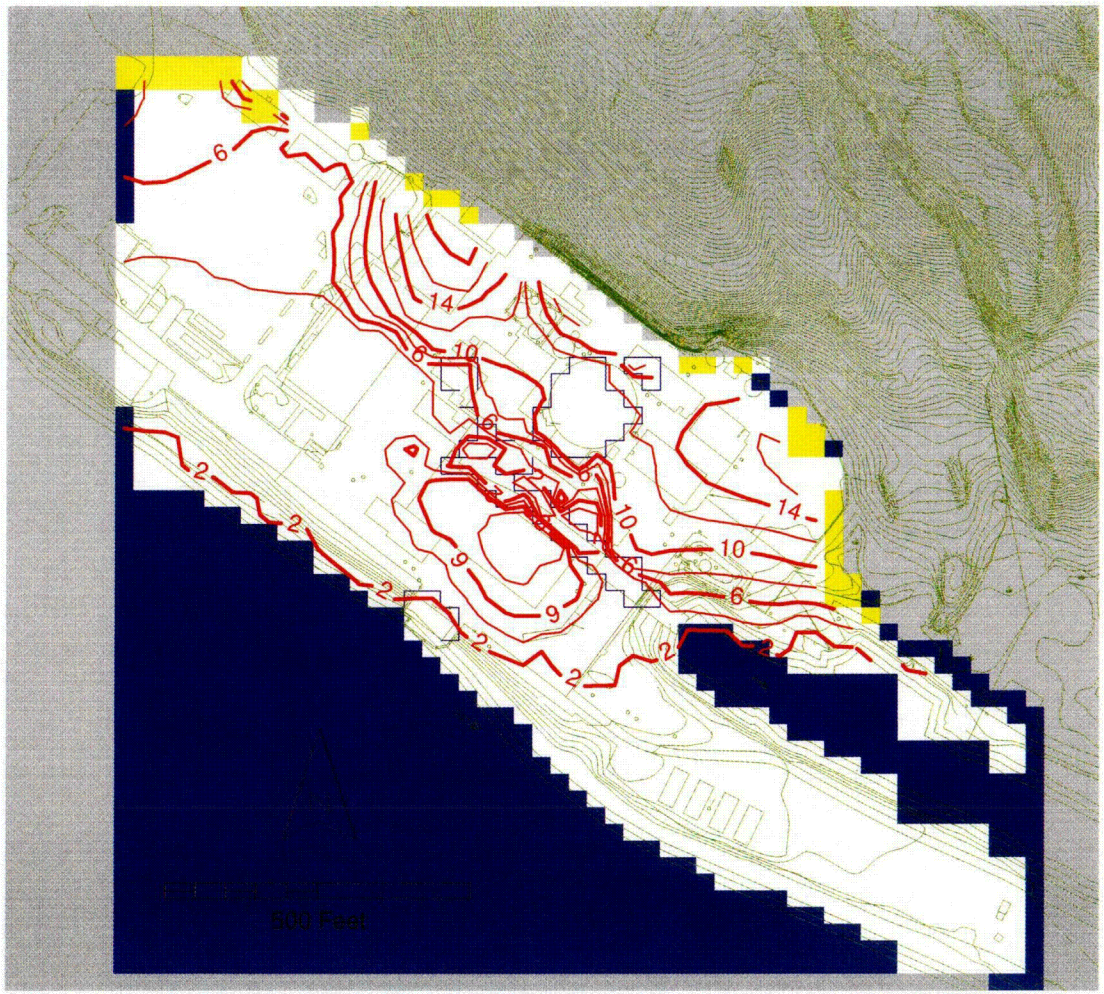

Legend

- Constant Head
- Drain
- Flow Barrier
- No Flow

Figure 50--Phreatic contours 60 days after dewatering north side of discharge tunnel

CY Groundwater Model

Heads are in feet above NGVD29, starting with average annual recharge conditions post demolition

8/24/05

STRATEX strategic consulting

C62

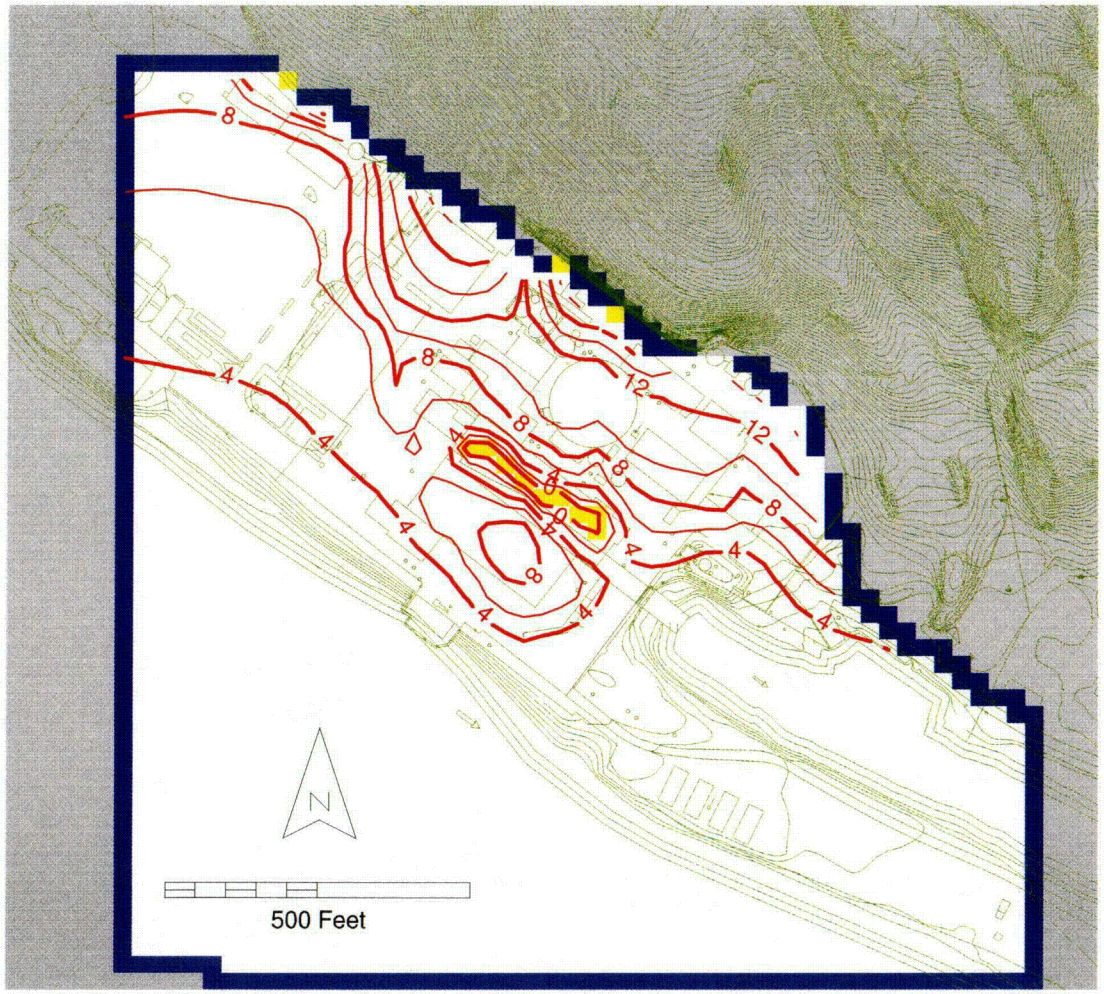

Legend

- Constant Head
- Drain
- No Flow

Figure 51--Layer 4 head contours 60 days after dewatering north side of discharge tunnel

CY Groundwater Model

Heads are in feet above NGVD29, starting with average annual recharge conditions post demolition

8/24/05

STRATEX strategic consulting

C63

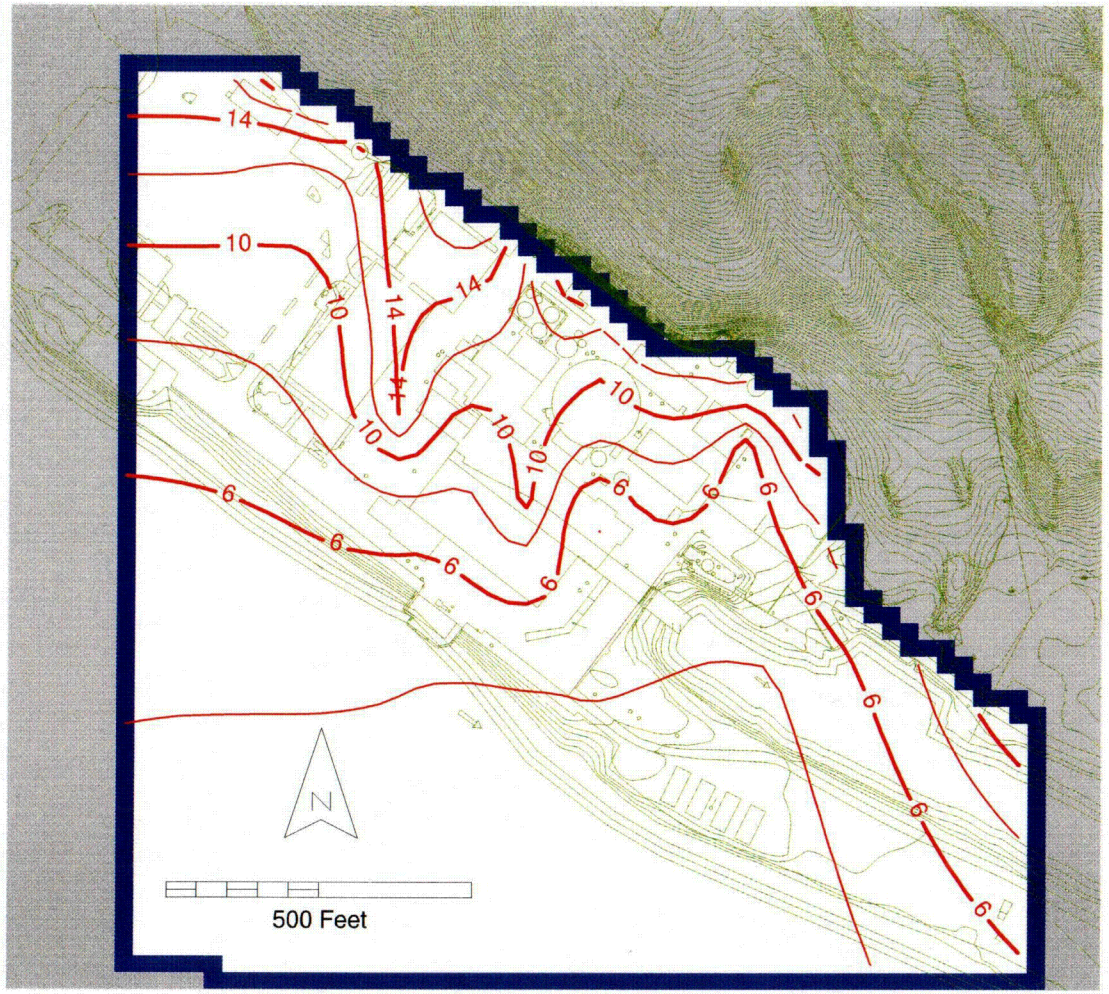

Legend

- Constant Head
- No Flow

Figure 52--Layer 6 head contours 60 days after dewatering north side of discharge tunnel

CY Groundwater Model

Heads are in feet above NGVD29, starting with average annual recharge conditions post demolition

8/24/05

STRATEX strategic consulting

C64

CY Groundwater Model

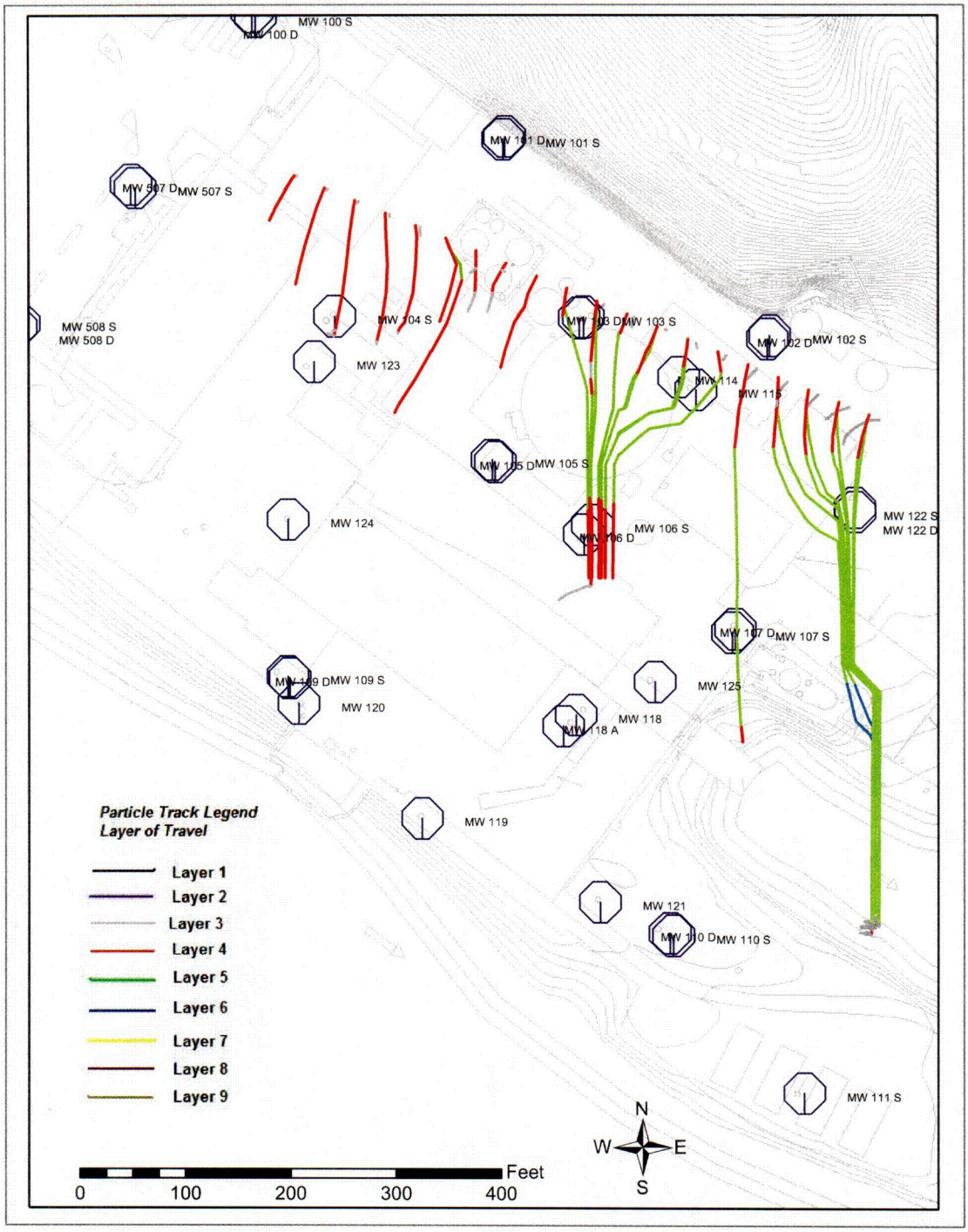

Legend

- Constant Head
- General Head Boundary
- Drain
- Barrier Wall

Forward Particle Tracking for 60 days from start of dewatering north of discharge tunnel during post demo conditions under average annual recharge

Particles started at 0.1 and 0.9 times depth of layer.
Particles were started in model layers 3 and 4

STRATEX
strategic consulting

8/24/05

Figure 53

C65

APPENDIX A

THE APPLICABILITY OF POROUS MEDIA THEORY TO FRACTURED ROCK GROUNDWATER FLOW

Introduction

Scientific methods are advancing rapidly in the field of bedrock groundwater fracture flow theory. The cubic law describes flow in a single fracture and the use of dual porosity theory is common in many problems. Fracture networks can be treated as having orientations, lengths, and fracture widths characterized by statistical distributions that can be sampled in a modeling environment such as with Monte Carlo techniques. The results of analyses such as time-of-first-arrival can be presented in probabilistic terms. However, deterministic porous media theory is presently much more practical for the analysis of typical regional bedrock ground water contamination problems. We have worked on many cases that provide evidence that supports the use of porous media theory in the evaluation of ground water flow and solute transport in fractured crystalline rock terranes[1].

We have found through bedrock pumping tests and site-specific studies of bedrock ground water contamination that porous media theory can usually be used to make reasonable predictions of fate and transport in crystalline fractured bedrock. Most of our experience is in southern Maine which consists of granitic intrusives and metamorphic rock of intermediate to high grade. Ground water flow takes place, for practical purposes, only in fractures formed by foliation, cleavage, joints, and faults. Secondary porosity matrix effects can be neglected in many solute transport problems except where bulk rock permeability is very low and/or contaminants are toxic at very low concentrations. In the latter cases, matrix diffusion may be important but even here the effects can often be approximated with general approaches available in MT3DMS.

New England bedrock fracture networks are often mapped as orthogonal sets with steeply dipping surfaces, simplifying the modeling of bedrock as either an isotropic or horizontally and/or vertically anisotropic aquifer. Because fractures are closely-spaced, we have found in Maine that the majority of drawdown curves from bedrock well pumping tests fit porous media type curves. Porous media theory modeling of site-specific bedrock flow and contamination produces surprisingly good results when applied at the proper scale. Lanter[2] describes the bedrock geology of the Connecticut Yankee site and vicinity. The rock is a crystalline fractured rock very similar to those we have studied in Maine. The fracture patterns are predominantly orthogonal and nearly vertical and horizontal[3], lending themselves to modeling with standard 3-D finite-difference techniques.

---

[1] Gerber, R.G., K.M. Bither, O.P. Muff, 1991, The applicability of porous media theory to fractured rock flow in Maine. NWWA Focus Conference on Eastern Regional Ground Water Issues, Oct. 29-31, Portland, ME, Proceedings

[2] Lanter, S., 2004, General Site Geology of the Connecticut Yankee Haddam Neck Plant. Technical Memorandum 3/13/04

[3] see stereonets and rose diagrams in Appendix C

A Problem of Scale

It was not very long ago that the analysis of flow in fractured rock was considered intractable. In fact the wellhead protection strategies for bedrock wells in many states, including Maine, defined a fixed radius of protection around the well, with no recognition that one might be able to define the true contributing area to the well. In the 1970's, hydrogeologists began to demonstrate success in locating high yield wells using remote sensing techniques. As pumping tests were made on these wells, it became obvious that many well drawdown plots fit the Theis curve or some other theoretical porous media "type" curve. The search for high level nuclear waste repositories spurred research in the 1980's into the hydraulic properties of fractured rocks. Technical papers began to flood the journals on double porosity models, parallel plate flow, and stochastic modeling of bedrock fracture patterns. Meanwhile, the petroleum industry, which had been quite knowledgeable about the subject for years, began to publish their findings in journals read by hydrogeologists. Gringarten's[4] landmark paper "Flow-Test Evaluation of Fractured Reservoirs" showed that much could be learned about fractured bedrock aquifers from a study of pumping test drawdown curves that did not fit the porous media type curves.

The problem for the practicing hydrogeologist is not whether but how to deal with fractured rock flow. The bedrock rarely escapes contamination once the overlying soils are contaminated. Hydrogeologists have become adept at modeling with porous media theory, but double porosity modeling, discrete fracture modeling, and stochastic modeling of fracture systems pose significantly more complexities. A huge and very costly field and laboratory effort is required to define the statistical distributions of the fracture orientations and lengths and aperture widths. It is one thing to do these studies over a cube of rock 100 meters on a side, such as at the Mirror Lake, New Hampshire, test site, but regional models covering large areas, such as the Connecticut Yankee model, may have many different statistical distributions within the model regime. Once the choice is made to use porous media theory models, the question will be how good the approximation is.

In crystalline rocks, such as those present at the Connecticut Yankee site, the major axis of the permeability ellipsoid is often coincident with the strike of the bedding or foliation planes. The fracture spacing commonly ranges from a fraction of an inch to a foot. More widely spaced (one to ten feet) are the joints lying perpendicular to the foliation and the conjugate joint set associated with folded rock. In the intrusive rocks, joints and jointed dikes form the most common avenues of ground water movement. These joints are commonly spaced from a foot to tens of feet apart, except within dikes where the spacing is commonly on the scale of inches. With the exception of shallow sheet jointing, the major joint sets are usually steeply-dipping to vertical. About two-thirds of the high yield bedrock wells in Maine have been found to be associated with fracture zones that can be confirmed by remote sensing techniques. These fracture concentrations are discrete zones of a few tens to a few hundreds of feet in width that must and can be treated as special cases when modeling with porous media theory.

---

[4] Gringarten, A.C., 1982, Flow-test evaluation of fractured reservoirs, in, Recent trends in hydrogeology, ed. by T.N. Narasimhan. Geol. Soc. of Am. Spec. Paper 189, p. 237-264

The problem is to define an appropriate scale at which the porous media approximation is valid. It certainly does not hold at the scale of the individual fracture, nor would it hold if one were trying to simulate the flow pattern in detail in a one-foot wide section of foliated rock. Many investigators (e.g., Hoek[5] and Neuman, et al.[6]) have used the rule of thumb that the scale of averaging should be something on the order of 100 times the average fracture spacing. For rocks like those found at the Connecticut Yankee site, the averaging scale would fall in the range of 10 to 100 feet. Fortunately, for regional groundwater modeling purposes, the typical grid cell width will lie within these ranges. For discrete fracture zones, which usually are linear and have a finite length on the scale of a few hundreds of feet, one can model these zones as a heterogeneity lying within what otherwise might be a more homogeneous rock mass for purposes of hydraulic analysis.

It should be noted that the presence of fractures does not insure ground water flow along those fractures. They must be sufficiently connected. The density of fractures among which enough intersections exist for flow to occur has been called the "percolation threshold" (de Marsily[7]). Whether the percolation threshold has been reached can be determined by several different approaches. One approach is to relate the average number of intersections of a single fracture with other fractures. Another evaluation of the threshold can be calculated by multiplying the density of fractures (plan-view) by the average length squared. Degree of randomness in orientation is important in interpreting these calculations. Although the science of fractal geometry seems to indicate that bedrock fractures can be described as a fractal process, the degree of connectivity has to be determined for each separate class of fractures independently. Our observation has been that most Maine bedrock has sufficiently connected fractures at the scale of hundreds to thousands of feet for porous media theory to apply. The Connecticut Yankee site and model area seem to be no different from our Maine experience.

Equivalent Porous Media Transmissivity and Porosity

Assuming one can use porous media approximations to work on a certain averaging scale with bedrock aquifers, how does one choose the important parameters of transmissivity and effective porosity? Choosing an equivalent porous media transmissivity is not too difficult. Bedrock pumping tests are one means of stressing a volume of rock on the scale of the averaging scale. Inverse modeling--back-calculating of transmissivity to match simulated with observed potentiometric elevations--is also a reasonable approach. Discrete fracture zones can produce tens to hundreds of gallons per minute (gpm) well yield and typically have transmissivities ranging from 25 to several thousand square feet

[5] Hoek, E., 1976, Rock slopes, in, Rock engineering for foundations and slopes, Proc. of Specialty Conf., Am. Soc. of Civil Engr., Univ. of Colorado, Boulder, Colorado, August 15-18, 1976, Vol. 11, p. 157-171

[6] Neuman, S.P., E.S. Simpson, P.A. Hsieh, J.W. Jones, C.L. Winter, 1985, Statistical analysis of hydraulic test data from fractured crystalline rock near Oracle, Arizona, in, Hydrogeology of rocks of low permeability. IAH Memoires, Vol. XVII, Part 1 Proc., Tucson, Arizona, Congress, p. 289-300

[7] Marsily, G. de, 1985, Flow and transport in fractured rocks: connectivity and scale effect, in, Hydrogeology of rocks of low permeability. IAH Memoires, Vol. XVII, Part 1 Proc., Tucson, Arizona, Congress, p. 267-277

per day. More typical rock yields one-quarter to 10 gpm and has a transmissivity of 1 to 25 square feet per day.

Estimating equivalent porous media effective porosity is a more difficult task. Typical bedrock fracture aperture widths lie in the 10 to 50 micron range below a typical depth of weathering, which may range from 10 to 50 feet in New England. If one can measure the density and aperture width distribution of fractures, there are theoretical methods of estimating porosity. However, not many studies will be sufficiently funded to be able to take this approach. Furthermore, it has been observed that the flow of water into a well is not related to fracture density over wide areas, so calculations relying on fracture density and aperture width might overstate the effective porosity.

We are not interested in being able to calculate the velocity of transport along a single fracture, but rather the average velocity along the theoretically equivalent porous media flowline. Therefore, the true secondary porosity of the fracture system may not resemble the one we need for our porous media approximations. Endo and Witherspoon[8] found that when there is a narrow distribution (small standard deviation) of fracture aperture widths, a theoretical fracture flow system behaves like an equivalent porous medium with the hydraulic effective porosity being slightly less than the total porosity. When the standard deviation of the aperture width is large, the hydraulic effective porosity becomes directionally dependent and larger than the total porosity.

There is usually a change of both permeability and porosity as a function of depth in bedrock. A three-dimensional porous media modeling approach can take this into account. The first major change in New England crystalline rock is at a depth of between 20 and 50 feet below the top of rock. This is the typical limit of the weathered zone. Both permeability and porosity will be higher in this zone than at deeper depths. Below about 50 feet, there may be a gradual decrease in permeability with depth as shown in Figure 3 of Neretnieks[9]. Aperture width appears to decrease with increasing normal stress and fracture lengths and densities decrease with depth. However, it is not uncommon to find high permeability fracture zones at great depth where the permeability of the adjacent fractured rock is otherwise low. In Maine our experience is limited to depths of about 1000 feet. For depths to at least 700 feet below top of rock, well yield per foot of drilling is more or less constant with depth below the weathered zone.

Equivalent Porous Media Permeability Anisotropy

It appears that anisotropy is a common feature of bedrock aquifers. It is theoretically possible to calculate the magnitude and orientation of the 3 orthogonal axes of the permeability ellipsoid. It has been shown that even if there are 3 or more sets of fractures that are not necessarily orthogonal, this permeability ellipsoid can be calculated. In some

[8] Endo, H.K. and P.A. Witherspoon, 1985, Mechanical transport and porous media equivalence in anisotropic fracture networks, in, Hydrogeology of rocks of low permeability. IAH Memoires, Vol. XVII, Part 2 Proc., Tucson, Arizona, Congress, p. 527-537

[9] Neretnieks, 1., 1985, Transport in fractured rocks, in, Hydrogeology of rocks of low permeability. IAH Memoires, Vol. XVII, Part 1 Proc., Tucson, Arizona, Congress, p.301-318

rocks the major axis of this ellipsoid will lie along the line formed by the intersections of two or more fracture planes. Fortunately, the primary fracture sets usually have a vertical or near-vertical dip and are often orthogonal. This leaves us with possible anisotropy, however, in horizontal plane. In addition to field mapping of fracture patterns, density, and lengths, pumping tests, tracer studies, and directional electrical resistivity surveys can often characterize the anisotropy. Sometimes the bulk anisotropy is due more to discrete high-yield fracture zones rather than anisotropy in the bulk rock matrix due to cleavage or foliation.

In foliated metamorphic rocks such as at Connecticut Yankee, joints perpendicular to foliation strike might be 10 to 100 times farther apart than individual foliation planes. Furthermore, the cross joints are often quite short (less than 10 feet). In this case, we might assume that the rock is highly anisotropic with the primary permeability along the plane of the foliation.

Summary

When the proper averaging scale is chosen, many crystalline fractured bedrock aquifer flow problems can be evaluated with porous media approaches. This is particularly true when the primary fracture planes are orthogonal and vertical or steeply-dipping as at Connecticut Yankee. Significant horizontal sheet joints (such as those that connect B-119, B-118, MW-109D and MW-110D at about 85 feet depth) can also be simulated with thin horizontal layers having higher than average transmissivity. Heterogeneities such as discrete high-yield fracture zones can be treated as such in the same fashion as heterogeneities are treated in porous media models. Several narrow linear zones of higher than average transmissivity have been used in the CY groundwater model. The appropriate averaging scale is on the order of 100 times the typical fracture spacing. For foliated rocks, model grid cells that are from 10 to 100 feet across would be appropriate.

Modeling of the CY site and vicinity has been reasonably successful in matching recession following recharge, responses to pumping, and responses to the rise and fall of the tide in the Connecticut River. The direction of movement predicted by particle tracking and solute transport modeling also seems to follow paths documented by water testing in the monitoring well network. Given the ability to reproduce these historical events, it is reasonable to assume that the model will have some predictive ability to evaluate future flow and transport.

Appendix B
Determination of River Elevations to Simulate May and September Groundwater Response to River Elevations
CY Groundwater Model

Tidal Fluctuations at the Site

Tidal fluctuation in the Connecticut River has been measured at the HNP site during a portion of 2004 using a data logger placed on the remains of the former pier at the site. Unfortunately, the vertical datum of the data logger is in question due to stretch in the transducer cable, uncertainty about the surveyed reference elevation at the pier, pier movement, and other potential sources of error. For purposes of calibrating the site groundwater model, it was necessary to define an accurate record of river fluctuation during a period in mid-May 2004 and a period in mid-September 2004. The raw data of the data logger (after correction for barometric pressure)[1] were used to establish the timing and magnitude of the sine curve defining the tidal fluctuation. Detailed analysis of predicted versus actual tidal fluctuations were made for the New London NOAA continuous tidal station. We also analyzed NOAA tidal index station predictions for Hartford, Haddam, and New London for the two periods of interest. A NOAA benchmark at Higganum Creek[2] on the Connecticut River was studied to relate tidal parameters such as mean sea level, mean tide level, mean low water and mean high water to NGVD 29. Finally, discharge flow in the Connecticut River was evaluated based on the Hartford USGS river flow gaging station site to evaluate tidal fluctuation at the Haddam Nuclear Plant (HNP) in relation to gaging station height at Hartford.

The graphic[3] on Figure B-1 is taken from the tidal benchmark on the Connecticut River at Higganum Creek. NGVD 29 at this tidal benchmark is 1.31 feet below the Mean Tide Level. NAVD88 is about 0.34' below MTL. Even without detailed analysis of other data, this indicates that the mean tide level at the site, without taking into account river flow, should be about 1.3 feet NGVD 29. Figure B-2 shows the NOAA predicted tide[4] at Haddam (all figures based on Eastern Standard Time, unless otherwise noted) on the Connecticut River for 2004, with a superimposed 15-day moving average of the high and low tides. The average of all highs and lows is 1.41' or 1.45' NGVD 29.

Figure B-3 shows the reported barometrically-corrected transducer data for the Connecticut River at the HNP dock compared with the gaged river height at Hartford[5]. Both data sets are reportedly referenced to NGVD 29. The HNP data are based on a 12-hour moving average of 5-minute interval measurements then data "sieved" to take only one value of the moving

---

[1] CYAPCo, 2004, Task 2 Supplemental Characterization Report, App. 6, *and*, CYAPCo, 2005, Semi-Annual Groundwater Monitoring Report, Third and Fourth Quarter 2004, Quarterly Sampling Events

[2] http://www.co-ops.nos.noaa.gov/benchmarks/8463836.html. The location where detailed tidal measurements were made over the 4- month period June 1987-September 1987 to calculate tidal constants and enable future predictions against the New London tide predictions.

[3] http://www.ngs.noaa.gov/cgi-bin/ngs_opsd.prl, Station ID 8463827

[4] http://www.co-ops.nos.noaa.gov/cgi-bin/get_pred.cgi?year=2004&stn=2555+New+London&secstn=Connecticut+River,+Haddam&thh=%2b2&thm=48&tlh=%2b3&tlm=8&hh=*0.97&hl=*0.95

[5] http://nwis.waterdata.usgs.gov/ct/nwis/discharge/?site_no=01190070

average per day for plotting purposes. Regardless of whether the HNP tidal values are correct in an absolute sense relative to NGVD 29, the chart shows that tidal levels at HNP do not rise above normal tidal fluctuation range (which would be the range within which the NOAA tide table predictions would be reasonably accurate) until the Connecticut River level at the Hartford gaging station rises above about 4 feet NGVD 29. The two periods of interest to the groundwater modeling calibration effort included several days in mid-May and several days in mid-September when the Hartford gaging station was generally below the 4' NGVD 29 height. Therefore, our evaluation of tidal fluctuation in these periods should be relatively un-influenced by River discharge rate.

Figure B-4 is a comparison of actual versus measured tidal fluctuation[6] at the New London Tide Gage on Long Island Sound, east of the Connecticut River, for the middle of May 2004. Note that for the period of interest the tide level was less than the predicted tide by 0.2' to 0.5'.

For Haddam, Figure B-5 shows the predicted tide versus the reported tide at the HNP dock. Notice that the measured tide is shown to be about 1.5 to 1.8 feet less than the predicted tide at that date and time. This is much more than the difference at the New London Tide Gage between predicted and measured tide there during that time.

Figure B-6 is a copy of the portion of the NOAA tide charts[7] for New London and the Connecticut River. Figure B-7 is additional NOAA tide prediction information for Haddam compared to the New London reference station. This shows that high tide is 2 hours and 48 minutes later at Haddam and low tide is 3 hours and 8 minutes later at Haddam than at New London. Figure B-8 shows the actual New London Tide measurements superimposed on Figure B-5. Notice that although the lag between low tide at New London and low tide at HNP is usually more than 3 hours, the lag between high tides is often in the range of only 2 hours.

A comparison of the actual New London Tide range for the mid-May 2004 period of interest with the measured HNP tide range shows that the average ratio of the ranges is 0.93 (versus the 0.96 average that Figure B-7 might predict). However, a complicated analysis of the ratio of the ranges over a number of tidal cycles shows that the multiplier that should be used to relate the ranges for the month of May 2004 generally increases with the overall tide range at New London.

NGVD 29 at Haddam is 0.92' lower relative to MLLW at Haddam than it is at New London. Since the tide range is approximately the same, then the Haddam tide level should be at least 0.92' higher than New London when river flows are small (e.g., gage height at Hartford is less than 4' NGVD 29). Figure B-9 is constructed to adjust the actual New London tide

---

[6] http://www.ngs.noaa.gov/cgi-bin/ngs_opsd.prl, Station ID 8461490; http://www.co-ops.nos.noaa.gov/cgi-bin/get_pred.cgi?year=2004&stn=2555+New+London; http://www.co-ops.nos.noaa.gov/cgi-bin/co-ops_qry_direct.cgi?stn=8461490+NEW+LONDON%2C+THAMES+RIVER+%2C+CT&dcp=1&ssid=WL&pc=W2+-+Hourly+heights&datum=MLLW&unit=1&bdate=20040501&edate=20040531&date=3&shift=1&level=-4&form=0&host=&addr=64.223.203.99&data_type=vwl&format=View+Data

[7] http://www.co-ops.nos.noaa.gov/tides05/tab2ec2a.html#15

highs and lows by raising them 0.92' and then comparing them with the actual measured HNP tide high and lows with 1.74' added using the time axis as consecutive half tide cycles in mid-May 2004 to remove the time lags. Adding 1.74' to the HNP data resulted in the low tide at HNP never going lower than the adjusted New London low tide of the same cycle. Although not presented here, similar evaluation of the mid-September tidal data suggested that adding 1.74' to the HNP data provided the best estimate of tide relative to NGVD 29, consistent with New London tide data.

Therefore, for the two tides of particular interest to the groundwater model calibration at HNP, the mid-May and mid-September HNP tide level readings should be corrected by adding 1.74' to the data as presented in the CH2M-Hill quarterly monitoring reports covering those periods. In general, for long-term average steady-state calibration and simulation of groundwater models at HNP, the mean tide level at HNP will be considered to be 1.74' NGVD 29.

Figure B-1
Tidal Benchmark Data for Connecticut River at Higganum Creek

Date created
Fri Apr 29 16:25:30 EDT 2005

Elevation Information for PID = LX0578, VM = 2242
Station_ID --- 8463827

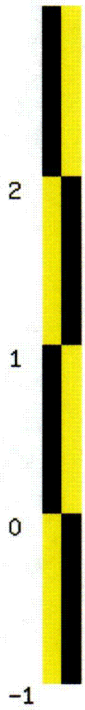

--- MHHW = 2.76 feet (0.841 meters)

--- MHW = 2.51 feet (0.765 meters)

--- MTL = 1.31 feet (0.399 meters)

--- NAVD88 = 0.97 feet (0.296 meters)

--- MLW = 0.10 feet (0.030 meters)

--- NGVD29 = -0.04 feet (-0.012 meters)

--- MLLW = 0.00 feet (0.000 meters)

The NAVD 88 and the NGVD 29 elevations related to MLLW were computed from Bench Mark, J 16, at the station.

Displayed tidal datums are Mean Higher High Water(MHHW), Mean High Water (MHW), Mean Tide Level(MTL), Mean Low Water(MLW), and Mean Lower Low Water(MLLW) referenced on 1983-2001 Epoch

Figure B-2
Predicted Tide at Haddam

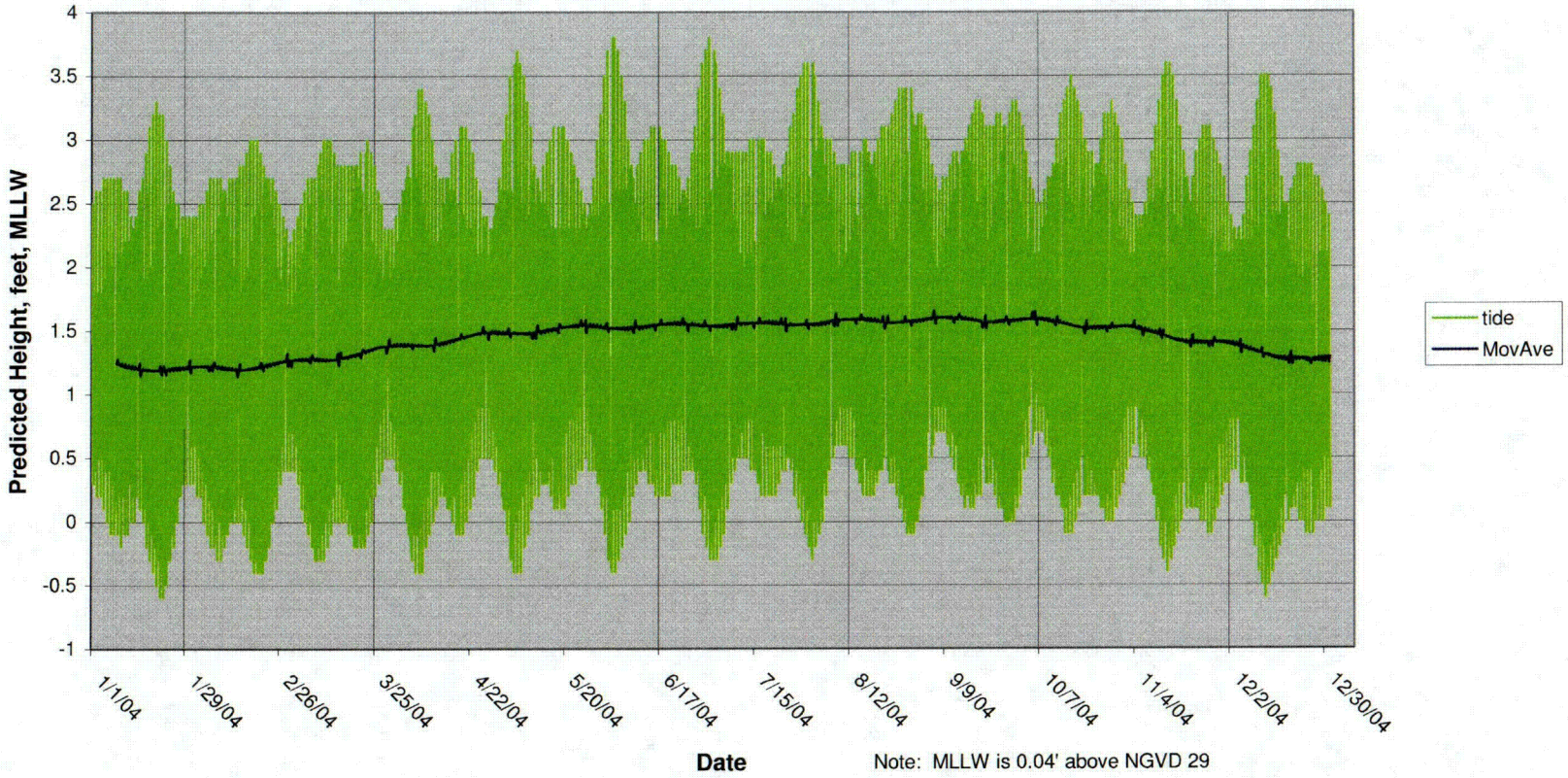

Note: MLLW is 0.04' above NGVD 29

Figure B-3
Conn River daily gage heights at Hartford compared with transducer measurements at HNP

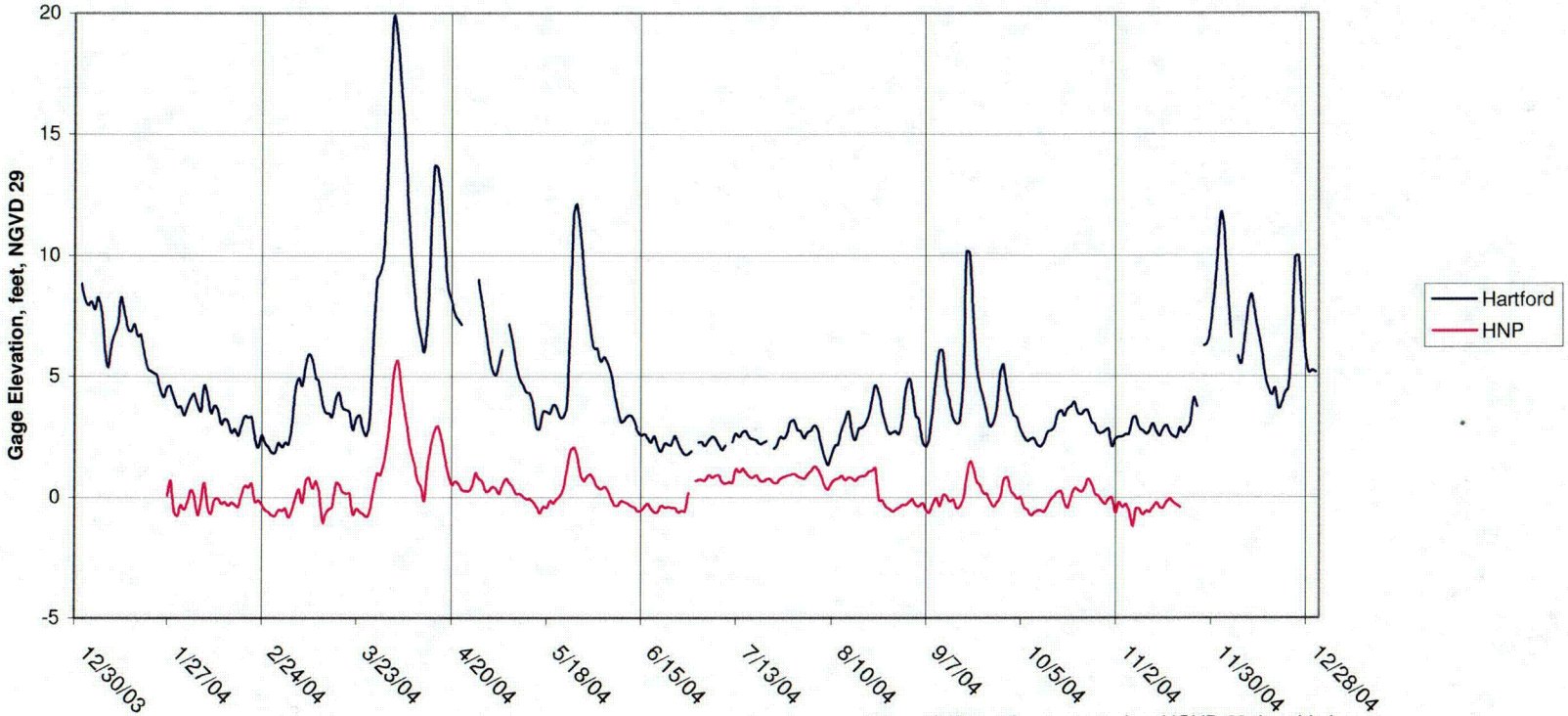

Note: HNP readings reported as NGVD 29, but this has been found to be in error.

C68

Figure B-4
Comparison of New London Tide Gage Predicted Versus Actual Heights, May 2004

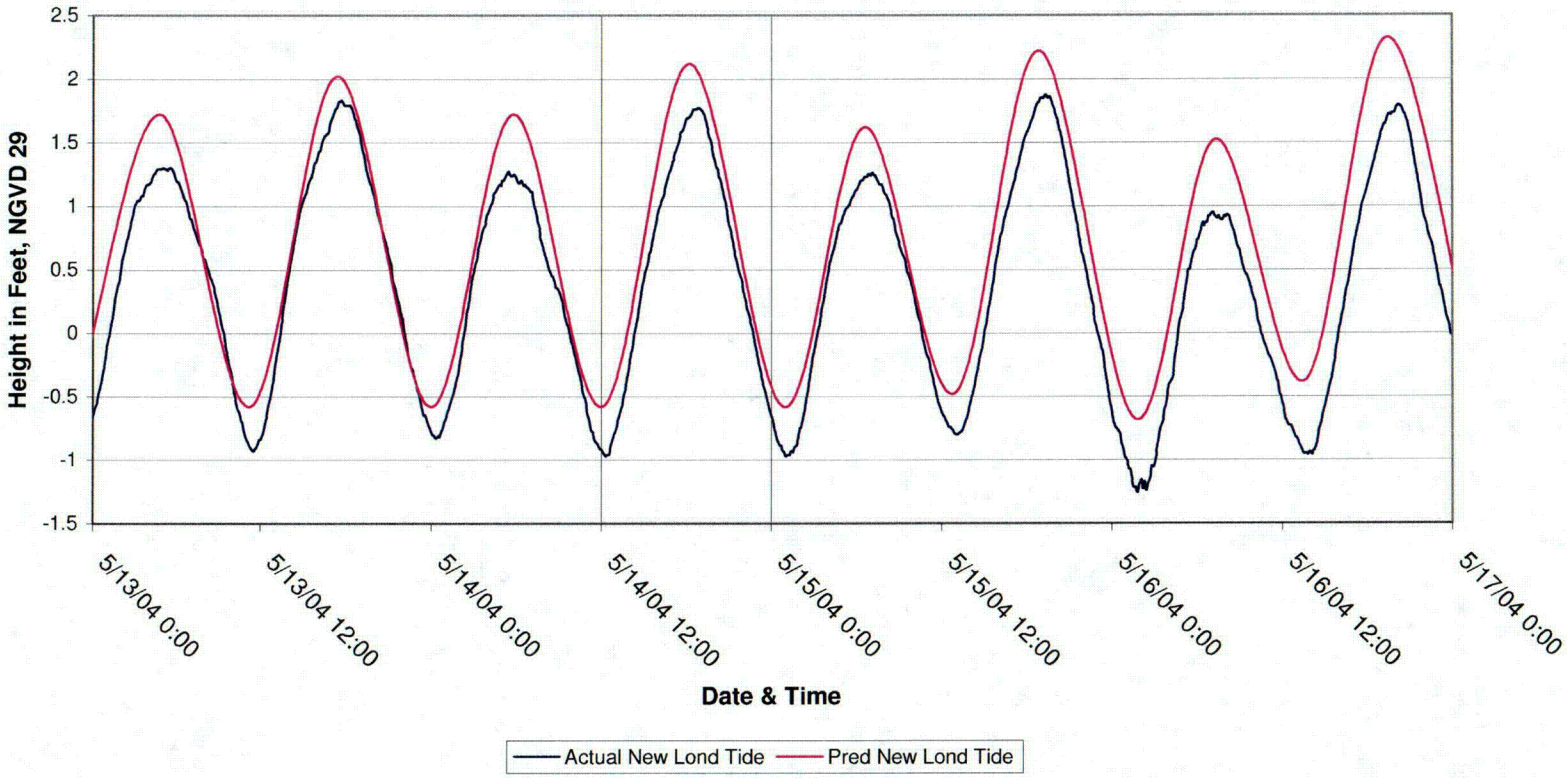

Figure B-5
Comparison of Measured HNP Tide Levels versus Predicted Haddam Tide Levels

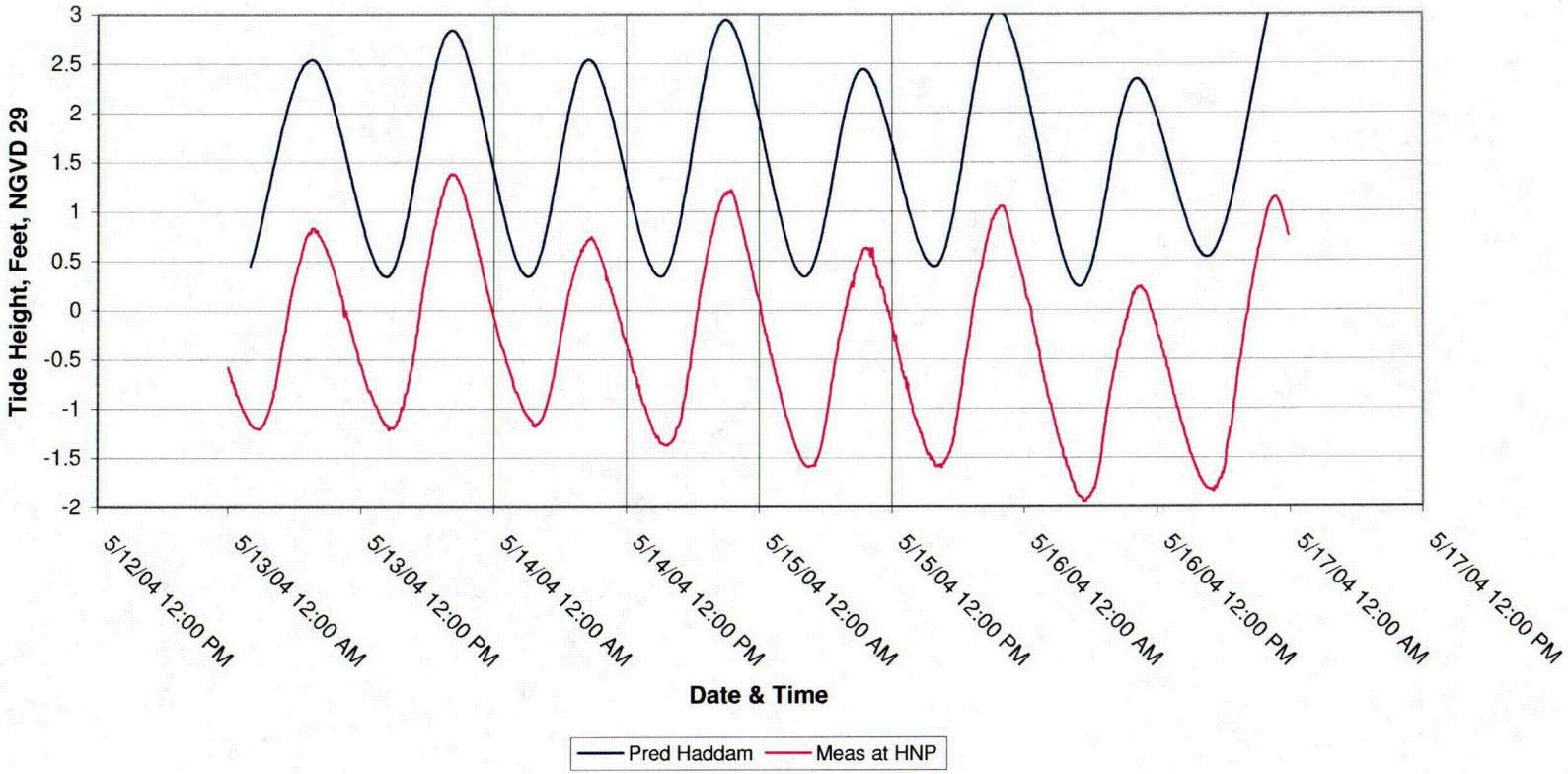

Figure B-6
NOAA Data on Tides on the Connecticut River

CONNECTICUT, Long Island Sound

Station	Latitude	Longitude	Mean Range (ft)	Spring Range (ft)	Mean Tide Level (ft)
Silver Eel Pond, Fishers Island, N.Y.	41°15.4'	72°01.8'	2.3	2.7	1.3
Thames River					
NEW LONDON, State Pier	41°21.6'	72°05.5'	2.56	3.05	1.47
Norwich	41°31.4'	72°04.7'	3	3.6	1.7
Connecticut River					
Saybrook Jetty	41°15.8'	72°20.6'	3.5	4.2	2
Saybrook Point	41°17.0'	72°21.0'	3.2	3.8	1.8
Lyme, highway bridge	41°19.3'	72°21.1'	3.1	3.7	1.7
Essex#7	41°20.9'	72°23.1'	3	3.6	1.7
Hadlyme#7	41°25.2'	72°25.7'	2.7	3.2	1.5
East Haddam#7	41°27.0'	72°27.8'	2.9	3.5	1.6
Haddam#7	41°28.9'	72°30.4'	2.5	3	1.4
Higganum Creek#7	41°30.1'	72°33.0'	2.6	3.1	1.5
Portland#7	41°33.7'	72°37.5'	2.2	2.6	1.3
Rocky Hill#7	41°39.0'	72°37.6'	2	2.4	1.2
Hartford#7	41°46.2'	72°40.1'	1.9	2.3	1.1

Figure B-7
NOAA Data Relating New London Tides to Haddam Tides

2004 Tide Predictions: Connecticut River, Haddam
(Reference station: New London,
Corrections Applied: Times: High +2 hr. 48 min.,
Low +3 hr. 8 min., Heights: High *0.97, Low *0.95)

Figure B-8
Comparison of Measured HNP Tide Levels versus Predicted Haddam Tide Levels

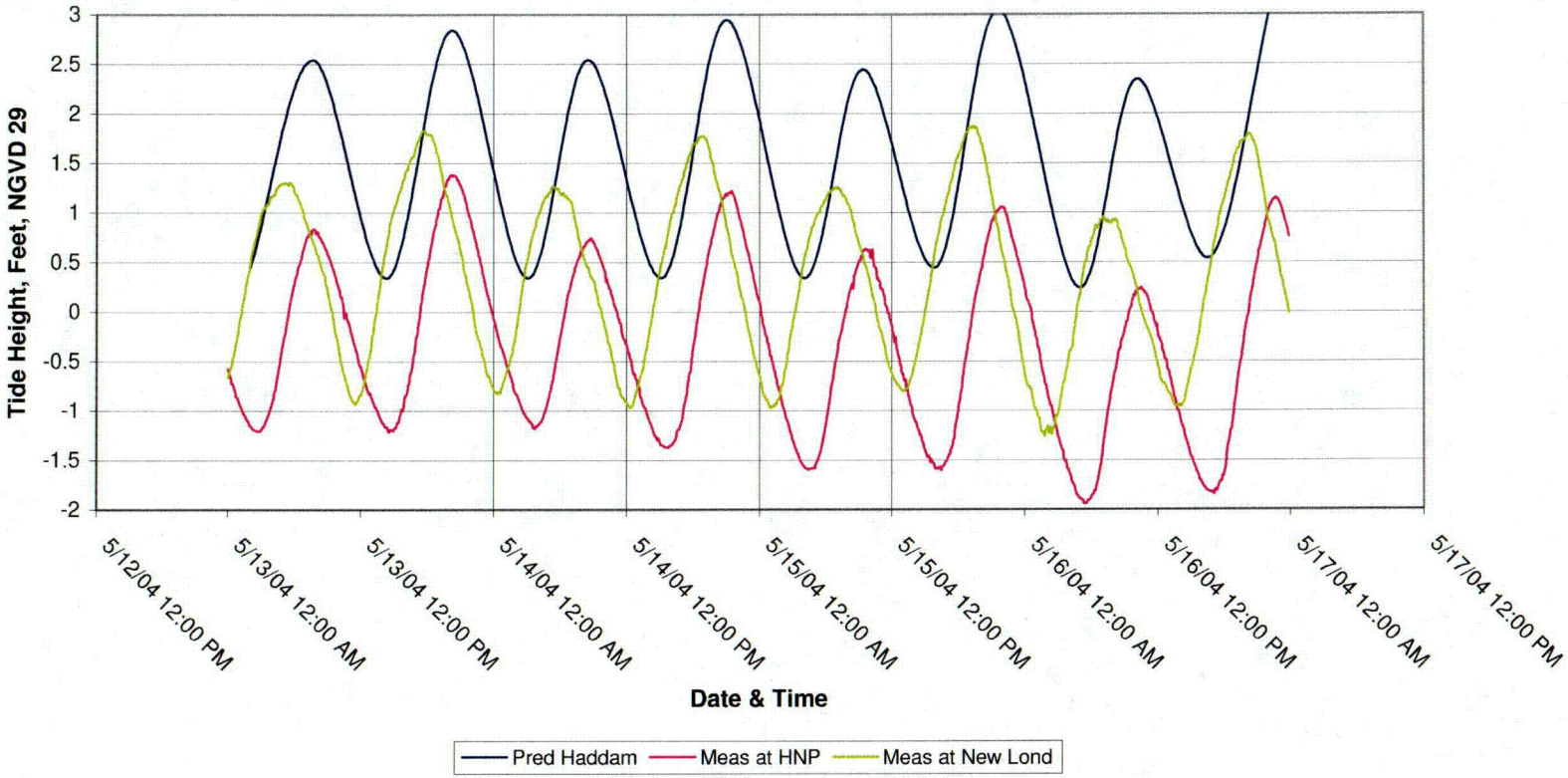

Figure B-9
Adjusted HNP Tide Relative to NGVD, compared to adjusted New London Tide in mid-May 2004

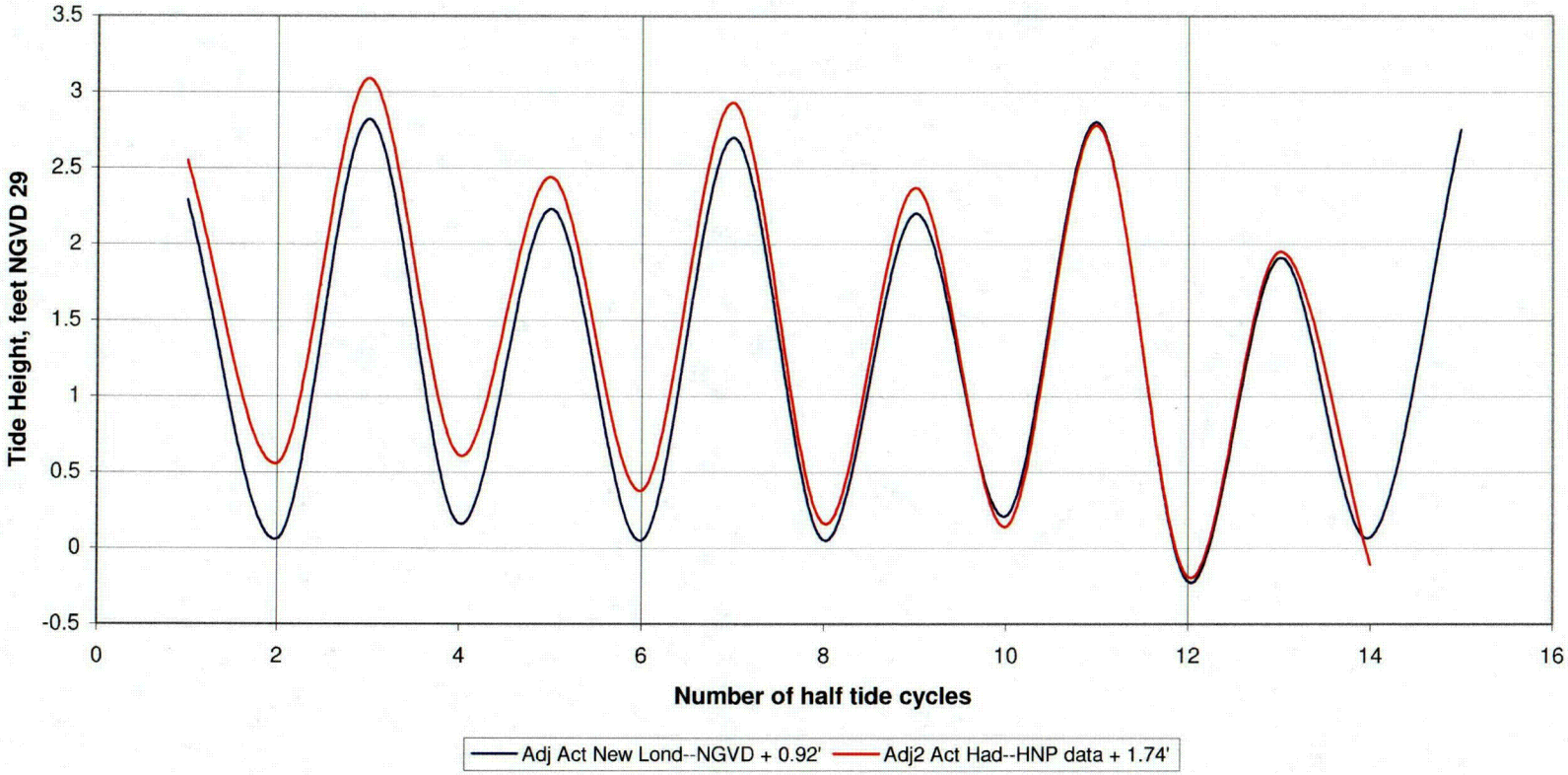

Figure C-1
Rose Diagram for Photolineaments interpreted on and near the CY Site
CY Groundwater Model

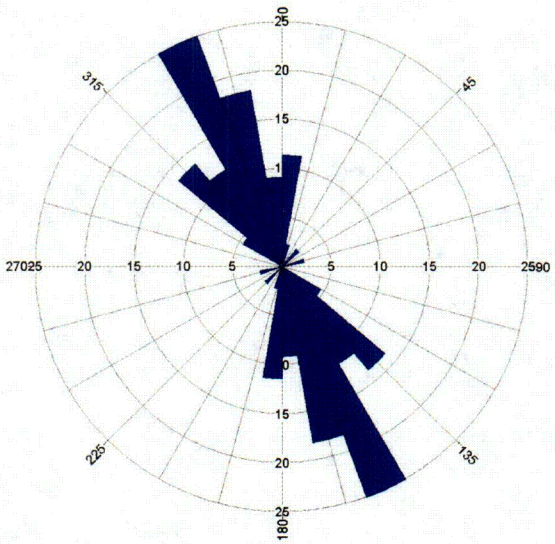

Lineament Rose Diagram--Connecticut Yankee

Calculation Method .... Frequency
Class Interval ..... 10 Degrees
Length Filtering ..... Deactivated
Azimuth Filtering ..... Deactivated
Data Type ..... Bidirectional
Population 44
Maximum Percentage .... 25.0 Percent
Mean Percentage ..... 10.0 Percent
Standard Deviation .... 7.39 Percent
Vector Mean ..... 322.63 Degrees
Confidence Interval ... 19.23 Degrees
R-mag 0.69

Rose diagram based on true north and photolinears digitized from Figure in Malcolm Pirnie, 1999

Figure C-2
Schmidt Diagram of Bedrock Foliation interpreted on and near the CY Site
CY Groundwater Model

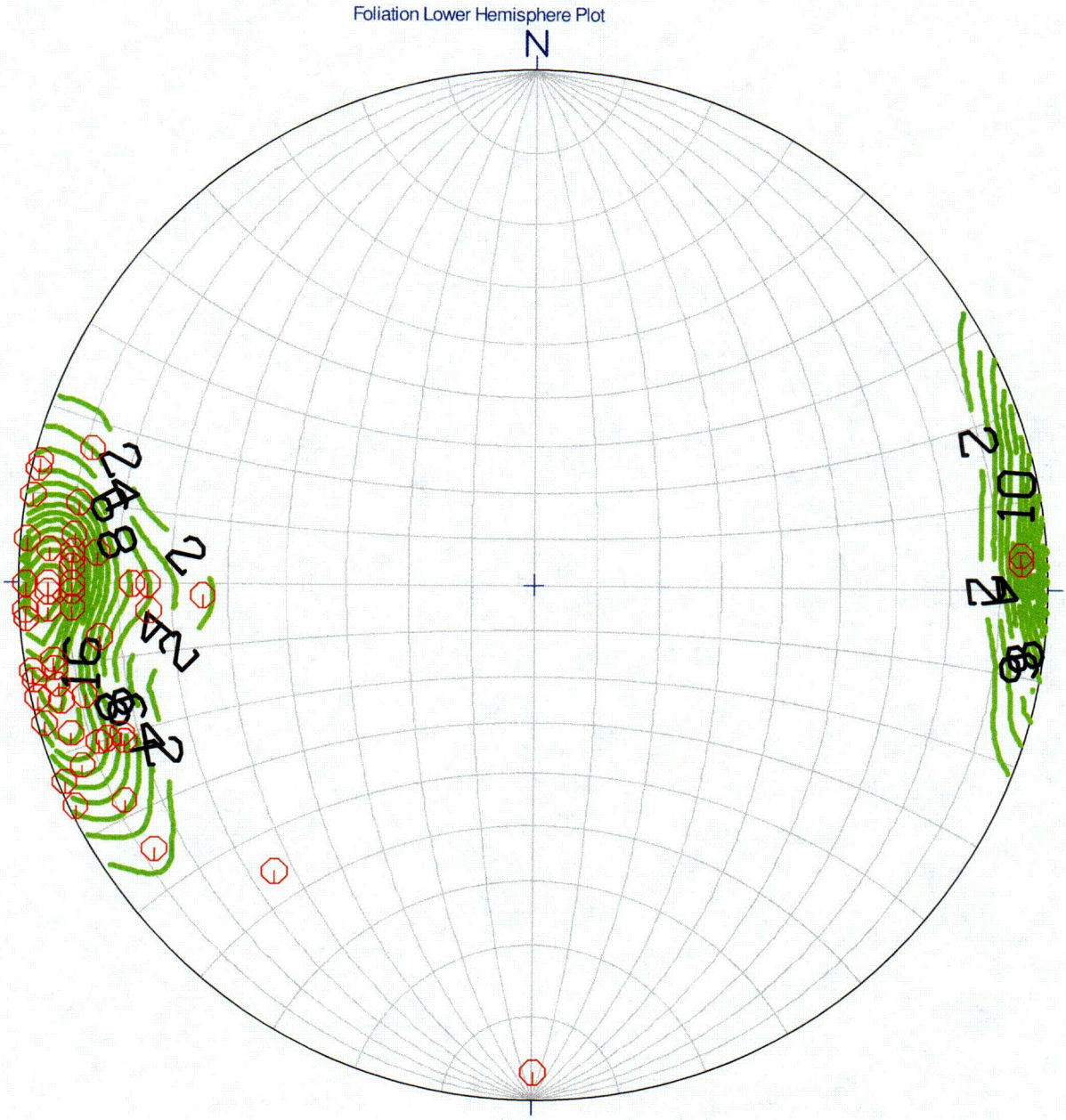

Schmidt Equal Area diagram based on true north and data digitized from Figure 1 in Lanter, 2004, "Technical Memorandum: General Site Geology of the Connecticut Yankee Haddam Neck Plant"

Figure C-3
Schmidt Diagram of Bedrock Joints interpreted on and near the CY Site
CY Groundwater Model

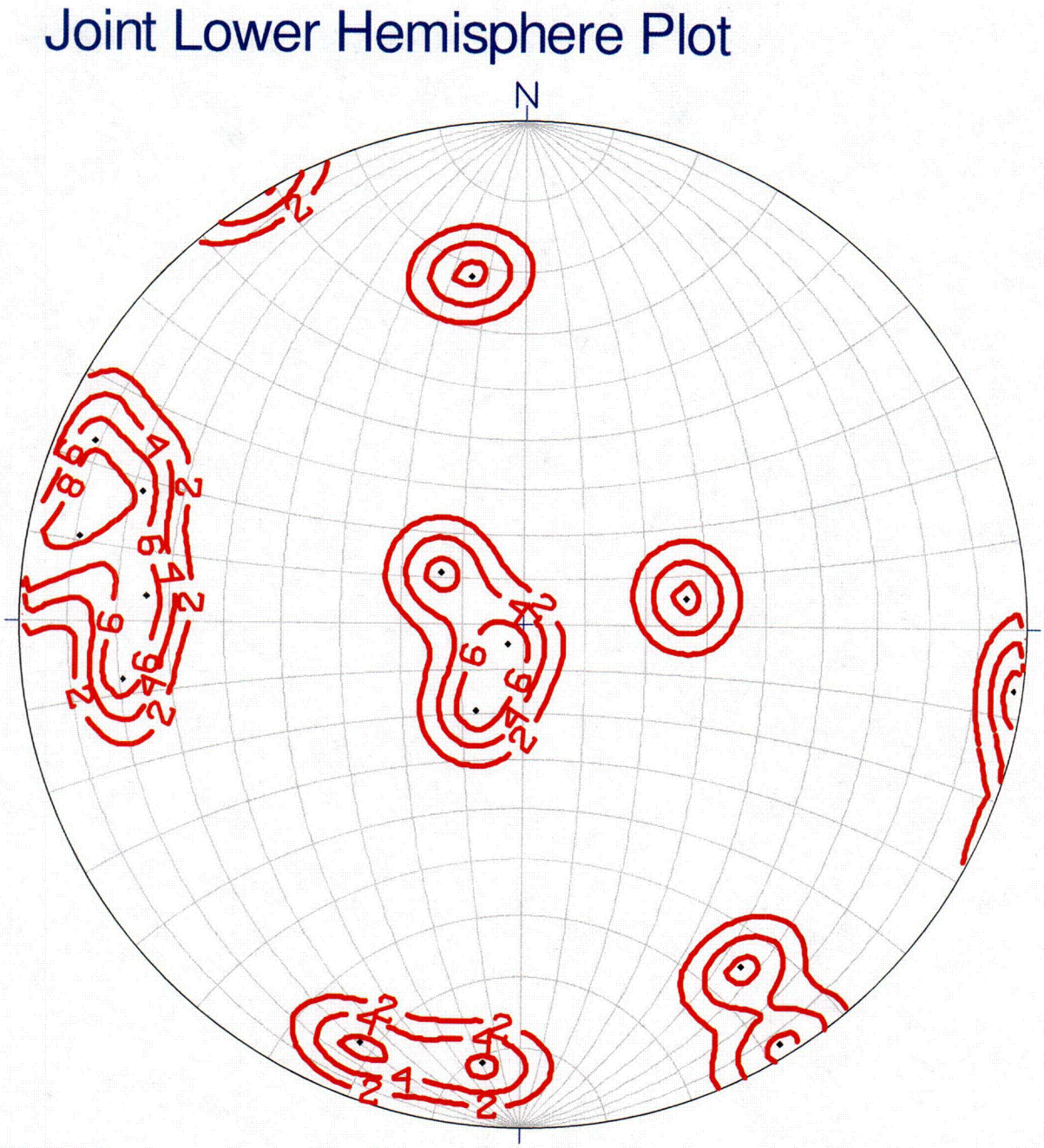

Schmidt Equal Area diagram based on true north and data digitized from Figure 1 in Lanter, 2004, "Technical Memorandum: General Site Geology of the Connecticut Yankee Haddam Neck Plant"

Figure C-4
Bedrock Foliation Rose Diagram interpreted from Data Recorded on and near the CY Site
CY Groundwater Model

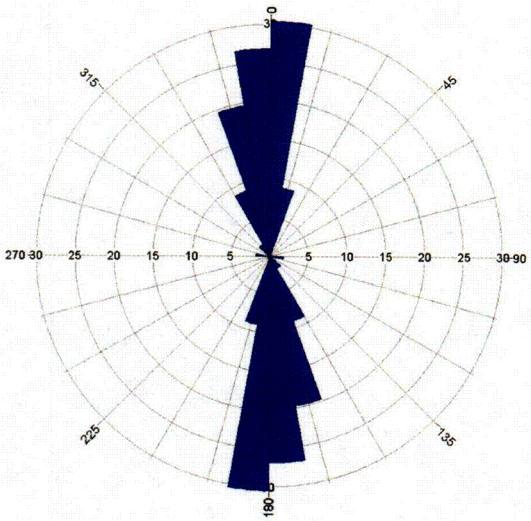

Foliation Strike Rose Diagram--Connecticut Yankee

```
Calculation Method .... Frequency
Class Interval ........ 10 Degrees
Length Filtering ...... Deactivated
Azimuth Filtering ..... Deactivated
Data Type ............. Bidirectional
Population ............ 56
Maximum Percentage .... 30.4 Percent
Mean Percentage ....... 12.5 Percent
Standard Deviation .... 11.22 Percent
Vector Mean ........... 313.52 Degrees
Confidence Interval ... 54.74 Degrees
R-mag ................ 0.25
```

Rose diagram based on true north and data digitized from Figure 1 in Lanter, 2004, "Technical Memorandum: General Site Geology of the Connecticut Yankee Haddam Neck Plant"

Figure C-5
Bedrock Joint Strike Rose Diagram interpreted from Data Recorded on and near the CY Site
CY Groundwater Model

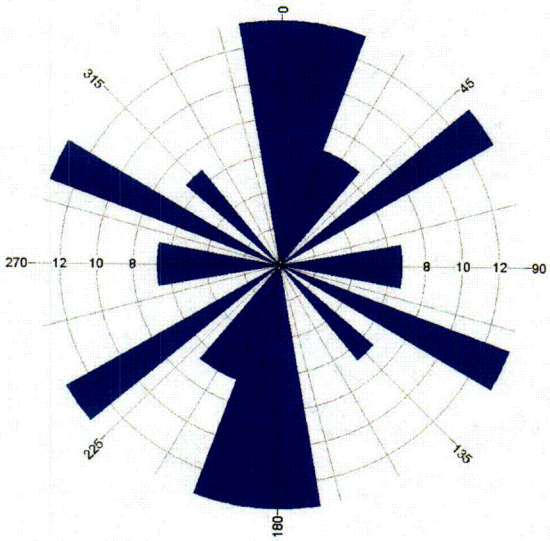

Joint Strike Rose Diagram--Connecticut Yankee

```
Calculation Method .... Frequency
Class Interval ........ 10 Degrees
Length Filtering ...... Deactivated
Azimuth Filtering ..... Deactivated
Data Type ............. Bidirectional
Population ............ 15
Maximum Percentage .... 13.3 Percent
Mean Percentage ....... 10.0 Percent
Standard Deviation .... 3.42 Percent
Vector Mean ........... 67.63 Degrees
Confidence Interval ... 40.84 Degrees
R-mag ................ 0.59
```

Rose diagram based on true north and data digitized from Figure 1 in Lanter, 2004, "Technical Memorandum: General Site Geology of the Connecticut Yankee Haddam Neck Plant"

CT1

Appendix D

Derivation of Inputs for Modeling Adsorption/Desorption of Radionuclides in Bedrock Under the Tank Farm CY Groundwater Model

In July 2005, just prior to completing the calibration of the CY Groundwater Model, we were asked to model solute transport of radionuclides that had been found sorbed on fracture surfaces and infilling material in bedrock fractures under the former "Tank Farm" located to the northwest of the containment building. CH2M-Hill provided laboratory analysis of the solid concentration of the fracture infilling material and also the estimated Kd value based on SPLP tests on the infilling material. Detectable concentrations of Am-241, Pu-238, Pu-239/240, Sr-90, Cs-134, Cs-137, and Co-60 were reported. CH2M-Hill also estimated, in consultation with us, estimates of the fracture porosity of the bedrock, porosity of the fracture infilling material, unit weights of the rock and the infilling material, relative percentage of each of the infilling materials that occupies the fracture void space at various depths in the rock, and the estimated distribution of fracture aperture widths.

We used MT3DMS (using inputs from MODFLOW) to do solute transport for Sr-90 and Cs-137, assuming that a linear isotherm would describe the process of sorption/desorption on the fracture and fracture infilling surfaces. This should be a conservative approach for Cs-137 as the literature indicates that Cs-137 may sorb irreversibly on micas in the rock. The problem was to convert the input parameters required by the porous media model to those that could simulate the sorption/desorption on fracture surfaces and fracture infillings. The conversion of the Kd values applicable to porous media calculations to equivalent Kd values for the fractured rock are given in Table D-1. In the process, metric units were converted to English measurement units to conform to those we had used in the flow model.

The translation process involves the assumption that all of the radionuclide weight was on the fracture surfaces or on the fracture infilling surfaces. In other words, no diffusive transfer of radionuclides into or out of the solid matrix was assumed. The total estimated weight of radionuclide solids as a fraction of the total bulk volume of rock was estimated for each model layer. The Kd of the infilling material had to be normalized to a Kd for the bulk rock. Finally an initial water concentration was estimated based on the laboratory tests. Transport simulations were run including radioactive decay in both the solute and on the solid surface, a linear isotherm Kd factor, and dispersivity. Final output was in pCi/pound and was converted back to pCi/liter.

Table D-1

CY Tank Farm Solute Transport Model Inputs

			granulite	mud	oxide volume
Model Layer 4	Constants	%infilled	15.00%	35.00%	0 ft3
Model Layers 5-8	Constants		granulite	mud	oxide volume
		%infilled	15.00%	0.00%	0 ft3
Model Layer 9	Constants		15.00%	0.00%	0 ft3

						ft/mm
spgrav	granulite	mud	oxide	amphib		0.003280833
	2.2	1.6	3.8	3.2		
Model Layer 4 aper. width	1	5	25 mm		Total Vol (ft3)	check
	50%	40%	10%		0.0120	0.012303125
Model Layers 5-8 aper. Width	0.10	0.50	2.50 mm			
	50%	40%	10%		0.0010	0.001230313
Model Layer 9 aper. Width	0.01	0.05	0.25 mm			
	50%	40%	10%		0.0001	0.000123031

Model Layer 4 eff. Por.	0.0120
Model Layer 5-8 eff. Por.	0.0010
Model Layer 9 eff. Por.	0.0001

surface area/vol 1.5

remaining granulite conc	pCi/g	pCi/g/40	pCi/kg	pCi/lb
Am-241	51.6	1.29	1290	585.03401
Pu-238	36.5	0.9125	912.5	413.8322
Pu-239/240	12.5	0.3125	312.5	141.72336
Sr-90	172	4.3	4300	1950.1134
Cs-134	659	16.475	16475	7471.6553
Cs-137	100000	2500	2500000	1133786.8
Co-60	1680	42	42000	19047.619

remaining mud conc	pCi/g	pCi/kg	pCi/lb
Am-241	1.25	1250	566.89342
Pu-238	0.883	883	400.45351
Pu-239/240	0.303	303	137.41497
Sr-90	12.6	12600	5714.2857
Cs-134	16.8	16800	7619.0476
Cs-137	2420	2420000	1097505.7
Co-60	18.1	18100	8208.6168

remaining oxide conc	pCi/g	pCi/kg	pCi/lb
Am-241	5670	5670000	0
Pu-238	4010	4010000	0
Pu-239/240	1370	1370000	0
Sr-90	18900	18900000	0
Cs-134	85900	85900000	0
Cs-137	11000000	11000000000	0
Co-60	110000	110000000	0

Granulite Solution Concentration	pCi/L	pCi/L/40	pCi/ft3
			0.0353
Am-241	156.93	3.92325	111.1402266
Pu-238	173.07	4.32675	122.5708215
Pu-239/240	48.11	1.20275	34.07223796
Sr-90	12804	320.1	9067.988669
Cs-134	1039.87	25.99675	736.4518414
Cs-137	170133.33	4253.33325	120491.0269
Co-60	6629.33	165.73325	4694.992918

Radioactive half-life	days
Am-241	157861.05
Pu-238	3.21E+04
Pu-239/240	3652500
Sr-90	10446.15
Cs-134	753.1455
Cs-137	11020
Co-60	1925.23275

Granulite Infilling Kd	L/Kg	ft3/lb
		0.01600907
Am-241	328.8090231	5.263926765
Pu-238	210.8973248	3.376270097
Pu-239/240	259.821243	4.159496543
Sr-90	13.43330209	0.215054677
Cs-134	633.7330628	10.14547715
Cs-137	587.7743062	9.409720185
Co-60	253.4192746	4.057006982

Mud infilling Kd	L/Kg	ft3/lb
		0.01600907
Am-241	119	1.905079365
Pu-238	76.2	1.219891156
Pu-239/240	93.9	1.503251701
Sr-90	121	1.937097506
Cs-134	229	3.666077098
Cs-137	212	3.393922902
Co-60	91.6	1.466430839

oxide infilling Kd	L/Kg	ft3/lb
		0.01600907
Am-241	329	0
Pu-238	211	0
Pu-239/240	260	0
Sr-90	134	0
Cs-134	634	0
Cs-137	588	0
Co-60	253	0

Calculate weighted percentage of rock that is radioactive, assuming only infillings and oxide are radioactive

Model Layer 4	granulite	mud	oxide	(pounds)	sum
	0.247104	0.419328	0		0.666432
Model Layers 5-8	0.020592	0	0		0.020592
Model Layer 9	0.0020592	0	0		0.0020592

Model Layer 4 Weight of 1 ft3 of amphibolite bulk rock	197.28384	pounds
Model Layers 5-8 Weight of 1 ft3 of amphibolite bulk rock	199.48032	
Model Layer 9 Weight of 1 ft3 of amphibolite bulk rock	199.660032	

Model Layer 4 Total weight amphibolite+infilling+oxide	197.950272
Model Layers 5-8 Total weight amphibolite+infilling+oxide	199.500912
Model Layer 9 Total weight amphibolite+infilling+oxide	199.6620912

(infilling + oxide)/total wgt Model layer 4	0.003366664
(infilling + oxide)/total wgt Model Layers 5-8	0.000103218
(infilling + oxide)/total wgt Model Layer 9	1.03134E-05

Bulk Kd of Model Layer 4 weighted Kd of granulite, mud, and oxide

	ft3/lb
Am-241	0.010606656
Pu-238	0.0067988
Pu-239/240	0.008376769
Sr-90	0.004371907
Cs-134	0.020430771
Cs-137	0.018935798
Co-60	0.008170831

Bulk Kd of Model Layers 5-8

	ft3/lb
Am-241	0.00054333
Pu-238	0.00034849
Pu-239/240	0.000429333
Sr-90	2.21974E-05
Cs-134	0.001047192
Cs-137	0.000971248
Co-60	0.000418754

Bulk Kd of Model Layer 9

	ft3/lb
Am-241	5.42891E-05
Pu-238	3.48209E-05
Pu-239/240	4.28987E-05
Sr-90	2.21795E-06
Cs-134	0.000104635
Cs-137	9.70464E-05
Co-60	4.18416E-05

Model Lyr 4 Bulk sorbed conc of solid	pCi
Am-241	1.287003262
Pu-238	0.909608448
Pu-239/240	0.311895643
Sr-90	9.689395614
Cs-134	16.97187676
Cs-137	2492.604167
Co-60	27.43442326

Model Layers 5-8 Bulk sorbed conc of soli	pCi
Am-241	0.001243464
Pu-238	0.000879582
Pu-239/240	0.000301227
Sr-90	0.004144881
Cs-134	0.015880677
Cs-137	2.409814363
Co-60	0.040484881

Model Lyr 9 Bulk sorbed conc of solid	pCi
Am-241	0
Pu-238	0
Pu-239/240	0
Sr-90	0
Cs-134	0
Cs-137	0
Co-60	0

Rev. 8/01/05 by RGG

Appendix E

Corrections to September 2004 Pumping Test Drawdown Observations

The analytical or curve matching analysis of pumping test data requires the application of corrections for effects causing trends in the data unrelated to the pumping stress. This is particularly true if the monitoring wells being used to determine drawdown are at great distance and drawdown is only a few tenths of a foot or less in the well. Under these conditions, changes in barometric pressure, earth tides, coastal tides, and the fall of a water level due to normal recession since the last precipitation event can make the drawdown due to pumping stress indistinguishable from these other effects.

During the September 2004 pumping test at Connecticut Yankee at AT-1 (pumped at 29 gallons per minute) a heavy rainfall occurred in the third day of the test. This rainfall was preceded by a significant decline in barometric pressure, which caused water levels to rise in monitoring wells. Although the transient computer model designed to simulate the pumping test included the effects of response to tide and recession, it does not include the ability to correct for barometric changes. In order to correct for this effect, the barometric efficiency of each well must be calculated. Since many of the wells also respond to tidal fluctuations on the Connecticut River, the tidal response was also increased in response to the increase in tide levels in proportion to the tidal efficiency. Finally, water levels were dropping during the first part of the pumping test in recession following a rainfall event several days prior to the test.

In order to determine the aquifer response characteristics pertinent to each well affected by the pumping test, we selected a later time interval (October 3 through October 14) to calculate tidal efficiencies and barometric efficiencies. Table E-1 summarizes the calculations and presents the graphs for monitoring wells OB-25, 104S, 109S, 109D, 123, 124, 508S and 508D. Notes to the right of the rows of each set of calculations summarize the steps.

We used the barometric efficiencies calculated across the range from October 8 to October 13. Tidal efficiencies were calculated separately for each well and are given on the top line of each set of calculations. Barometric efficiencies ranged from 0% for MW-123 to 22% for MW-109S. Tidal efficiencies ranged from 0% from MW-508S and MW-104S to 9% to 508D. Because of the rather tedious procedures to capture and process the data for each well, we did not calculate the efficiencies for the other wells that were not affected by the pumping tests.

Table E-1
September 2004 Pumping Test Drawdown Corrections
CY Groundwater Model

Analysis of Barometric Efficiency in period 10/05/04 to 10/14/04 — Tidal Efficiency 0.086207

Well 508D

	5-Oct	6-Oct	7-Oct	8-Oct	9-Oct	10-Oct	11-Oct	12-Oct	13-Oct	14-Oct	
Bar	30.43	30.72	30.71	30.75	30.63	30.39	30.34	30.19	30.03	30.01	barometric pressure in inches of Hg
tide	-0.2	-0.5	-0.8	-0.8	-0.75	-0.65	-0.55	-0.45	-0.25	-0.1	Measured Tide elevation
tide corr	0	-0.3	-0.6	-0.6	-0.55	-0.45	-0.35	-0.25	-0.05	0.1	Measured change in Tide elevation from Oct. 5
barometric change	0	0.32857	0.31724	0.36256	0.2266	-0.04532	-0.10197	-0.27192	-0.4532	-0.47586	Theoretical change in tide in feet due to barometric pressure from Oct. 5
Tide offset by bar.	-0.2	-0.17143	-0.48276	-0.43744	-0.5234	-0.69532	-0.65197	-0.72192	-0.7032	-0.57586	Tide elevation with barometric change taken out
tide bar corr		-0.62857	-0.91724	-0.96256	-0.7766	-0.40468	-0.24803	0.02192	0.4032	0.57586	Tide correction since Oct. 5 with barometric change offset
tide corr by eff.		-0.05419	-0.07907	-0.08298	-0.066948	-0.034886	-0.021382	0.00189	0.034759	0.049643	Tide correction from Oct. 5 multiplied by tidal efficiency of well
recession	0	-0.0267	-0.0534	-0.0801	-0.1068	-0.1335	-0.1602	-0.1869	-0.2136	-0.2403	amount of decline since Oct. 5 due to lack of recharge
well	3.2	3.1	3.05	2.97	2.92	2.9	2.9	2.9	2.91	2.93	Actual well water elevation measured
well-rec	3.2	3.1267	3.1034	3.0501	3.0268	3.0335	3.0602	3.0869	3.1236	3.1703	Well elevation corrected for recession (add recession back)
well-rec+tide corr	3.2	3.28089	3.33247	3.363079	3.373748	3.368386	3.381582	3.38501	3.378841	3.390657	Correct well elevation with recession by offsetting tidal effect
bar efficiency		-0.24618	4.55299	-0.67535	0.078471	-0.019719	0.232934	0.020173	-0.03403	0.521426	Calculate barometric efficiency of well day by day
										0.019322	Calculate barometric efficiency of well from Oct 8 to Oct 13

Time	BarPress	Uncorr	Corr Head
38245.55486	30.711	3.1839	3.1839
38245.55564	30.711	3.1839	3.1839
38245.55841	30.711	3.1862	3.1862
38245.56189	30.711	3.1862	3.1862
38245.56883	30.711	3.1908	3.1908
done 38245.58333	30.659	3.1746	3.1736
38245.6105	30.659	3.1539	3.1529
38245.66667	30.633	3.0708	3.06929
38245.77716	30.631	2.9094	2.90785
38246	30.566	3.0016	2.9988
38246.44383	30.475	2.8356	2.83104
38247.33333	30.343	2.6441	2.63699

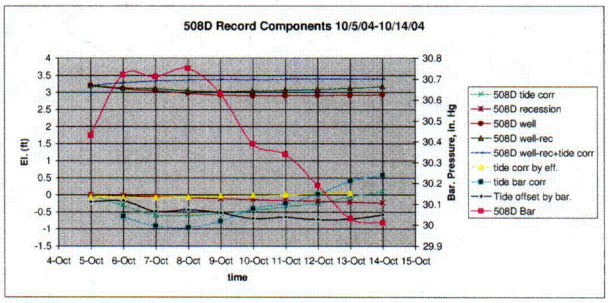

Analysis of Barometric Efficiency in period 10/05/04 to 10/14/04 — Tidal Efficiency 0

Well 508S

	5-Oct	6-Oct	7-Oct	8-Oct	9-Oct	10-Oct	11-Oct	12-Oct	13-Oct	14-Oct	
Bar	30.43	30.72	30.71	30.75	30.63	30.39	30.34	30.19	30.03	30.01	barometric pressure in inches of Hg
tide	-0.2	-0.5	-0.8	-0.8	-0.75	-0.65	-0.55	-0.45	-0.25	-0.1	Measured Tide elevation
tide corr	0	-0.3	-0.6	-0.6	-0.55	-0.45	-0.35	-0.25	-0.05	0.1	Measured change in Tide elevation from Oct. 5
barometric change	0	0.32857	0.31724	0.36256	0.2266	-0.04532	-0.10197	-0.27192	-0.4532	-0.47586	Theoretical change in tide in feet due to barometric pressure from Oct. 5
Tide offset by bar.	-0.2	-0.17143	-0.48276	-0.43744	-0.5234	-0.69532	-0.65197	-0.72192	-0.7032	-0.57586	Tide elevation with barometric change taken out
tide bar corr		-0.62857	-0.91724	-0.96256	-0.7766	-0.40468	-0.24803	0.02192	0.4032	0.57586	Tide correction since Oct. 5 with barometric change offset
tide corr by eff.		0	0	0	0	0	0	0	0	0	Tide correction from Oct. 5 multiplied by tidal efficiency of well
recession	0	-0.0689	-0.1378	-0.2067	-0.2756	-0.3445	-0.4134	-0.4823	-0.5512	-0.6201	amount of decline since Oct. 5 due to lack of recharge
well	12.4	12.3	12.25	12.23	12.2	12.2	12.15	12.1	11.95	11.9	Actual well water elevation measured
well-rec	12.4	12.3689	12.3878	12.4367	12.4756	12.5445	12.5634	12.5823	12.5012	12.5201	Well elevation corrected for recession (add recession back)
well-rec+tide corr	12.4	12.3689	12.3878	12.4367	12.4756	12.5445	12.5634	12.5823	12.5012	12.5201	Correct well elevation with recession by offsetting tidal effect
bar efficiency		0.09465	1.66814	-1.07899	0.286114	0.253383	0.333628	0.111209	-0.4473374	0.834069	Calculate barometric efficiency of well day by day
										0.079067	Calculate barometric efficiency of well from Oct 8 to Oct 13

Time	BarPress	Uncorr	Corr Head
38245.55486	30.711	12.6877	12.6877
38245.55564	30.711	12.6877	12.6877
38245.55841	30.711	12.6877	12.6877
38245.56189	30.711	12.6854	12.6854
38245.56883	30.711	12.6877	12.6877
done 38245.58333	30.659	12.6877	12.6836
38245.6105	30.659	12.6831	12.679
38245.66667	30.633	12.6784	12.6723
38245.77716	30.631	12.6761	12.6698
38246	30.566	12.6646	12.6531
38246.44383	30.475	12.66	12.6413
38247.33333	30.343	12.6231	12.594

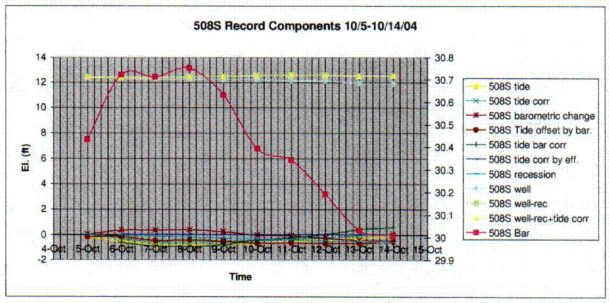

Analysis of Barometric Efficiency in period 10/05/04 to 10/14/04 — Tidal Efficiency 0.047034

Well 109D

	5-Oct	6-Oct	7-Oct	8-Oct	9-Oct	10-Oct	11-Oct	12-Oct	13-Oct	14-Oct	
Bar	30.43	30.72	30.71	30.75	30.63	30.39	30.34	30.19	30.03	30.01	barometric pressure in inches of Hg
tide	-0.2	-0.5	-0.8	-0.8	-0.75	-0.65	-0.55	-0.45	-0.25	-0.1	Measured Tide elevation
tide corr	0	-0.3	-0.6	-0.6	-0.55	-0.45	-0.35	-0.25	-0.05	0.1	Measured change in Tide elevation from Oct. 5
barometric change	0	0.32857	0.31724	0.36256	0.2266	-0.04532	-0.10197	-0.27192	-0.4532	-0.47586	Theoretical change in tide in feet due to barometric pressure from Oct. 5
Tide offset by bar.	-0.2	-0.17143	-0.48276	-0.43744	-0.5234	-0.69532	-0.65197	-0.72192	-0.7032	-0.57586	Tide elevation with barometric change taken out
tide bar corr		-0.62857	-0.91724	-0.96256	-0.7766	-0.40468	-0.24803	0.02192	0.4032	0.57586	Tide correction since Oct. 5 with barometric change offset
tide corr by eff.		-0.02956	-0.04314	-0.04527	-0.036527	-0.019034	-0.011666	0.001031	0.018964	0.027085	Tide correction from Oct. 5 multiplied by tidal efficiency of well
recession	0	-0.0611	-0.1222	-0.1833	-0.2444	-0.3055	-0.3666	-0.4277	-0.4888	-0.5499	amount of decline since Oct. 5 due to lack of recharge
well	3.75	3.65	3.55	3.5	3.45	3.41	3.4	3.39	3.4	3.41	Actual well water elevation measured
well-rec	3.75	3.7111	3.6722	3.6833	3.6944	3.7155	3.7666	3.8177	3.8888	3.9599	Well elevation corrected for recession (add recession back)
well-rec+tide corr	3.75	3.74066	3.71534	3.728574	3.730927	3.734534	3.776266	3.816669	3.869836	3.932815	Correct well elevation with recession by offsetting tidal effect
bar efficiency		0.02841	-2.235	-0.29196	0.01731	0.013265	0.771969	0.225967	0.293285	2.779304	Calculate barometric efficiency of well day by day
										0.173166	Calculate barometric efficiency of well from Oct 8 to Oct 13

Time	BarPress	Uncorr	Corr Head
38245.55486	30.711	3.0364	3.0364
38245.55564	30.711	3.0433	3.0433
38245.55841	30.711	3.0433	3.0433
38245.56189	30.711	3.0779	3.0779
done 38245.56883	30.711	3.0295	3.0295
38245.58333	30.659	3.0433	3.0343
38245.6105	30.659	2.9995	2.9905
38245.66667	30.633	2.9649	2.95139
38245.77716	30.631	2.8657	2.85185
38246	30.566	2.8934	2.86829
38246.44383	30.475	2.8126	2.77173
38247.33333	30.343	2.5889	2.52517

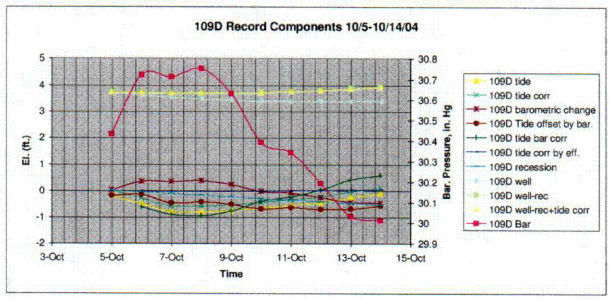

C78

Table E-1
September 2004 Pumping Test Drawdown Corrections
CY Groundwater Model

Analysis of Barometric Efficiency in period 10/05/04 to 10/14/04 — Tidal Efficiency 0.053333

Well 109S

	5-Oct	6-Oct	7-Oct	8-Oct	9-Oct	10-Oct	11-Oct	12-Oct	13-Oct	14-Oct	
Bar	30.43	30.72	30.71	30.75	30.63	30.39	30.34	30.19	30.03	30.01	barometric pressure in inches of Hg
tide	-0.2	-0.5	-0.8	-0.8	-0.75	-0.65	-0.55	-0.45	-0.25	-0.1	Measured Tide elevation
tide corr	0	-0.3	-0.6	-0.6	-0.55	-0.45	-0.35	-0.25	-0.05	0.1	Measured change in Tide elevation from Oct. 5
barometric change	0	0.32857	0.31724	0.36256	0.2266	-0.04532	-0.10197	-0.27192	-0.4532	-0.47586	Theoretical change in tide in feet due to barometric pressure from Oct. 5
Tide offset by bar.	-0.2	-0.17143	-0.48276	-0.43744	-0.5234	-0.69532	-0.65197	-0.72192	-0.7032	-0.57586	Tide elevation with barometric change taken out
tide bar corr		-0.62857	-0.91724	-0.96256	-0.7766	-0.40468	-0.24803	0.02192	0.4032	0.57586	Tide correction since Oct. 5 with barometric change offset
tide corr by eff.		-0.03352	-0.04892	-0.05134	-0.041419	-0.021583	-0.013228	0.001169	0.021504	0.030713	Tide correction from Oct. 5 multiplied by tidal efficiency of well
recession	0	-0.05	-0.1	-0.15	-0.2	-0.25	-0.3	-0.35	-0.4	-0.45	amount of decline since Oct. 5 due to lack of recharge
well	2.35	2.25	2.17	2.08	2.06	2.03	2.01	2.03	2.08	2.16	Actual well water elevation measured
well-rec	2.35	2.3	2.27	2.23	2.26	2.28	2.31	2.38	2.48	2.61	Well elevation corrected for recession (add recession back)
well-rec+tide corr	2.35	2.33352	2.31892	2.281337	2.301419	2.301583	2.323228	2.378831	2.458496	2.579287	Correct well elevation with recession by offsetting tidal effect
bar effficiency		0.05015	-1.28899	0.829279	0.147706	0.000604	0.382089	0.327171	0.439459	5.330603	Calculate barometric efficiency of well day by day
										0.217171	Calculate barometric efficiency of well from Oct 8 to Oct 13

	Time	BarPress	Uncorr	Corr Head
	38245.55486	30.711	3.0083	3.0083
	38245.55564	30.711	3.0083	3.0083
	38245.55841	30.711	3.0083	3.0083
	38245.56189	30.711	2.999	2.999
done	38245.56883	30.711	3.0129	3.0129
	38245.58333	30.659	3.0106	2.99931
	38245.6105	30.659	3.0083	2.99701
	38245.66667	30.633	2.9783	2.96136
	38245.77716	30.631	2.8722	2.85483
	38246	30.566	2.8283	2.79681
	38246.44383	30.475	2.6899	2.63865
	38247.33333	30.343	2.5654	2.48548

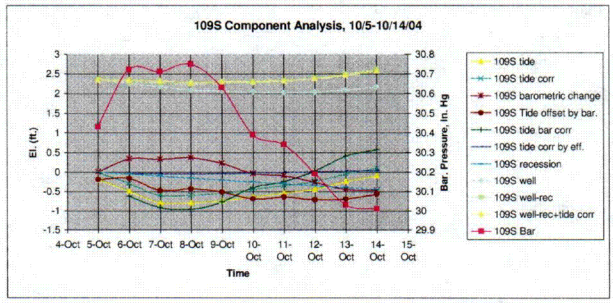

Analysis of Barometric Efficiency in period 10/05/04 to 10/14/04 — Tidal Efficiency 0.045966

Well 123

	5-Oct	6-Oct	7-Oct	8-Oct	9-Oct	10-Oct	11-Oct	12-Oct	13-Oct	14-Oct	
Bar	30.43	30.72	30.71	30.75	30.63	30.39	30.34	30.19	30.03	30.01	barometric pressure in inches of Hg
tide	-0.2	-0.5	-0.8	-0.8	-0.75	-0.65	-0.55	-0.45	-0.25	-0.1	Measured Tide elevation
tide corr	0	-0.3	-0.6	-0.6	-0.55	-0.45	-0.35	-0.25	-0.05	0.1	Measured change in Tide elevation from Oct. 5
barometric change	0	0.32857	0.31724	0.36256	0.2266	-0.04532	-0.10197	-0.27192	-0.4532	-0.47586	Theoretical change in tide in feet due to barometric pressure from Oct. 5
Tide offset by bar.	-0.2	-0.17143	-0.48276	-0.43744	-0.5234	-0.69532	-0.65197	-0.72192	-0.7032	-0.57586	Tide elevation with barometric change taken out
tide bar corr		-0.62857	-0.91724	-0.96256	-0.7766	-0.40468	-0.24803	0.02192	0.4032	0.57586	Tide correction since Oct. 5 with barometric change offset
tide corr by eff.		-0.02889	-0.04216	-0.04424	-0.035697	-0.018601	-0.011401	0.001008	0.018533	0.02647	Tide correction from Oct. 5 multiplied by tidal efficiency of well
recession	0	-0.085	-0.17	-0.255	-0.34	-0.425	-0.51	-0.595	-0.68	-0.765	amount of decline since Oct. 5 due to lack of recharge
well	5.95	5.85	5.75	5.65	5.55	5.48	5.4	5.35	5.25	5.2	Actual well water elevation measured
well-rec	5.95	5.935	5.92	5.905	5.89	5.905	5.91	5.945	5.93	5.965	Well elevation corrected for recession (add recession back)
well-rec+tide corr	5.95	5.96389	5.96216	5.949245	5.925697	5.923601	5.921401	5.943992	5.911467	5.93853	Correct well elevation with recession by offsetting tidal effect
bar effficiency		-0.04228	-0.15279	0.285014	-0.173196	-0.007706	-0.038844	0.132931	-0.179423	1.194333	Calculate barometric efficiency of well day by day
										0	Calculate barometric efficiency of well from Oct 8 to Oct 13

	Time	BarPress	Uncorr	Corr Head
	38245.55486	30.711	4.4062	4.4062
	38245.55564	30.711	4.4062	4.4062
	38245.55841	30.711	4.4016	4.4016
	38245.56189	30.711	4.3393	4.3393
	38245.56883	30.711	4.4362	4.4362
done	38245.58333	30.659	4.3209	4.3209
	38245.6105	30.659	4.3624	4.3624
	38245.66667	30.633	4.3462	4.3462
	38245.77716	30.631	4.3116	4.3116
	38246	30.566	4.3209	4.3209
	38246.44383	30.475	4.2447	4.2447
	38247.33333	30.343	4.1248	4.1248

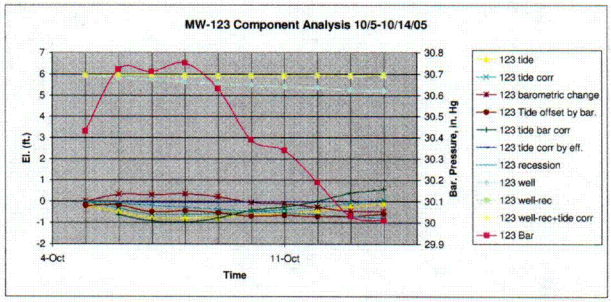

Analysis of Barometric Efficiency in period 10/05/04 to 10/14/04 — Tidal Efficiency 0

Well 104

	5-Oct	6-Oct	7-Oct	8-Oct	9-Oct	10-Oct	11-Oct	12-Oct	13-Oct	14-Oct	
Bar	30.43	30.72	30.71	30.75	30.63	30.39	30.34	30.19	30.03	30.01	barometric pressure in inches of Hg
tide	-0.2	-0.5	-0.8	-0.8	-0.75	-0.65	-0.55	-0.45	-0.25	-0.1	Measured Tide elevation
tide corr	0	-0.3	-0.6	-0.6	-0.55	-0.45	-0.35	-0.25	-0.05	0.1	Measured change in Tide elevation from Oct. 5
barometric change	0	0.32857	0.31724	0.36256	0.2266	-0.04532	-0.10197	-0.27192	-0.4532	-0.47586	Theoretical change in tide in feet due to barometric pressure from Oct. 5
Tide offset by bar.	-0.2	-0.17143	-0.48276	-0.43744	-0.5234	-0.69532	-0.65197	-0.72192	-0.7032	-0.57586	Tide elevation with barometric change taken out
tide bar corr		-0.62857	-0.91724	-0.96256	-0.7766	-0.40468	-0.24803	0.02192	0.4032	0.57586	Tide correction since Oct. 5 with barometric change offset
tide corr by eff.		0	0	0	0	0	0	0	0	0	Tide correction from Oct. 5 multiplied by tidal efficiency of well
recession	0	-0.289	-0.578	-0.867	-1.156	-1.445	-1.734	-2.023	-2.312	-2.601	amount of decline since Oct. 5 due to lack of recharge
well	11	10.7	10.4	10.05	9.75	9.45	9.15	8.9	8.65	8.4	Actual well water elevation measured
well-rec	11	10.989	10.978	10.917	10.906	10.895	10.884	10.923	10.962	11.001	Well elevation corrected for recession (add recession back)
well-rec+tide corr	11	10.989	10.978	10.917	10.906	10.895	10.884	10.923	10.962	11.001	Correct well elevation with recession by offsetting tidal effect
bar effficiency		0.03348	-0.97087	1.345984	-0.080906	-0.040453	-0.194175	0.229479	0.215137	1.721094	Calculate barometric efficiency of well day by day
										0.055163	Calculate barometric efficiency of well from Oct 8 to Oct 13

	Time	BarPress	Uncorr	Corr Head
	38245.55486	30.711	7.8313	7.8313
	38245.55564	30.711	7.8313	7.8313
	38245.55841	30.711	7.8267	7.8267
	38245.56189	30.711	7.806	7.806
	38245.56883	30.711	7.8175	7.8175
done	38245.58333	30.659	7.8221	7.81923
	38245.6105	30.659	7.8152	7.81233
	38245.66667	30.633	7.799	7.7947
	38245.77716	30.631	7.7644	7.75999
	38246	30.566	7.6999	7.6919
	38246.44383	30.475	7.5937	7.58068
	38247.33333	30.343	7.3792	7.3589

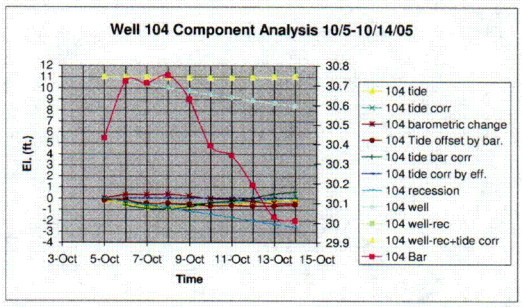

Table E-1
September 2004 Pumping Test Drawdown Corrections
CY Groundwater Model

Analysis of Barometric Efficiency in period 10/05/04 to 10/14/04 — Tidal Efficiency 0.008621

Well 124	5-Oct	6-Oct	7-Oct	8-Oct	9-Oct	10-Oct	11-Oct	12-Oct	13-Oct	14-Oct	
Bar	30.43	30.72	30.71	30.75	30.63	30.39	30.34	30.19	30.03	30.01	barometric pressure in inches of Hg
tide	-0.2	-0.5	-0.8	-0.8	-0.75	-0.65	-0.55	-0.45	-0.25	-0.1	Measured Tide elevation
tide corr	0	-0.3	-0.6	-0.6	-0.55	-0.45	-0.35	-0.25	-0.05	0.1	Measured change in Tide elevation from Oct. 5
barometric change	0	0.32857	0.31724	0.36256	0.2266	-0.04532	-0.10197	-0.27192	-0.4532	-0.47586	Theoretical change in tide in feet due to barometric pressure from Oct. 5
Tide offset by bar.	-0.2	-0.17143	-0.48276	-0.43744	-0.5234	-0.69532	-0.65197	-0.72192	-0.7032	-0.57586	Tide elevation with barometric change taken out
tide bar corr		-0.62857	-0.91724	-0.96256	-0.7766	-0.40468	-0.24803	0.02192	0.4032	0.57586	Tide correction since Oct. 5 with barometric change offset
tide corr by eff.		-0.00542	-0.00791	-0.0083	-0.006695	-0.003489	-0.002138	0.000189	0.003476	0.004964	Tide correction from Oct. 5 multiplied by tidal efficiency of well
recession	0	-0.0375	-0.075	-0.1125	-0.15	-0.1875	-0.225	-0.2625	-0.3	-0.3375	amount of decline since Oct. 5 due to lack of recharge
well	3.4	3.33	3.26	3.19	3.14	3.11	3.08	3.06	3.07	3.1	Actual well water elevation measured
well-rec	3.4	3.3675	3.335	3.3025	3.29	3.2975	3.305	3.3225	3.37	3.4375	Well elevation corrected for recession (add recession back)
well-rec+tide corr	3.4	3.37292	3.34291	3.310798	3.296695	3.300989	3.307138	3.322311	3.366524	3.432536	Correct well elevation with recession by offsetting tidal effect
bar effficiency		0.08242	-2.64885	0.708502	-0.10373	0.015791	0.108554	0.089278	0.243894	2.913131	Calculate barometric efficiency of well day by day
										0.068312	Calculate barometric efficiency of well from Oct 8 to Oct 13

	Time	BarPress	Uncorr	Corr Head
	38245.55486	30.711	2.8356	2.8356
	38245.55564	30.711	2.8356	2.8356
	38245.55841	30.711	2.8333	2.8333
	38245.56189	30.711	2.8333	2.8333
	38245.56883	30.711	2.8286	2.8286
done	38245.58333	30.659	2.8148	2.81125
	38245.6105	30.659	2.794	2.79045
	38245.66667	30.633	2.7525	2.74717
	38245.77716	30.631	2.6879	2.68244
	38246	30.566	2.5934	2.58349
	38246.44383	30.475	2.4688	2.45268
	38247.33333	30.343	2.2497	2.22456

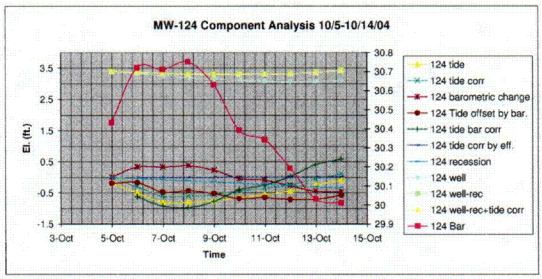

Analysis of Barometric Efficiency in period 10/05/04 to 10/14/04 — Tidal Efficiency 0.013793

Well OB-25	5-Oct	6-Oct	7-Oct	8-Oct	9-Oct	10-Oct	11-Oct	12-Oct	13-Oct	14-Oct	
Bar	30.43	30.72	30.71	30.75	30.63	30.39	30.34	30.19	30.03	30.01	barometric pressure in inches of Hg
tide	-0.2	-0.5	-0.8	-0.8	-0.75	-0.65	-0.55	-0.45	-0.25	-0.1	Measured Tide elevation
tide corr	0	-0.3	-0.6	-0.6	-0.55	-0.45	-0.35	-0.25	-0.05	0.1	Measured change in Tide elevation from Oct. 5
barometric change	0	0.32857	0.31724	0.36256	0.2266	-0.04532	-0.10197	-0.27192	-0.4532	-0.47586	Theoretical change in tide in feet due to barometric pressure from Oct. 5
Tide offset by bar.	-0.2	-0.17143	-0.48276	-0.43744	-0.5234	-0.69532	-0.65197	-0.72192	-0.7032	-0.57586	Tide elevation with barometric change taken out
tide bar corr		-0.62857	-0.91724	-0.96256	-0.7766	-0.40468	-0.24803	0.02192	0.4032	0.57586	Tide correction since Oct. 5 with barometric change offset
tide corr by eff.		-0.00867	-0.01265	-0.01328	-0.010712	-0.005582	-0.003421	0.000302	0.005561	0.007943	Tide correction from Oct. 5 multiplied by tidal efficiency of well
recession	0	-0.04667	-0.09337	-0.14007	-0.186767	-0.233467	-0.280167	-0.326867	-0.373567	-0.420267	amount of decline since Oct. 5 due to lack of recharge
well	3.43	3.37	3.29	3.2	3.17	3.15	3.12	3.11	3.13	3.16	Actual well water elevation measured
well-rec	3.43	3.41667	3.38337	3.340067	3.356767	3.383467	3.400167	3.436867	3.503567	3.580267	Well elevation corrected for recession (add recession back)
well-rec+tide corr	3.43	3.42534	3.39602	3.353343	3.367478	3.389048	3.403588	3.436564	3.498005	3.572324	Correct well elevation with recession by offsetting tidal effect
bar effficiency		0.01419	-2.58767	0.941635	0.103965	0.079325	0.256652	0.194037	0.338929	3.279721	Calculate barometric efficiency of well day by day
										0.177334	Calculate barometric efficiency of well from Oct 8 to Oct 13

	Time	BarPress	Uncorr	Corr Head
	38245.55486	30.711	2.6957	2.6957
	38245.55564	30.711	2.6934	2.6934
	38245.55841	30.711	2.6911	2.6911
	38245.56189	30.711	2.6865	2.6865
	38245.56883	30.711	2.6796	2.6796
done	38245.58333	30.659	2.6519	2.64268
	38245.6105	30.659	2.6127	2.60348
	38245.66667	30.633	2.5573	2.54347
	38245.77716	30.631	2.465	2.45081
	38246	30.566	2.3451	2.31939
	38246.44383	30.475	2.1652	2.12335
	38247.33333	30.343	1.9298	1.86464

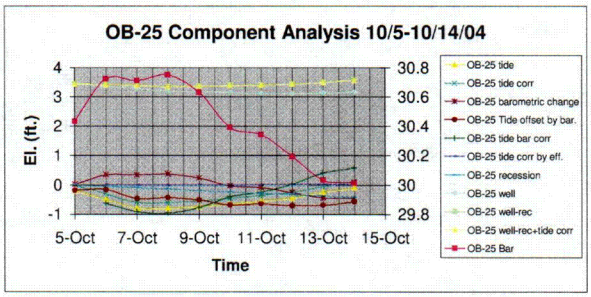

C80